Tectonics®

RESEARCH ARTICLE
10.1029/2025TC008824

Salt Diapirs and Minibasins Along a Transect Across the Basque-Cantabrian Pyrenees: Implications for Cover-Basement Interaction During Rifting and Inversion

Mark G. Rowan[1], Josep Anton Muñoz[2], Eduard Roca[2], Eloi Carola[2], Rodolfo Uranga[2], Iñaki Garcia[3], and Oriol Ferrer[2]

[1]Rowan Consulting, Inc., Boulder, CO, USA, [2]Institut de Recerca UB-Geomodels, Departament de Dinàmica de la Terra i de l'Oceà, Facultat de Ciències de la Terra, Universitat de Barcelona, Barcelona, Spain, [3]Retired, Bilbao, Spain

Abstract The Basque-Cantabrian Pyrenees experienced Early Cretaceous rifting and latest Cretaceous to Cenozoic inversion, with the presence of prerift Upper Triassic Keuper salt influencing how deformation was accommodated. Considerable disagreement exists on the degree of decoupling of supra- and subsalt deformation, the amount of thin-skinned translation of the cover relative to basement, and the dip polarity of the primary extensional and contractional lithospheric detachment. To address these issues, we use surface and subsurface data to evaluate six diapirs and associated minibasins along a transect across the Basque-Cantabrian Pyrenees. Key findings include: (a) the Burgalesa Platform and the Alavesa Platform to southern limb of the Bilbao Anticlinorium are ramp-syncline basins, with prekinematic rafts, that record Cretaceous thin-skinned extension and translation over north-dipping basement faults; (b) whereas Bakio and Villasana de Mena had early extensional triggers and long-lived passive diapirism, Poza de la Sal and Salinas de Rosío began as salt anticlines, with the onset of steep passive diapirism in the late Albian and Cenozoic, respectively; (c) although Sopelana and Montorio were squeezed shut to form vertical welds, Villasana de Mena was not noticeably shortened; (d) the salt layer was still continuous after extension ceased; (e) the salt served as a ramp-flat thrust fault during inversion; and (f) although the initiation and evolution of diapirs were influenced by basement faults, they are not located over those faults today. The deformation to the south of the Bilbao Anticlinorium was thus decoupled above and below a major north-dipping salt décollement during both extension and contraction.

Key Points:

- Diapirs and minibasins along a transect across the Basque-Cantabrian Pyrenees have varying geometries, origins, and evolutionary histories
- The salt-related cover deformation was largely decoupled from basement structures during both rifting and inversion
- The results support models with significant cover translation and contradict those with direct links between cover and basement structures

Correspondence to:
J. A. Muñoz,
jamunoz@ub.edu

Citation:
Rowan, M. G., Muñoz, J. A., Roca, E., Carola, E., Uranga, R., Garcia, I., & Ferrer, O. (2025). Salt diapirs and minibasins along a transect across the Basque-Cantabrian Pyrenees: Implications for cover-basement interaction during rifting and inversion. *Tectonics*, *44*, e2025TC008824. https://doi.org/10.1029/2025TC008824

Received 17 JAN 2025
Accepted 25 APR 2025

Author Contributions:
Conceptualization: Mark G. Rowan, Josep Anton Muñoz, Eduard Roca
Formal analysis: Mark G. Rowan, Josep Anton Muñoz, Eduard Roca
Funding acquisition: Josep Anton Muñoz, Oriol Ferrer
Investigation: Mark G. Rowan, Josep Anton Muñoz, Eduard Roca, Eloi Carola, Rodolfo Uranga, Iñaki Garcia, Oriol Ferrer
Methodology: Mark G. Rowan, Josep Anton Muñoz, Eduard Roca, Oriol Ferrer
Resources: Josep Anton Muñoz, Eduard Roca
Validation: Mark G. Rowan, Josep Anton Muñoz, Eduard Roca, Eloi Carola, Rodolfo Uranga, Iñaki Garcia, Oriol Ferrer
Visualization: Mark G. Rowan, Josep Anton Muñoz, Eduard Roca, Iñaki Garcia

1. Introduction

Rift basins and rifted margins commonly contain evaporite sequences that influence how deformation is accommodated during both extension and any subsequent inversion. The details vary by basin but are largely controlled by the relative timing between rifting and evaporite deposition. The salt may be prerift, early synrift, late synrift, or postrift (Jackson & Vendeville, 1994; Rowan, 2014). Whereas early synrift salt basins are characterized by only moderate decoupling between cover and basement deformation during thick-skinned extension, late synrift and early postrift salt basins are dominated by thin-skinned, gravity-driven deformation with little direct relation to underlying rift geometries (Rowan, 2014). Prerift salt basins are more enigmatic and may contain a combination of styles.

The degree of decoupling between cover and basement deformation during rifting varies (e.g., Jackson & Vendeville, 1994; Stewart et al., 1996; Withjack & Callaway, 2000). Deformation may be completely coupled, in which case faults cut through the salt layer. At the other end of the spectrum is complete decoupling, with no spatial link between basement-involved and suprasalt extensional structures. In between is a wide variety of moderately decoupled geometries that include (Figure 1): (a) drape folds of the cover, whether faulted or not, over basement faults; (b) salt anticlines, salt rollers, reactive diapirs, and passive diapirs typically set back somewhat above the footwalls of the subsalt faults; and (c) ramp-syncline basins, or landward-shifting depocenters formed during basinward translation over base-salt steps. Corresponding and coeval supra- and subsalt deformation can be offset laterally by many tens of kilometers (Rowan, 2022; Rowan & Jarvie, 2020; Rowan & Krzywiec, 2014). However, an important point is that the degree of coupling tends to increase over time as the amount of basement fault offset increases and the salt thickness decreases due to stretching and flow into diapirs (Ferrer, Carola, & McClay, 2023; Stewart & Clark, 1999). Moreover, although the cited work on decoupling is primarily from low-β settings such as the North Sea, the same concepts can be applied to high-β provinces such as the necking and

Writing – original draft: Mark G. Rowan
Writing – review & editing: Josep Anton Muñoz, Eduard Roca, Eloi Carola, Rodolfo Uranga, Oriol Ferrer

hyperextension domains on rifted margins (Clerc & Lagabrielle, 2014; Ducoux et al., 2021; Izquierdo-Llavall et al., 2020; Jammes et al., 2010; Labeaume & Teixell, 2020; Lagabrielle et al., 2019, 2020).

Deformation can also be partially decoupled during subsequent inversion of low-β rift basins (e.g., Dooley & Hudec, 2020; Ferrer, Carola, McClay, & Bufaliza, 2023; Ferrer et al., 2017; Letouzey et al., 1995) and high-β rifted margins (e.g., Ducoux et al., 2021; Ghazian & Buiter, 2014; Gomar et al., 2024; Izquierdo-Llavall et al., 2020; Labeaume & Teixell, 2020; Lagabrielle et al., 2019). The role of salt during contraction depends largely on the distribution of salt after the cessation of rifting (Ferrer, Carola, McClay, & Bufaliza, 2023). Again, because salt tends to thin over time during extensional deformation, one might expect discontinuous salt, especially where the salt is completely offset on major rift faults, so that inversion will locally be hard-linked between basement and cover (e.g., Hansen et al., 2021; Stewart, 2014; Stewart & Clark, 1999). However, a combination of surface, well, and seismic data documents that salt can still be connected between the foot- and hanging walls of basement faults with 2–5 km of extensional throw (e.g., Ducoux et al., 2021; Ford & Vergés, 2021; Mencos et al., 2015).

The Pyrenean system is considered an example of prerift salt (e.g., Ferrer et al., 2012; Jammes et al., 2010; Rowan, 2014). Although it was deposited during the latest stages of Triassic rifting, a prekinematic Lower-Middle Jurassic cover was deposited prior to the main Early Cretaceous rift event that led to mantle exhumation in the onshore Pyrenees and in the central Bay of Biscay and ultimately to oceanic spreading in the western Bay of Biscay (Jammes et al., 2010; Lescoutre et al., 2021; Roca et al., 2011; Tugend et al., 2014). Despite an abundance of both surface and subsurface data and published studies, especially in recent years, there are numerous topics of ongoing controversy. These include, but are not limited to: (a) the symmetry or asymmetry of the rift basin; (b) if asymmetric, whether the main extensional lithospheric detachment dipped toward the north or south; (c) the regional stress orientation during both extension and contraction; (d) the prevalence, location, and timing of any significant strike-slip movement; (e) the total magnitudes of both tectonic divergence and convergence; (f) the degree of decoupling between the supra- and subsalt deformation; and (g) the amount of thin-skinned translation of the cover relative to basement (see recent reviews by Cámara, 2017; Ducoux et al., 2020; Ford et al., 2022; Lagabrielle et al., 2020; Manatschal et al., 2021; Muñoz, 2019; Pedrera et al., 2021, 2023; Teixell et al., 2018).

The focus here is on the Basque-Cantabrian Pyrenees, located south of the eastern Bay of Biscay between the Cantabrian Mountains to the west and the Aragonese-Catalan Pyrenees (or Pyrenees *sensu stricto*) to the east (see Muñoz, 2002, 2019, for terminology). The Basque-Cantabrian Pyrenees is a Late Cretaceous-Cenozoic doubly-vergent fold-and-thrust belt characterized by a thick pre-orogenic, Late Jurassic to Late Cretaceous depocenter known as the Basque-Cantabrian Basin. Like the Arzacq Basin in SW France (Ducoux et al., 2021), the extensional Basque-Cantabrian Basin preserves the rift architecture despite the later orogenic overprint. The Basque-Cantabrian Basin contains about 25 diapirs of Upper Triassic Keuper salt, six of which are aligned along or close to a regional transect across the western Basque-Cantabrian Pyrenees oriented roughly in the direction of both extension and contraction (Figure 2). Multiple interpretations covering either portions or all of this transect can be divided into two broad styles of contractional deformation during the Pyrenean Orogeny: (a) one in which the salt was mostly, but not entirely, continuous, with largely decoupled deformation between the cover and faulted basement and, depending on the interpretation, variable amounts of thin-skinned translation (Figure 3a; Cámara, 2017; Cámara et al., 2023; Carola et al., 2015; Gómez et al., 2002; Hernaiz Huerta & Solé Pont, 2000; Jourdon et al., 2020; Malagón et al., 1994; Manatschal et al., 2021; Miró et al., 2021, 2023; Mirumbrales Ayllón et al., 2023; Muñoz, 2019; Roca et al., 2011; Serrano & Martínez del Olmo, 1990; Serrano et al., 1994; Serrano Oñate et al., 1989); and (b) one in which major contractional structures emanated in Variscan basement and cut through the salt and cover, such that there was little decoupling and thin-skinned shortening (Figure 3b; Pedrera et al., 2017, 2021; Quintana et al., 2015; Ramos et al., 2022a, 2022b; Tavani & Granado, 2015; Tavani et al., 2013).

In this contribution, we do not address explicitly most of the crustal-scale controversies mentioned above. Instead, we focus on the salt structures, both diapirs and intervening minibasins. What do their geometries and evolutionary histories tell us about the interaction between basement faulting and cover deformation? How much coupling or decoupling was there, first, during rifting, and second, during subsequent inversion of the rift basin? Do the present-day diapir locations, geometries, and evolution reflect underlying basement structures? We address these questions by examining the six diapirs close to the transect (Figure 2), starting with the Bakio diapir to the north (on which our team has already published; Roca et al., 2021) and moving south to the Sopelana salt weld, the Villasana de Mena, Salinas de Rosío, and Poza de la Sal diapirs, and finally the Montorio complex near

10.1029/2025TC008824

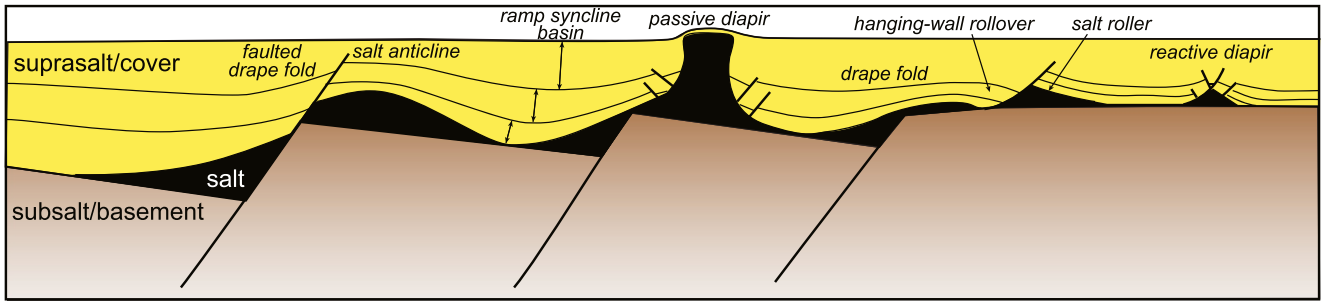

Figure 1. Schematic representation of typical salt and cover geometries and nomenclature in partially decoupled, thick-skinned, low-β extension (modified from Rowan, 2022). Figure not to scale, but cover and basement extension are intended to be equal and coeval. Double-headed arrows indicate laterally-shifting depocenters.

the south Pyrenean thrust front. But we also evaluate the intervening minibasin geometries and stratal thicknesses/ages for clues about the amount and timing of lateral translation of the cover above the salt. We do this using a combination of surface geology, subsurface seismic and well data, and some quantitative restorations. In short, the geometries demonstrate that: (a) different diapirs had quite different origins and histories; (b) large areas of the Basque-Cantabrian Basin suprasalt cover experienced significant thin-skinned, lateral translation of the cover relative to basement during and even after rifting; and (c) that the salt layer was still continuous over considerable stretches of the basin after rifting, so that inversion also resulted in long-distance thin-skinned translation of the cover relative to underlying basement. The results place critical constraints on the construction and restoration of regional, crustal-scale transects, not only for the Basque-Cantabrian Pyrenees but also for the rifting and inversion of the entire Pyrenean system and similar settings worldwide, such as the Alps, Hellenides, Betic-Rif system, Atlas Mountains, and the Flinders Ranges of South Australia.

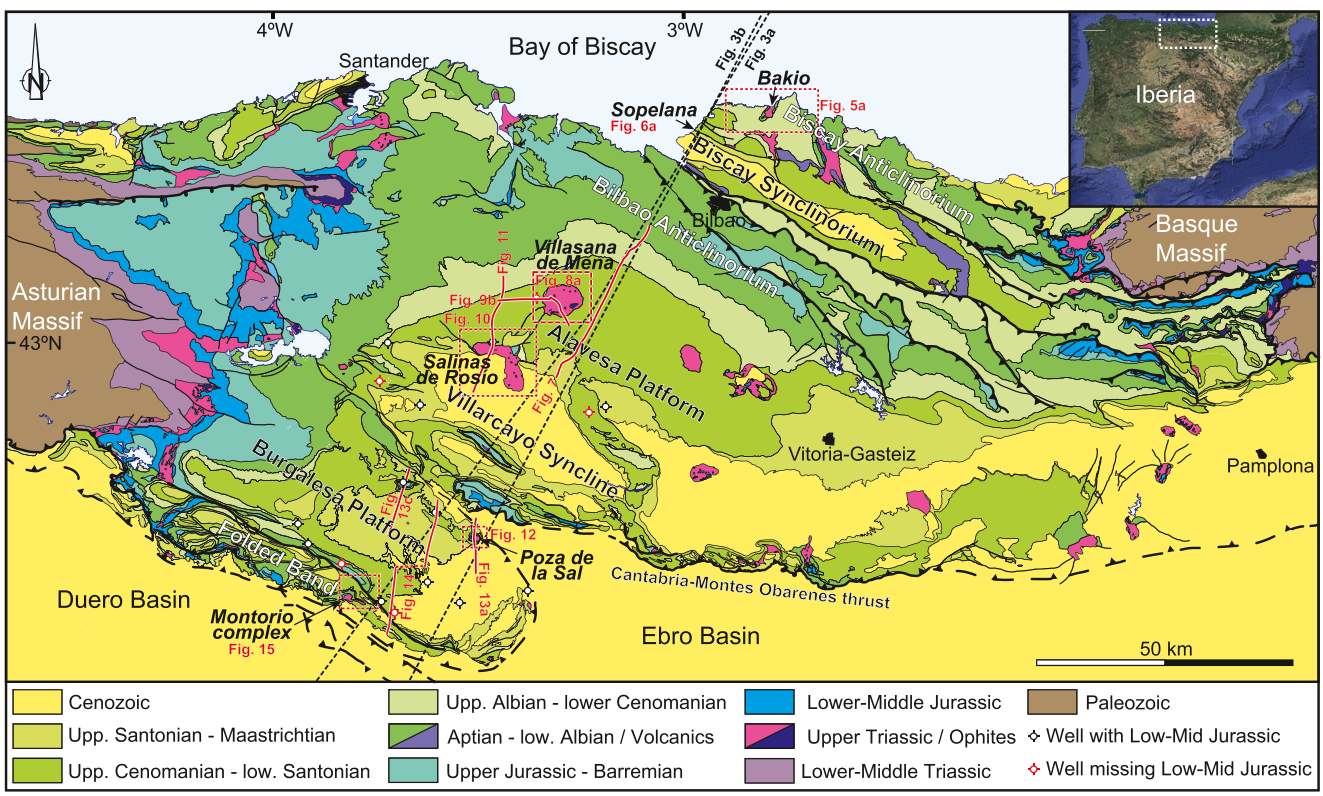

Figure 2. Geologic map of the Basque-Cantabrian Pyrenees, bounded by the Bay of Biscay to the north and the Ebro and Duero foreland basins to the south, and by the Asturian and Basque basement massifs to the west and east, respectively (modified from Miró et al., 2021). The structural domains and the six diapirs near the regional transects of Figure 3 are labeled, as are the locations of other figures.

10.1029/2025TC008824

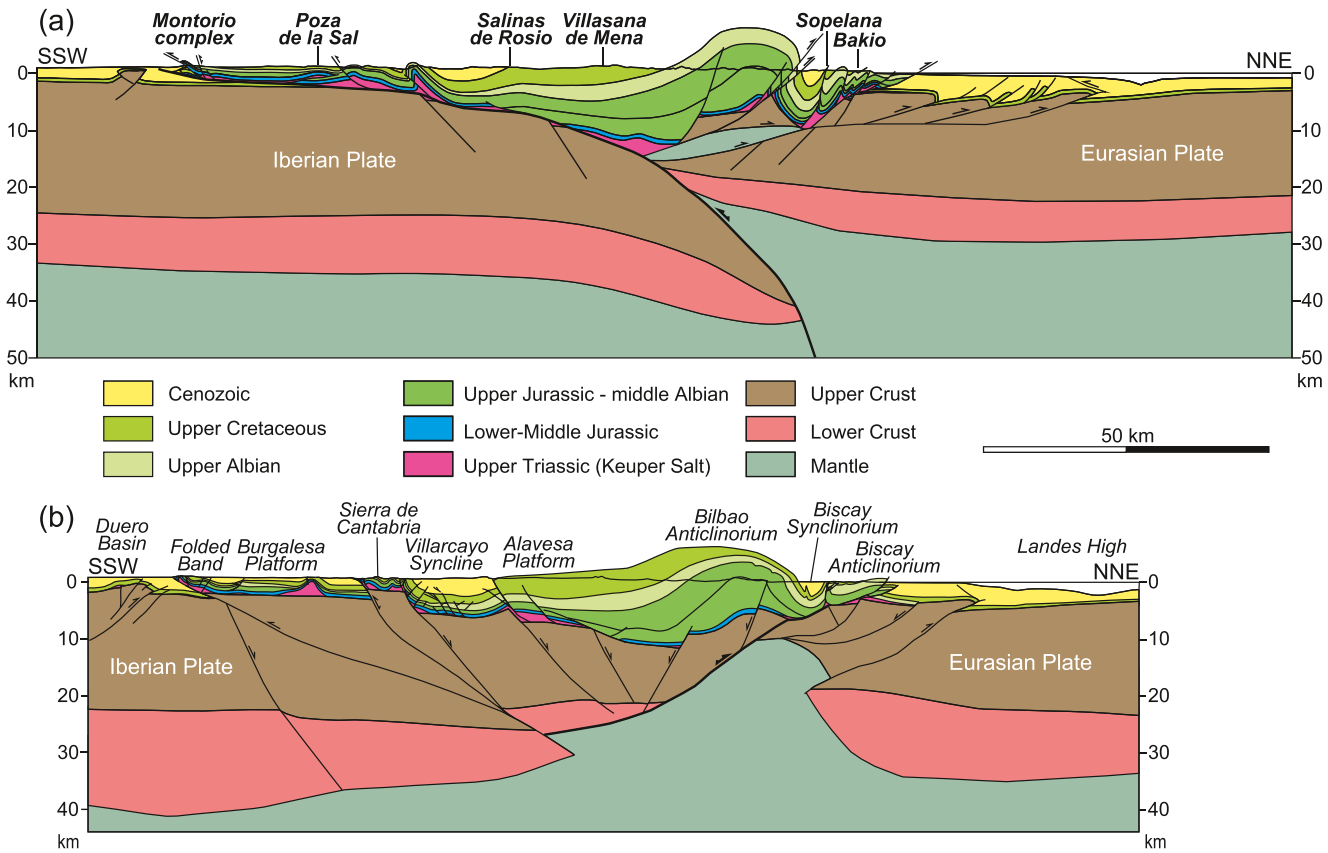

Figure 3. Two regional transects across the same area of the Basque-Cantabrian Pyrenees shown at the same 1:1 scale and with the same color scheme (locations shown in Figure 2): (a) with a crustal root, a dominant N-dipping detachment, and mostly decoupled deformation above and below the salt layer (Muñoz, 2019); and (b) with no crustal root, a dominant S-dipping detachment, and mostly coupled deformation (Pedrera et al., 2021). The diapirs and structural domains addressed in this paper are indicated above (a, b), respectively. Note the top of the upper Albian unit in panel (b) is actually within the Cenomanian, and that the Upper Jurassic-Barremian and Aptian-lower Albian units in Figure 2 are combined into one Upper Jurassic to middle Albian unit in this figure.

2. Geologic Setting

2.1. Tectonics

2.1.1. Tectonic Evolution

The overall tectonic development of northern Iberia was marked by several episodes of extension and contraction, with each phase of the deformation controlled to varying degrees by the inherited structure (Manatschal et al., 2021). For the purposes of this paper, we begin with the breakup of Pangea during the Triassic, after the post-orogenic collapse of the Paleozoic Variscan orogen. The Variscan itself is considered part of the basement so is not addressed (Figure 4).

The change of tectonic setting from the extensional collapse of the Variscan orogen to rifting related to breakup of Pangea was characterized by a change of volcanism from calc-alkaline to alkaline, coeval with a change of structural style from narrow and scattered extensional basins developed in a transtensional setting to more widespread extensional basins filled with synrift uppermost Permian to Lower Triassic nonmarine strata (López-Gómez, Alonso-Azcárate, et al., 2019). These sediments were overlain by shallow-marine to nonmarine strata, including the Upper Triassic Keuper evaporites (Figure 4). However, the lack of large-scale accommodation space suggests that crustal thinning at this time was at most minor (Manatschal et al., 2021). The Keuper salt has traditionally been considered to be early postrift (García-Mondéjar et al., 1986; see also Serrano Oñate et al., 1989), but even in this scenario there would have been areas of thicker salt due to flexural loading, thermal subsidence, and differential compaction of the main Permo-Triassic depocenters. It is also possible that rifting continued, at least locally, into the Late Triassic (Angrand et al., 2020; López-Gómez, Martín-González,

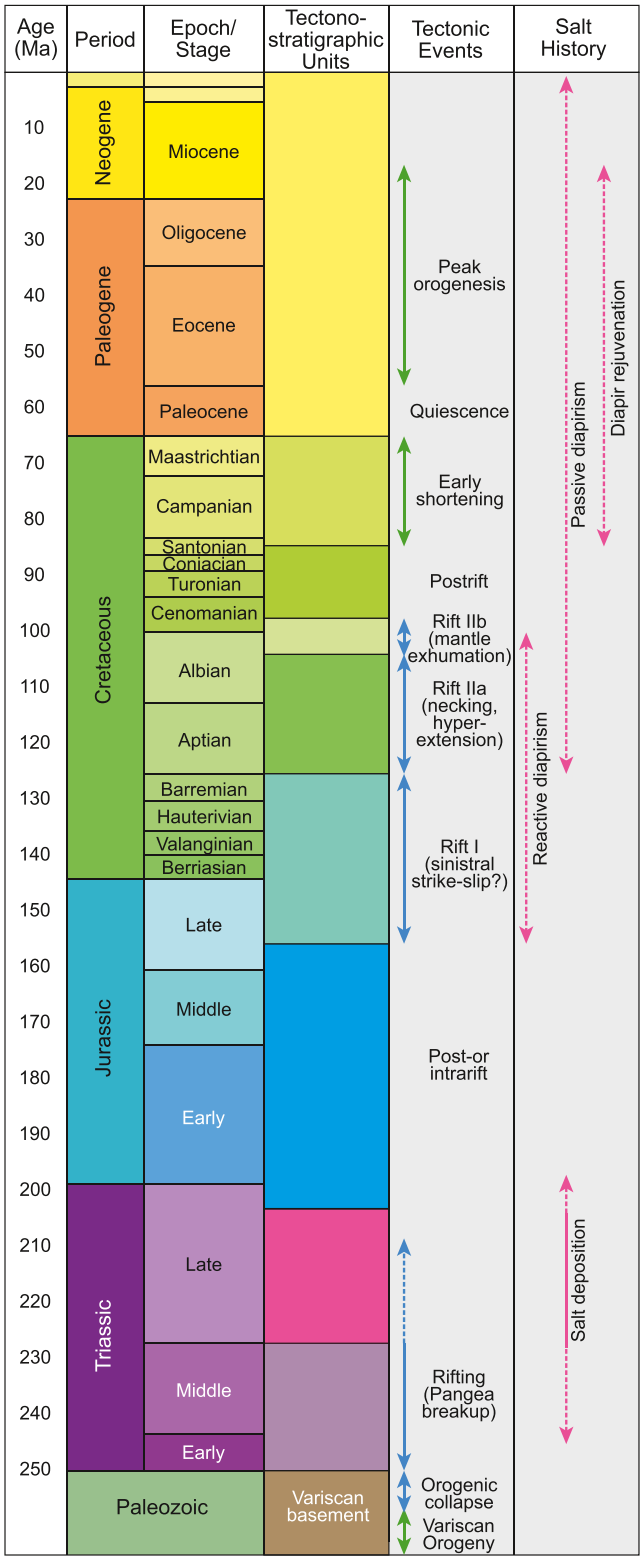

Figure 4.

et al., 2019; Manatschal et al., 2021), in which case the Keuper salt would have thickened abruptly across basement faults.

Whether or not the Keuper salt was postrift relative to the breakup of Pangea, the overlying Early-Middle Jurassic was a time of tectonic quiescence (Figure 4). Thus, the salt and its immediate overburden are considered as prerift relative to the main Late Jurassic to Early Cretaceous rifting. This extensional event has seen evolving interpretations of its timing and nature over the past decades, and here we adopt some of the most recent thinking (Angrand et al., 2020; Cadenas et al., 2020; DeFelipe et al., 2019; Frasca et al., 2021; Lescoutre et al., 2021; Manatschal et al., 2021; Miró et al., 2021). The Basque-Cantabrian Basin developed during the opening of the North Central Atlantic and its connection with the Alpine Tethys along the Bay of Biscay and Pyrenean rift arm (Stampfli & Hochard, 2009; Tavani et al., 2018). It formed as the Iberian plate moved eastward and away from the Eurasian plate in a transtensional sense. This left-lateral movement resulted in a diffuse plate boundary with several depocenters formed along both the northern Iberian margin and the Iberian Range south of the Ebro Basin (Asti et al., 2022). These depocenters have been interpreted to be the product of multi-stage rifting (Miró et al., 2021; Figure 4): an initial, sinistral transtensional phase during the Late Jurassic to Barremian (rift stage I); and subsequent N-S directed hyperextension and mantle exhumation during the Aptian to middle Cenomanian (rift stage II). Although we have not observed any significant shift or discontinuity in the sedimentary record of the Basque-Cantabrian Basin compatible with the proposed two distinct rift stages, we nevertheless maintain the separation of the synrift stratigraphy into two successions (Figure 4). Moreover, we further divide the second rift stage into two sub-stages (IIa and IIb) because of the regional importance of a middle-late Albian unconformity (García-Mondéjar et al., 2004). This unconformity may mark the onset of mantle exhumation and associated changes in regional uplift and subsidence patterns (Rowan, 2014).

Much of the Late Cretaceous was a time of postrift loading and thermal subsidence (Figure 4). The onset of orogenic contraction is uncertain in the Basque-Cantabrian Pyrenees. Although it is well dated as late Santonian farther east (e.g., Ford et al., 2022; Muñoz, 2002), Upper Cretaceous contractional growth strata are unknown from the study area, and it may be that initial shortening was accommodated by mantle subduction. In any case, the main contractional deformation in the Basque-Cantabrian Pyrenees occurred during the Eocene-early Miocene and ceased at middle Miocene times (Miró et al., 2021; Muñoz, 2019).

2.1.2. Cover Geometry Along the Transect

Regardless of the differing interpretations of basement geometry and the amount of linkage or decoupling across the Upper Triassic salt (Figure 3), the cover geometry is mostly well constrained by surface and subsurface data.

Figure 4. Stratigraphic chart of the Basque-Cantabrian Pyrenees showing the tectonostratigraphic units and colors used here, the regional tectonic events (based primarily on the compilation of Manatschal et al., 2021, and references therein), and the published history of salt deposition and salt tectonics (see text for explanation and references). Note that in the legends to subsequent figures, the Keuper salt is termed "Upper Triassic" and the uppermost Triassic to intra-Upper Jurassic is termed "Lower-Middle Jurassic."

The primary features between the bounding foreland basins are, from north to south (Figures 2 and 3): (a) the Biscay Anticlinorium, in the hanging wall of one or more N-directed thrust faults, containing pre-, syn-, and postrift strata and multiple diapirs of varying plan-view shapes (including Bakio diapir); (b) the Biscay Synclinorium, an asymmetric tight syncline with thick synorogenic strata, cut by several thrust faults and containing several narrow outcrops of salt (including the Sopelana thrust weld); (c) the Bilbao Anticlinorium, a large, N-directed thrusted anticline with almost 15 km of synrift strata but no exposed diapirs; (d) the Alavesa Platform, comprising a panel of subhorizontal syn-to postrift strata approximately 20 km wide between Villasana de Mena and Salinas de Rosío diapirs; (e) the Villarcayo Syncline, filled with synorogenic sediment above thin syn- to postrift strata; (f) the relatively short-wavelength salt-cored Oña and Tudanca anticlines that are the northwestern prolongation of the Sierra Cantabria thrust front; (g) the Burgalesa Platform, another panel of subhorizontal, but reduced-thickness, syn-to postrift strata about 20 km wide and bounded to the north by Poza de la Sal diapir and a N-directed thrust fault; and (h) the Folded Band, a belt of S-directed, short-wavelength thrust faults and folds in thin cover, with a few outcrops of salt near the transect that we term the Montorio complex. Note that these domains, including linear WNW-ESE trends of diapirs, generally extend for tens of km along strike (Figure 2) and are thus more than just local features.

2.2. Stratigraphy

The stratigraphy of the area is broken up here into tectonostratigraphic packages that match, at least approximately, the different tectonic stages (Figure 4). Again, the divisions and descriptions are compiled from multiple sources (Brinkmann & Lögters, 1968; Cámara, 2017; Cumberpatch et al., 2021; García-Mondéjar et al., 1986, 1996; Martín-Chivelet et al., 2002, 2019; Martinez-Braceras et al., 2017; Payros et al., 2006; Pedrera et al., 2017, 2021; Poprawski et al., 2016; Pujalte et al., 2000; Rat, 1988; Roca et al., 2021; Serrano Oñate et al., 1989; and references therein). We avoid formation names, focusing on the ages instead, except for the European-wide Triassic strata.

The strata between Variscan basement and the salt comprise Permian to Lower Triassic Buntsandstein redbeds and carbonate-dominated strata of the Middle Triassic Muschelkalk. The salt is generally considered to consist of the Upper Triassic (Carnian to Norian) Keuper mixture of halite, anhydrite (gypsum at the surface), clays, carbonates, and volcanic to shallow intrusive dolerites (traditionally termed ophites in the Pyrenees). However, clasts of underlying Muschelkalk and overlying Rhaetian to Hettangian (uppermost Triassic to lowermost Jurassic) carbonates are mapped in some of the diapirs, suggesting that evaporite deposition may have spanned more than just the Late Triassic (Figure 4; Serrano Oñate et al., 1989).

The Rhaetian to Middle Jurassic interval overlying the salt consists of platform carbonates with only minor and gradual thickness changes, and thus represents the prekinematic overburden between the salt and Upper Jurassic-Lower Cretaceous synrift strata (Figure 4). The synrift strata, as well as the overlying postrift sequences, contain a mixture of carbonates and siliciclastics, with nonmarine to shallow-marine depositional environments in the south transitioning to deepwater facies in the basin center. There is a similar proximal-to-distal transition, but narrower and with opposite vergence, on the northern margin of the Basque-Cantabrian Basin. Finally, Cenozoic synorogenic strata comprise nonmarine conglomerates, sandstones, siltstones, and shales in the south that grade to deepwater turbidites in the Biscay Synclinorium.

2.3. Salt Tectonics

The salt diapirs and associated suprasalt structures of the Basque-Cantabrian Pyrenees have been studied since the 1950s (Agirrezabala et al., 2002; Belenguer Oliver, 2017; Bodego et al., 2018; Boess, 1984; Brinkmann & Lögters, 1968; Cámara, 2017, 2020; Canérot et al., 2005; Carola et al., 2015; Cuevas & Tubia, 1985; Cumberpatch et al., 2021; Ducoux et al., 2020; Frankovic, 2010; Frankovic et al., 2016; García-Mondéjar et al., 1996; Guerrero, 2017; Guerrero et al., 2023; Hempel, 1967; Hernaiz et al., 1994; Hernaiz Huerta & Solé Pont, 2000; Klimowitz et al., 1999; Lotze, 1953; Málagon et al., 1994; Mas Tudó, 2011; Pedrera et al., 2017; Pflug, 1967; Poprawski et al., 2014, 2016; Quintà et al., 2012; Ramos et al., 2022a, 2022b; Roca et al., 2021; Rodríguez Cañas et al., 1994; Schroeder & Willems, 1983; Serrano et al., 1994; Serrano & Martínez del Olmo, 1990, 2004; Serrano Oñate et al., 1989; Soto et al., 2017; Tavani et al., 2011, 2013, 2022; Tavani & Granado, 2015). Here we summarize only the general findings; relevant detailed observations and interpretations from the literature are mentioned below when appropriate to the discussions of the diapirs along the transect.

Most diapirs, given the regional tectonic history, have been interpreted to have been triggered by extension. However, the reported timing of the onset of salt movement ranges from the Late Jurassic to as late as the Albian-Cenomanian transition. Moreover, the extension has variably been interpreted as thin- or thick-skinned, and some have noted that diapirs formed along or at the intersections of faults, whether extensional, strike-slip, or contractional. Whatever the timing and origin, many diapirs show evidence of ongoing near-surface passive diapirism, with flanking stratal thinning and upturn, unconformities, and local occurrences of reworked sediment in Lower Cretaceous to Cenozoic strata. Moreover, diapirs closer to the basin margins were squeezed during orogenic contraction, whereas those in the central zone were at most only slightly modified.

3. Diapirs and Minibasins

In this section, we address the diapirs and intervening minibasins along and near our regional transect (Figures 2 and 3a), starting on the coast in the north and moving toward the Duero Basin in the south. Where we cite already published work, we present both observations and interpretations; however, for new analyses carried out for this paper, we only describe the observations in this section and offer our interpretations in a subsequent section. Note also that we use the term minibasin in the broad sense of a depocenter, regardless of size, adjacent to one or more diapirs or other salt structures, with accommodation generated at least in part by subsidence into the underlying salt and/or growth of flanking salt structures (Rowan & Giles, 2021); this is in contrast to earlier, more restrictive definitions (Jackson & Hudec, 2017; Jackson & Talbot, 1991).

3.1. Bakio Diapir and the Biscay Anticlinorium

One of the most studied diapirs in the Basque-Cantabrian Pyrenees is Bakio diapir, within the Biscay Anticlinorium on the coast north of Bilbao (Figure 2), due to recent research programs by several groups (Cumberpatch et al., 2021; Poprawski et al., 2014, 2016, 2021; Roca et al., 2021; Soto et al., 2017). Here, we preferentially summarize the observations and interpretations from our team (Roca et al., 2021), which are not substantially different from others published.

Bakio diapir is approximately 2.5 by 1.5 km in size in outcrop, although based on seabed morphological facies, it continues for another 4 km off the coast with a narrowing in the center (Figure 5a). The salt wall trends NNE-SSW, slightly oblique to both the early extension and late shortening directions. The geometries of surrounding minibasins, combined with the diapir orientation, suggest that it formed over a west-dipping relay ramp between two south-dipping extensional faults. This in turn implies that the diapir was triggered by extension.

Near-diapir strata comprise Neocomian to lower Cenomanian marls, carbonate turbidites, and siliciclastic turbidites. They are characterized by several features that are anomalous for the area: (a) the strata thin and turn up to vertical and overturned attitudes within 400 m of the diapir; (b) there is a series of stacked angular unconformities within the same deformation halo; and (c) there are common debrites containing mostly carbonate platform facies. Thus, these strata form tapered composite halokinetic sequences (Giles & Rowan, 2012) and document ongoing passive diapirism during at least the Aptian to Albian. We infer that the diapir began as a reactive diapir in the earliest Cretaceous and transitioned, through a brief active stage, to passive diapirism by the Aptian at the latest (Figure 5b).

Nearby well and seismic data show that Bakio diapir and the Biscay Anticlinorium are located in the hanging wall of a N-vergent thrust-fault system, detached in the salt, with about 10 km of displacement. This is interpreted to be the reactivation of a Late Jurassic-Early Cretaceous S-dipping extensional salt detachment with a ramp-flat geometry caused by underlying basement faults, with Bakio diapir and flanking minibasins, including prekinematic Lower to Middle Jurassic strata, first translating basinward (to the south) during the Aptian to Albian (Figure 5c). Pyrenean shortening not only moved the diapir back to the north, over two ramps, but also squeezed the diapir somewhat as indicated by several contractional anticlinoria intersecting the diapir: one connecting it to Mungia diapir to the south, and one connecting it to Bermeo diapir to the east (Figure 5a). Moreover, the narrow central part of Bakio diapir gives it a Q-tip geometry (Dooley et al., 2009; Rowan & Vendeville, 2006), compatible with oblique squeezing during shortening. Note that, although not shown in Figure 5, there are likely wedges of remnant salt at the basement steps which would have facilitated translation in both directions.

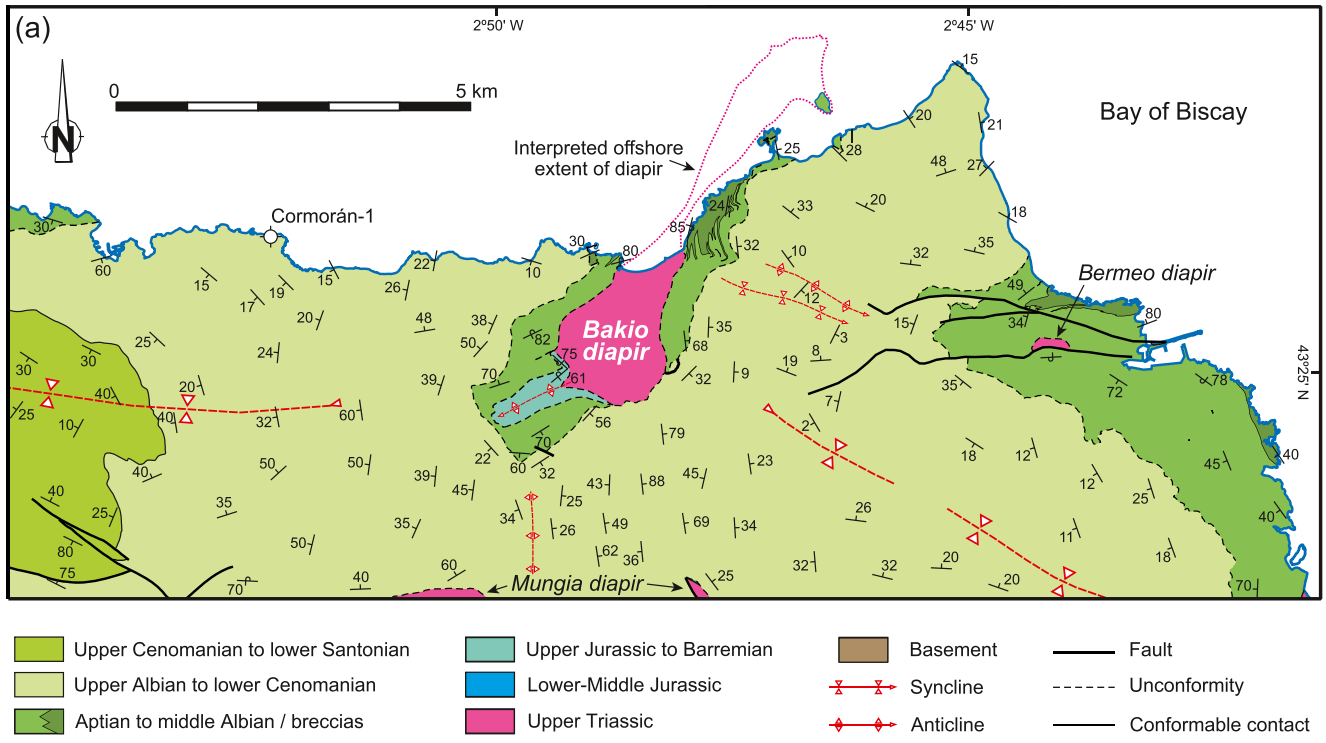

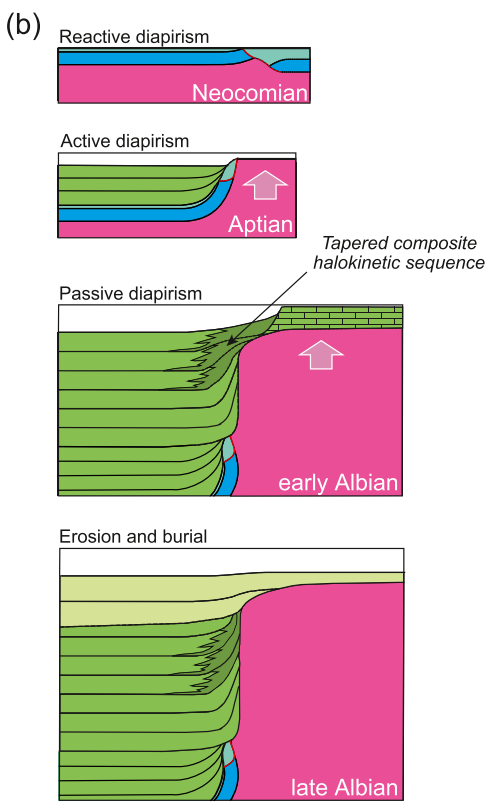

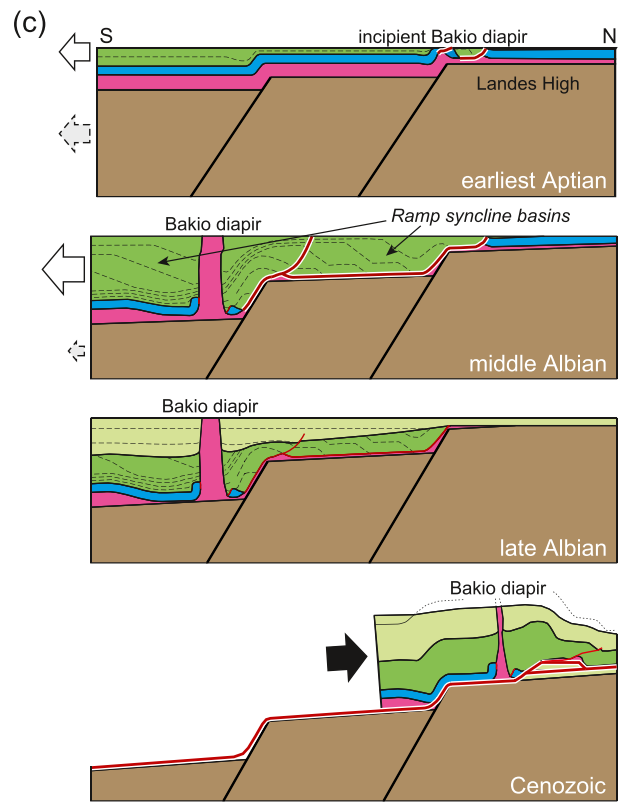

Figure 5.

3.2. Sopelana Weld and the Biscay Synclinorium

The Sopelana salt weld is exposed on the coast just NW of Bilbao, on the northern limb of the Biscay Synclinorium in a zone of linear thrust faults and narrow bodies of salt that extends for at least 30 km along strike to the ESE (Figure 2). The Sopelana weld is a steeply-dipping, 20 m wide body of Keuper lithologies (Figure 6a) that has been interpreted as a partly inverted normal fault (Rodríguez et al., 2008), a squeezed diapir between Maastrichtian and Paleocene strata (Miró et al., 2021), or the welded core of an anticline formed of Santonian to Maastrichtian rocks (Pedrera et al., 2021). The latter interpretation is contradicted by robust biostratigraphic data indicating a Maastrichtian age for the northern side and an early Eocene age for the southern side (Elorza et al., 1984; Martínez-Braceras et al., 2017).

The exposures display a series of WNW-ESE trending, N-vergent thrust faults on both sides of the weld and an interpreted thrust fault extending off the western tip of the salt body (Figure 6a). The strata immediately to the south of the weld are highly deformed, with S-C fabrics in a shear zone dipping 35°S (Figure 6b) also documenting N-vergent thrusting. This shear zone cuts down-section and, although not exposed, probably truncates the narrow body of Keuper (Figure 6c). The lower Eocene strata to the south strike approximately parallel to the weld, with moderate to overturned dips, in a tight, asymmetric anticline-syncline pair dissected by minor thrust faults (Figure 6c). In contrast, Maastrichtian strata to the north of the weld, although they also have moderate to steep dips, strike almost perpendicular to the weld (Figure 6a). This difference in strike on either side of the weld is also incompatible with an interpretation in which the weld is the squeezed core of an anticline, as put forward by Pedrera et al. (2021).

3.3. Bilbao Anticlinorium

The Bilbao Anticlinorium is the most prominent feature of the Basque-Cantabrian Pyrenees. It comprises a succession of Cretaceous synrift to postrift strata, close to 15 km in thickness, that forms a N-vergent, thrusted structure with the Biscay Synclinorium in its footwall (Figure 3a). Interestingly, there are no exposures of diapirs in this domain (Ábalos et al., 2008).

The northern limb of the Bilbao Anticlinorium is complexly faulted and folded at the surface (e.g., Quintana et al., 2015; Ábalos et al., 2008), but the deep structure is largely unconstrained due to inadequate seismic and well data. The southern limb, however, is imaged reasonably well (Figure 7a) and comprises a >20 km wide panel of moderately-dipping Kimmeridgian to Albian strata, at least 12 km in cumulative thickness, above a north-dipping band of brighter reflections that ties to known salt farther south. The strata form a series of subtle depocenters (Figure 7a, red double-headed arrows) that shift toward the south (landward) moving up through the stratigraphy —a pattern that continues into the Alavesa Platform. This geometry has been interpreted either as an expulsion-rollover structure driven by differential loading (Ábalos et al., 2008) or as a ramp-syncline basin associated with a large hanging-wall rollover structure on a major south-dipping extensional fault with a ramp-flat geometry (Pedrera et al., 2021). Just above the continuous band of north-dipping reflections at the base of the seismic profile is a series of isolated packages of bright reflections (Figure 7a, blue arrows) interpreted as blocks of the pre-kinematic Lower-Middle Jurassic strata (Figure 7b).

3.4. Villasana de Mena diapir

Villasana de Mena diapir is located at the boundary between moderately S- to SE-dipping strata on the southern limb of the Bilbao Anticlinorium and subhorizontal to slightly S-dipping strata at the western end of the Alavesa Platform (Figures 2 and 3a). At the surface, Villasana de Mena diapir is almost circular in map view (8 km by 6 km) and has no contractional structures extending away from it (Figure 8a), although two NE-SW trending faults of uncertain origin link it to Salinas de Rosío diapir (Figure 2).

Figure 5. Geology of the Bakio diapir and nearby areas (modified and adapted from Roca et al., 2021): (a) geologic map (location shown in Figure 2); (b) interpreted origin and evolution of the diapir using, in part, the observed composite halokinetic sequences flanking the diapir (not to scale, but the zone of near-diapir folding is roughly 500–800 m wide); and (c) restored schematic cross section (not to scale, but the diapir is approximately 4 km tall) showing the extensional origin, lateral translation, and subsequent contraction, but not the near-diapir halokinetic sequences of (b) (see text for explanation). The arrows in panel (c) show: solid white—thin-skinned extension of the salt and its cover; dashed gray—thick-skinned basement extension; and black—thin-skinned, ramp-flat thrusting of the salt and its cover (note that there are likely wedges of remnant salt against the basement faults that would make thin-skinned translation over the ramps more feasible). Color scheme as in Figure 4.

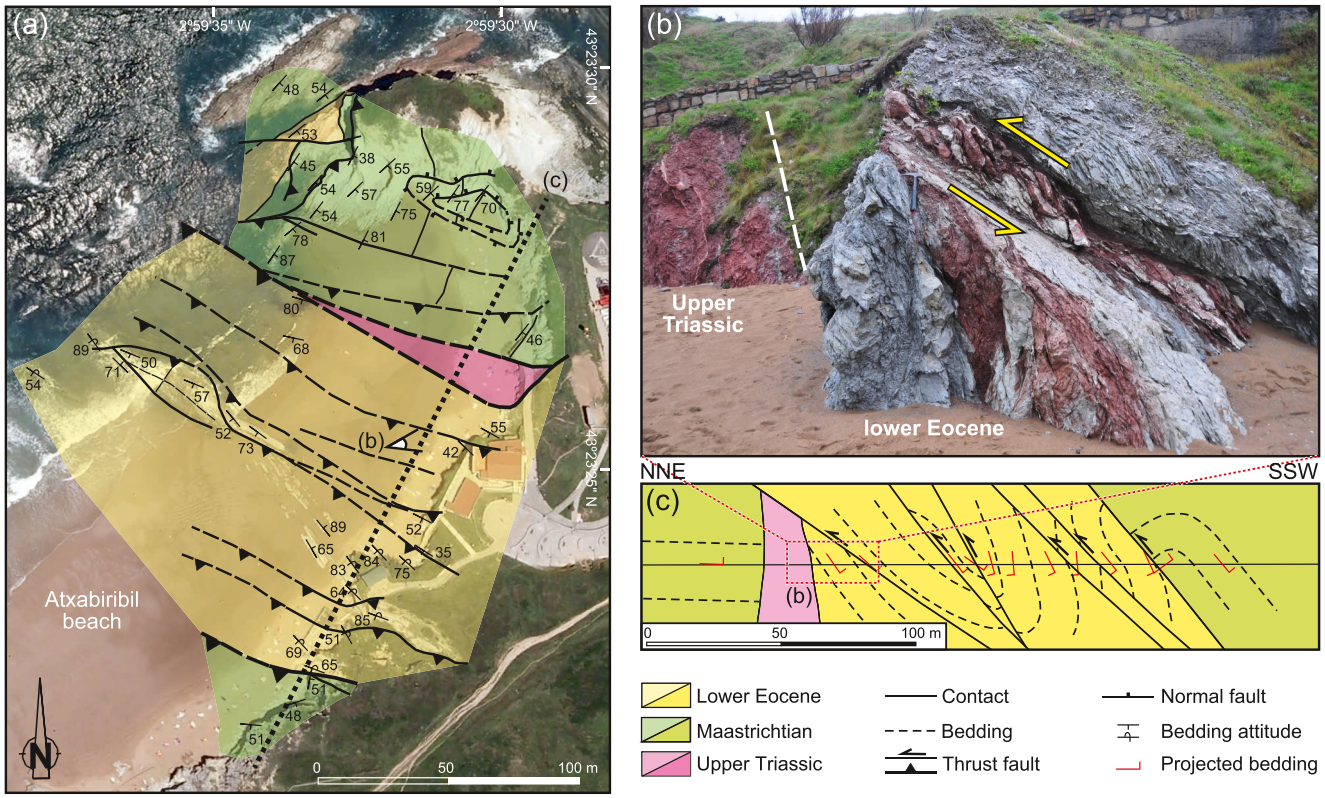

Figure 6. Surface observations at the Sopelana salt weld: (a) geologic map; (b) photo of intensely sheared Eocene marls on southern side of Keuper weld comprising 20 m wide zone of gypsum, red mudstones, and ophite blocks (see (a, c) for location of photo); (c) cross section oriented with SSW to the right in order to match the view from the beach (section indicated in panel (a)). See Figure 2 for location.

Villasana de Mena diapir is surrounded by upper Cenomanian to upper Coniacian marls and limestones except for a fringe of upper Albian to lower Cenomanian sandstones on its northwestern edge (Figure 8, locations ***1***) and upper Albian carbonates that formed on a paleo-high (Fernández-Mendiola & García-Mondéjar, 1997) on its northern edge (Figure 8a, location ***2***). The diapir contains clasts of mostly ophites as well as carbonates that are likely Muschelkalk or Rhaetian in age, plus a single mapped decametric-scale clast each of Paleozoic quartzite conglomerate and Paleocene rocks. A tectonic breccia is locally developed at the edge of the diapir (Figure 8, locations ***3***) and contains clasts of lithologies affiliated with the Triassic salt but none of the flanking Upper Cretaceous rocks. On the western flank, the breccia contains shear zones dipping 37–52° to the east (Figures 8b and 8c), with possible sense-of-shear indicators implying the east (diapir) side moved up relative to the outlying strata.

Strata all around the diapir, regardless of their regional dip, are folded upward within less than 0.5 km from the diapir edge (Figure 8a). This can be seen especially well on the western side of the diapir, where upper Albian to lowermost Coniacian strata turn up within 200 m of the salt (Figures 8b and 8c). Those closest to the salt have overturned dips of 36–49°, that is, sub-parallel to the shear fabric just inside the edge of salt, suggesting that the diapir flares up to at least the middle Turonian in this location (Figure 8c). The flanking strata, in addition to decreasing in dip away from the diapir, contain one significant but local unconformity (at the base of upper Turonian marls), with upturned underlying strata truncated beneath thinning and onlapping overlying strata, as well as several minor angular unconformities (Figures 8b and 8c).

The flaring of the western diapir edge is confirmed by the Encarnación-1 and Sopeñano-4 wells (Figure 9a), both of which spudded within the Triassic salt but drilled out of salt and into Cenomanian and Albian strata, respectively (Lanaja, 1987). The calculated dip of the base salt from these penetrations is 40° to the east, effectively parallel to the flanking overturned strata exposed at the surface. The Sopeñano-4 well reentered the salt at the bottom of the hole, with Aptian strata in contact with the salt. Away from the diapir, the Vivanco-1 well (Figure 9a) went from synrift "Weald" facies (Upper Jurassic or Neocomian) directly into the Triassic salt without

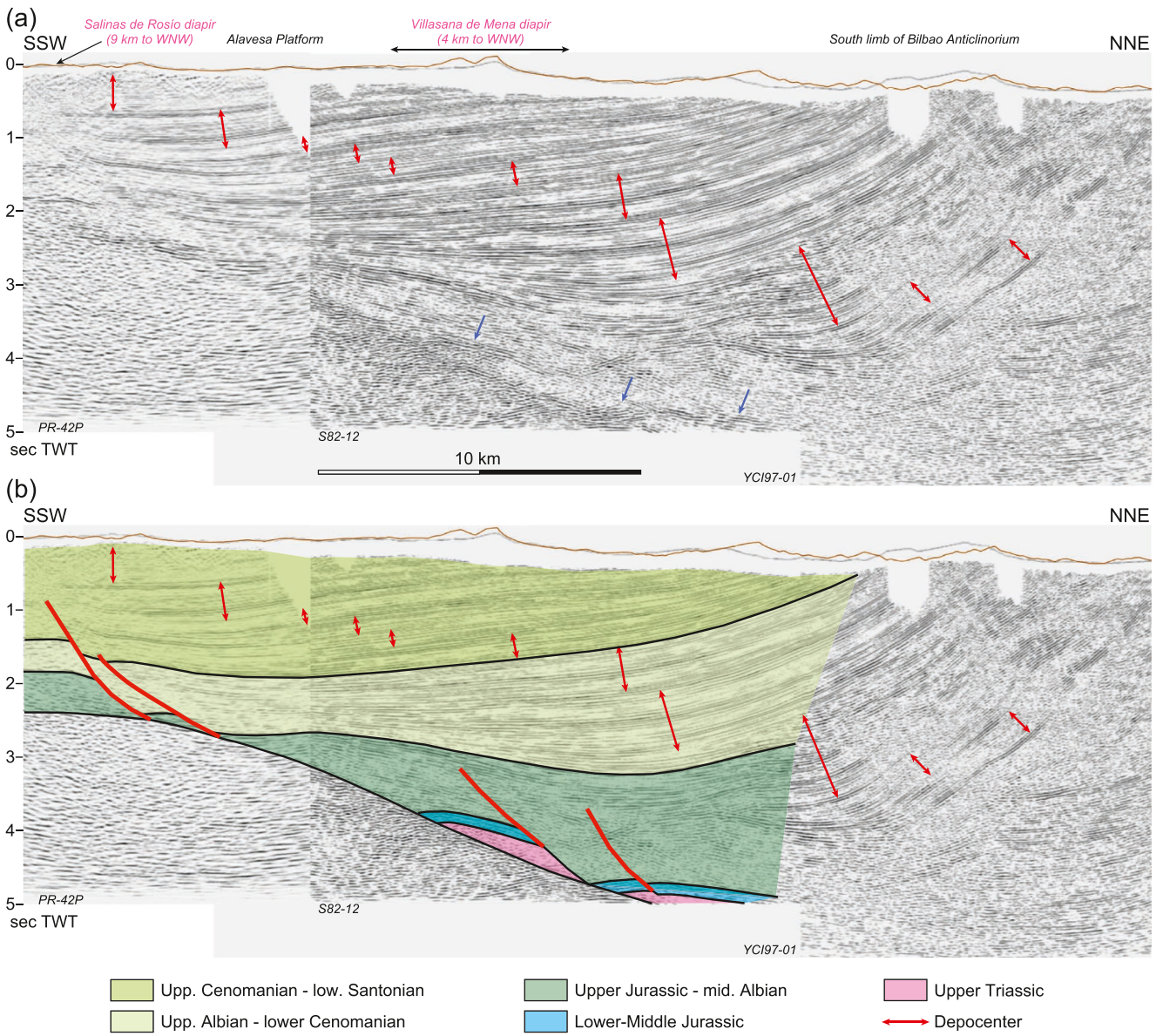

Figure 7. Composite time-migrated seismic profile (lines YCI97-01, S82-12, and PR-42P; courtesy of B. López-Mir) showing the southern limb of the Bilbao anticlinorium and extending past Villasana de Mena diapir to a position along strike from Salinas de Rosío diapir (location shown in Figure 2). (a) Uninterpreted profile: red double-headed arrows indicate landward/southward-shifting depocenters defined purely geometrically; blue arrows highlight a discontinuous package of bright reflections at depth above a basinward-dipping band of reflections. (b) Interpretation of the central to southern portion of the composite profile (the geometries relevant to this paper), where the deep reflections (blue arrows in panel (a)) are identified as extended prekinematic Lower-Middle Jurassic strata beneath synrift growth strata, with ages of the latter adopted from Pedrera et al. (2021). The profile is at approximately 1:1 scale assuming an average velocity of 4,600 m/s.

encountering any Lower-Middle Jurassic strata. The well likely drilled a location equivalent to one of the gaps in the probable prekinematic blocks on Figure 7. According to seismic data (Figure 9b and regional correlations), the salt at the base of the well is the top of a thick pedestal. Moreover, there are very different minibasin geometries on the two flanks of the diapir: whereas synrift strata in the western minibasin thin toward the salt; those in the eastern minibasin thicken somewhat into the diapir (Figure 9b, yellow arrows).

3.5. Alavesa Platform

The area between Villasana de Mena and Salinas de Rosío diapirs forms the western end of the WNW-ESE trending Alavesa Platform (Figure 2). At the surface, mostly postrift Upper Cretaceous strata are

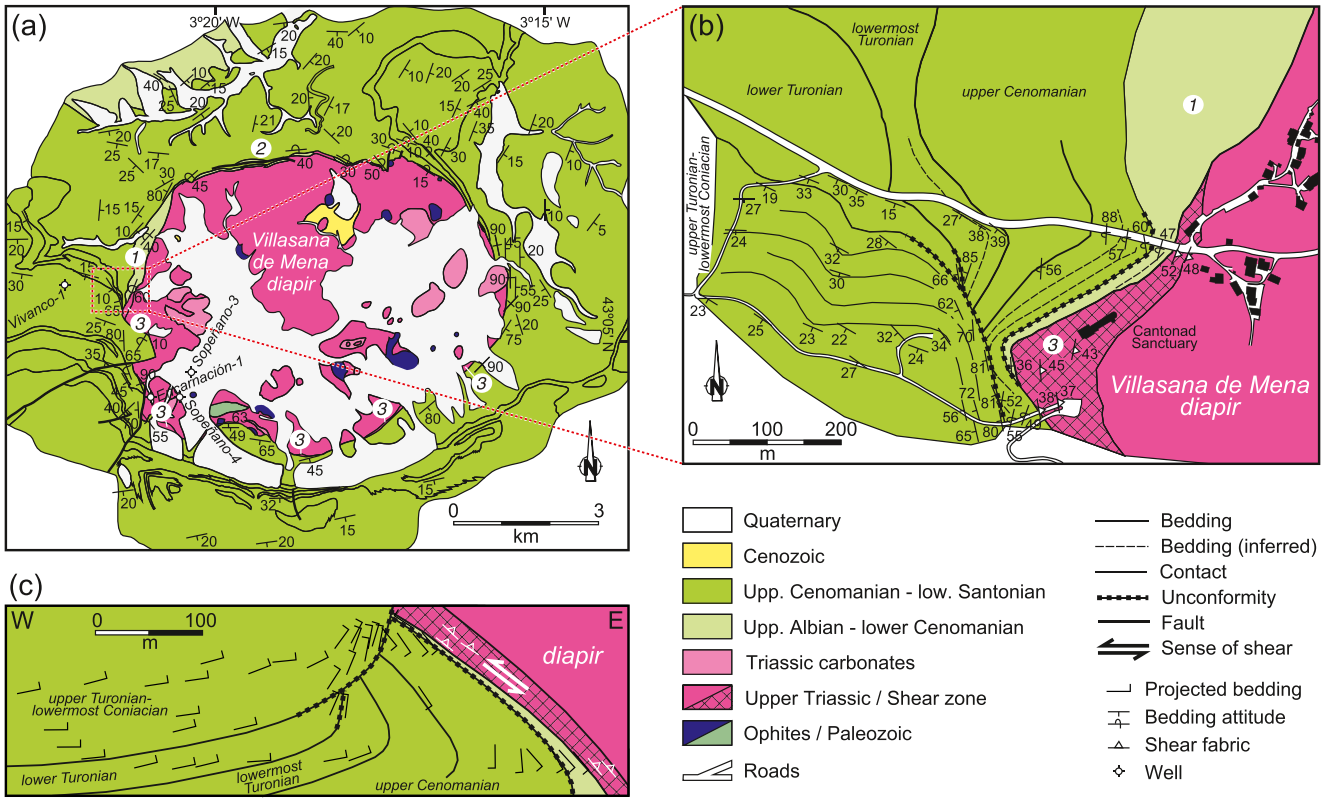

Figure 8. Surface observations at Villasana de Mena diapir: (a) geologic map (location shown in Figure 2); (b) detailed map of part of the western flank of the diapir (location in panel (a)); (c) data in panel (b) projected orthogonally onto a plane striking 100° and dipping to the north 70°, that is, perpendicular to regional bedding away from the diapir (projected using Move™). Numbers in circles indicate features discussed in the text.

subhorizontal, with maximum dips of 10° to the south, over a N-S distance of about 20 km. With increasing depth, the strata gradually dip slightly more toward the south, then flatten before reversing to slight northward dips (Figure 7), thereby representing a continuation of the landward-shifting depocenters on the southern limb of the Bilbao Anticlinorium.

3.6. Salinas de Rosío diapir

Salinas de Rosío diapir is located at the hinge between the subhorizontal Alavesa Platform and the south-dipping northern limb of the Villarcayo Syncline (Figures 2 and 3a), along the S-vergent La Hoz anticline (Hernaiz Huerta & Solé Pont, 2000). This location also marks the southern end of the landward-shifting depocenters of the Alavesa Platform and southern limb of the Bilbao Anticlinorium (Figure 7). Passive diapirism has been interpreted to have occurred during rifting (Belenguer Oliver, 2017) or as late as the Cenozoic orogeny (Hernaiz Huerta & Solé Pont, 2000).

Salinas de Rosío diapir has a distinctive shape in map view, comprising two elongate components at high angles to each other (Figure 10a): (a) a 9 km long segment trending roughly E-W, aligned with the regional strike direction; and (b) a 6.5 km long segment trending NNW-SSE, slightly oblique to the regional dip direction. The E-W segment is exposed in the core of a doubly-plunging, south-vergent asymmetric anticline (Figures 10a and 10b). At the eastern end of the diapir (Figure 10a, location ***1***), Upper Jurassic prerift and Lower Cretaceous synrift strata dip moderately to the east and are bounded by: (a) the diapir to the west and southwest; (b) an extensional fault with juxtaposed Maastrichtian strata to the north; and (c) an unconformity at the base of the upper Albian to the east (Figure 10e). Note that there is also an unconformity at the base of the synrift, with the Berriasian locally lying directly on salt (Figure 10a, location ***2***). This entire E-plunging panel is bounded on its southern side by some small, E-W trending faults. At the western end of the diapir (Figure 10a, location ***3***, Figure 10e), moderately west-dipping upper Albian to lower Cenomanian strata unconformably overlie the Triassic salt, with bedding parallel to the diapir edge. These strata are bounded to the north and south by steep, E-W trending extensional

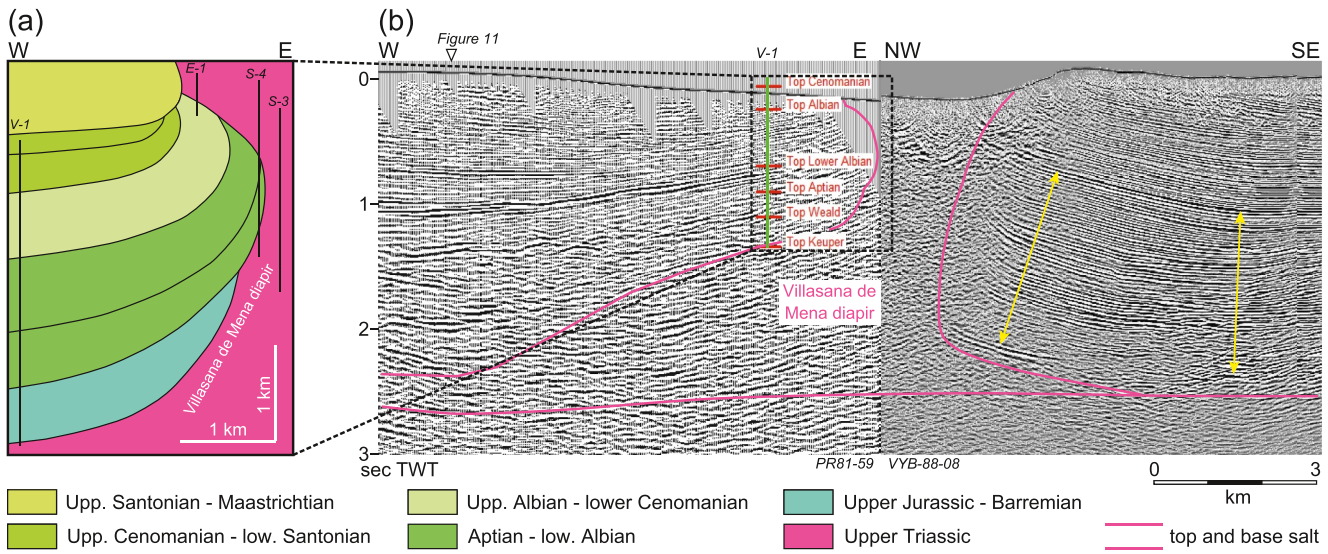

Figure 9. Subsurface observations at Villasana de Mena diapir: (a) well-tie cross section trending E-W across the western side of the diapir (no vertical exaggeration, wells shown in Figure 8a), with wells projected taking into account the regional northward dip and the NE-trending extensional fault south of the Vivanco-1 well (well data from Lanaja, 1987); (b) composite time-migrated, strike-oriented seismic profile (lines VYB-88-08 and PR81-59) across the diapir (location shown in Figure 2) with only the salt (pink lines) interpreted. V-1, E-1, S-3, and S-4 indicate, respectively, the Vivanco-1, Encarnacion-1, Sopeñano-3, and Sopeñano-4 wells; the yellow arrows highlight slight thickening of synrift strata toward the diapir; note that the prekinematic Lower-Middle Jurassic section is absent in Vivanco-1 even though it reached the Triassic salt at depth. The profile is at approximately 1:1 scale assuming an average velocity of 4,600 m/s; the triangle above the line shows the intersection with the seismic profile of Figure 11.

faults that die out or are truncated upward in upper Cenomanian to lower Coniacian (postrift) units. The northern faults on both ends of the diapir are coincident with the northern edge of the diapir, which is flanked by upper Albian to Maastrichtian strata, and are part of the system that connects to Villasana de Mena diapir (Figure 2). The hanging wall of this fault-diapir-fault system at Salinas de Rosío has a structural culmination south of the Ribero-1 well, with strata dipping away along strike to both the west and east. According to Hernaiz Huerta and Solé Pont (2000), the displacement on the fault system increases with depth, with the Lower Cretaceous interval much thicker on the northern side.

In contrast to the E-W segment of the diapir, the N-S segment is surrounded only by lower-to middle-Miocene syn- to post-orogenic clastics (Figure 10a). The salt truncates the Miocene strata along its eastern and western contacts and has been interpreted as a salt tongue (Figure 10d; Belenguer Oliver, 2017; Hernaiz Huerta & Solé Pont, 2000). The subsalt strata, along with those flanking the southern edge of the E-W segment of Salinas de Rosío diapir, comprise part of the southern limb of La Hoz anticline. These Miocene clastics form a growth wedge with conglomerates adjacent to the salt but sandstones and mudstones farther away (Figures 10a, 10c, and 10d); the conglomerates include clasts of both Cretaceous shallow-water carbonates and Keuper lithologies (e.g., ophites).

Like Villasana de Mena diapir, Salinas de Rosío diapir contains clasts mostly of ophites and Triassic carbonates, but also a single instance each of Miocene and Paleozoic clasts plus several blocks of upper Albian to lower Cenomanian rocks. Interestingly, the distribution of intrasalt clasts differs between the two segments of Salinas de Rosío diapir: whereas Triassic carbonate clasts are confined to the E-W segment, ophite clasts are almost exclusively found in the N-S salt tongue (Figure 10a).

In contrast to Bakio and Villasana de Mena diapirs, where all the flanking strata turn up and thin within 500 and 200 m, respectively, of the diapirs, exposed strata around Salinas de Rosío diapir have widely varying relationships to the salt. First, Jurassic strata next to the salt on the eastern flank dip away from the diapir slightly less than more outboard Berriasian strata, with the two separated by an angular unconformity (Figure 10a, location ***1***, Figure 10e). Second, Cretaceous strata north of the diapir have orientations that change dramatically from east to west: (a) a thin sliver of steeply-dipping Lower Cretaceous rocks unconformably overlain by Maastrichtian strata that dip slightly toward the salt (Figure 10a, location ***4***); (b) Maastrichtian limestones dipping 70° to the south (into the salt) and unconformably overlying older Upper Cretaceous strata (Figure 10a, location ***5***)

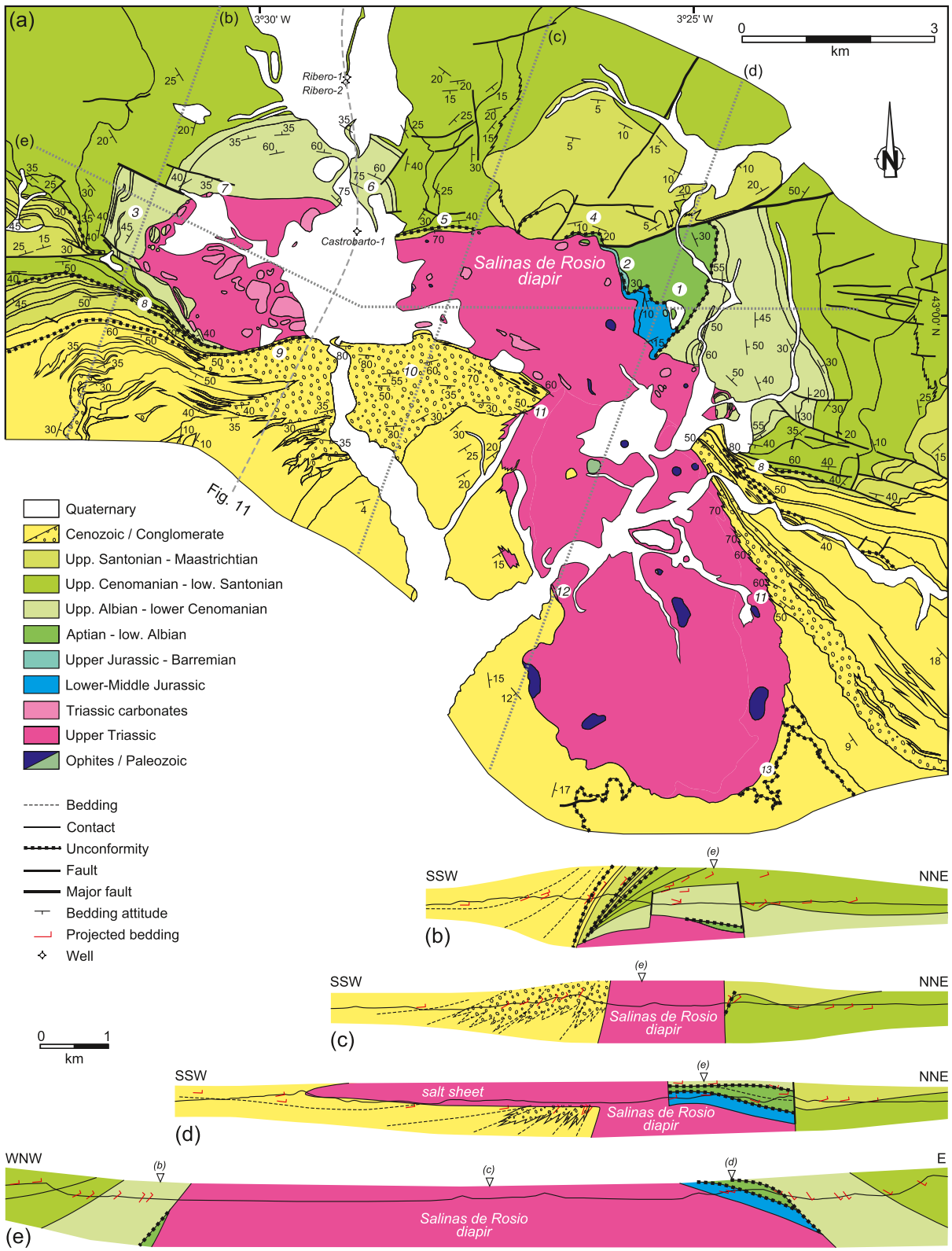

Figure 10. Surface observations at Salinas de Rosío diapir: (a) geologic map (location shown in Figure 2); (b–e) cross sections (locations shown on map; data projected using Move™). Numbers in circles indicate features discussed in the text.

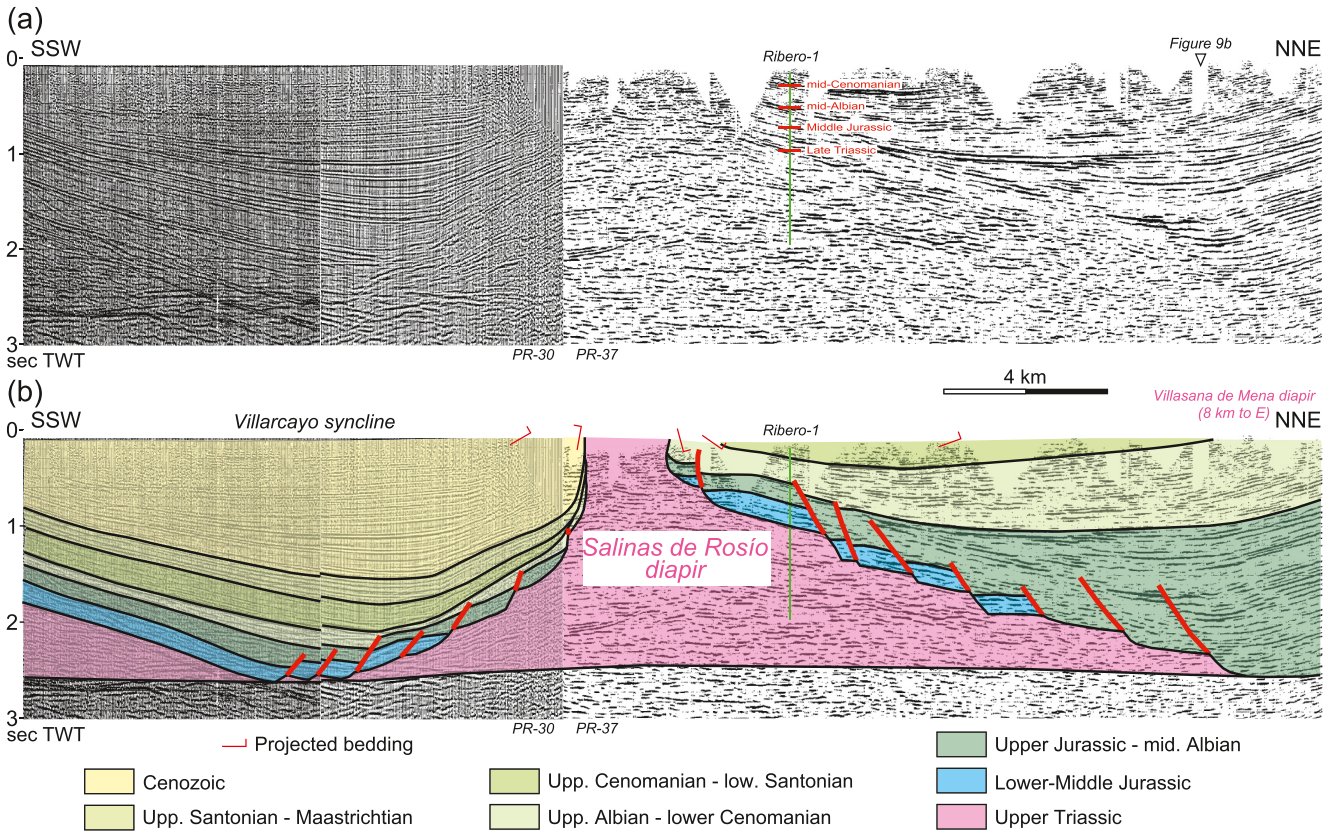

Figure 11. 2-D, time-migrated composite seismic profile (lines PR-37 and PR-30) across Salinas de Rosío diapir (location shown on Figures 2 and 10a): (a) uninterpreted; (b) interpreted (constrained by both surface outcrops and well-tie seismic correlations). The interpreted gaps in the prekinematic Lower-Middle Jurassic sequence are based on nearby wells and the local absence of the bright reflection package that ties to this interval in the Ribero-1 well. The profile is at approximately 1:1 scale assuming an average velocity of 4,600 m/s, and the plotted bedding attitudes are at 1:1 scale. The triangle above the line in panel (a) shows the intersection with the seismic profile of Figure 9b. Note that well tops for the Ribero-1 well have been removed in panel (b) for clarity.

that form a series of short-wavelength folds (Figure 10c); (c) upper Albian and younger units dipping steeply to moderately away from the diapir (Figure 10a, location ***6***); and (d) upper Albian to Upper Cretaceous strata in a series of short-wavelength folds with moderate dips (Figure 10a, location ***7***) that continue to the west in the hanging wall of a steep fault (Figure 10b). Third, Upper Cretaceous to Paleogene postrift and synorogenic strata on both the southwestern and southeastern sides of the diapir thin toward the salt over a distance of several km, are folded to steep southerly dips, and contain several near-diapir unconformities (Figure 10a, locations ***8***, Figure 10b); the oldest is at the base of Campanian calcarenites and the youngest is at the base of the Miocene, with no preserved upper Eocene to Oligocene strata. Fourth, the western third of the southern edge of the E-W segment is flanked by thin, concordant Paleocene carbonates unconformably overlain by Miocene conglomerates (Figure 10a, location ***9***). Fifth, the Miocene synorogenic clastics increase in dip toward the diapir within 700 m of the salt-sediment interface (Figure 10a, location ***10***). Sixth, the same Miocene strata abut directly against the western and eastern edges of the N-S segment, without any thinning or upturn (Figure 10a, locations ***11***). Seventh, along the western edge of the tongue is a locally 10 m thick breccia containing mostly clasts of Keuper lithologies with rare and small pieces of Miocene rocks (Figure 10a, location ***12***); it appears to be cut by a low-angle, S-vergent thrust fault but contains no internal shear zones or other small-scale structures. Finally, the middle Miocene at the southeastern tip of the N-S segment folds from subhorizontal to near-vertical within 20 m of the salt (Figure 10a, location ***13***).

Seismic data (Figure 11) confirm that the exposed Salinas de Rosío diapir is at the crest of the large, S-vergent, salt-cored La Hoz anticline (Belenguer Oliver, 2017; Hernaiz Huerta & Solé Pont, 2000). The Ribero-1 well, on the northern flank of Salinas de Rosío diapir (Figure 11a), drilled over 2,600 m of Keuper halite, anhydrite, dolomite, and shale (Lanaja, 1987). The well penetrated apparent Buntsandstein siliciclastics at 4,150 m below

the surface (at the bottom of the green wellbore in Figure 11), leading some (Cámara, 2017; Hernaiz Huerta & Solé Pont, 2000) to suggest that basement was abnormally shallow in this area. However, the well data show that there is abundant anhydrite and halite intermixed with the siliciclastics, suggesting that this section may be part of a layered evaporite sequence rather than strata beneath the salt. One prominent feature of the seismic data, as constrained by well ties, is the difference in the minibasins on either side of the diapir (Figure 11). Whereas the minibasin to the north, which forms the western end of the Alavesa Platform (Figure 2), has thick, gently-dipping synrift strata that thin toward the anticline, the southern minibasin (Villarcayo Syncline) has a very thin synrift section, with steeper dips adjacent to the salt, and is filled predominantly with Neogene synorogenic strata that thicken into the core of the syncline. The prekinematic and synrift sequences in both minibasins are interpreted to be cut by numerous small extensional faults, and the Lower-Middle Jurassic prerift section is shown as missing in some locations above the Upper Triassic salt based on the apparent absence of the higher-amplitude reflections characteristic of this unit.

3.7. Villarcayo Syncline and Oña/Tudanca Anticlines

The Villarcayo Syncline is a 15 km wide, south-vergent structure cored by Cenozoic synorogenic strata (Figures 2 and 3) and involving a thin Mesozoic succession as mentioned above (Figure 11). Farther south, a system of salt-cored anticlines with relatively short wavelength involves an even thinner Mesozoic cover comprising a thin synrift succession that directly overlies the Triassic salt or a reduced Jurassic series (as observed at the surface and seen in exploration wells such as the Navajo-1 well; Lanaja, 1987). These folds developed during the Paleogene and Neogene, as revealed by synorogenic strata preserved in the cores of the synclines, and are part of the hanging wall of the Cantabria-Montes Obarenes thrust, which represents the frontal thrust of the Basque-Cantabrian Pyrenees farther to the east (Figure 2).

3.8. Poza de la Sal diapir

Poza de la Sal diapir is a domal structure located along the northeastern margin of the Burgalesa Platform (Figure 2) at the corner between the SE-vergent Hontomin anticline and the NE-vergent Villalta anticline (Figure 12), both with synorogenic Cenozoic growth strata. The latter anticline is in the hanging wall of a SW-dipping thrust fault that repeats Upper Triassic salt to Lower Cretaceous strata, with some of the shortening occurring during the synrift Early Cretaceous (Carola et al., 2015). In plan view, the diapir is approximately 5 by 3 km in size, thus having an axial ratio of 1.7 elongated in a WNW-ESE direction (Figure 12). Different interpretations of its origin have been proposed: (a) that it broke through a thick roof along two lines of weakness, specifically radial faults (Hempel, 1967); (b) that salt movement was triggered during extension, with inflation due to differential loading, erosion and burial, and breakthrough during Pyrenean shortening (Klimowitz et al., 1999; Mas Tudó, 2011; Quintà et al., 2012); or (c) that it formed in a small pull-apart basin during strike-slip movement (Tavani et al., 2011).

At the surface, the diapir comprises mostly typical Keuper gypsum and red mudstones, along with ophite clasts and one carbonate clast. It is flanked by faulted strata that dip (up to 90° and slightly overturned on the SE side) and young away from the diapir in all directions (Figures 12a–12c). The faults have generally radial orientations and die out up-section away from the diapir. The salt-sediment interface is conformable on the SW and NE sides, with uppermost Triassic to lowermost Jurassic strata adjacent to the salt (Figure 12a, areas ***A*** and ***E–F***, Figure 12b). In contrast, in two fault-bounded compartments on the NW and SE sides (Figure 12a, area ***D*** and ***G–H***, Figure 12c), strata adjacent to the salt are mostly late Albian in age but are as young as Coniacian along the southeastern edge (area ***G***). Four unconformities are identified near the diapir. The first is the regional base-upper Albian unconformity (García-Mondéjar et al., 2004), with highly variable missing section around the diapir (Figure 12d). The second occurs at the base of the Coniacian only on the SE side of the diapir (Figure 12a, locations ***I***), where it is slightly angular (<10°; Figure 12b) and locally cuts out upper Albian to Turonian strata. The youngest two, located on the SE and NE flanks, are synorogenic and separate Oligocene strata from underlying upper Santonian to Campanian units and overlying Miocene rocks.

The seismic data show that the subsurface part of Poza de la Sal diapir, like that of Salinas de Rosío diapir, forms a large domal structure with a concordant and conformable Upper Jurassic section except at its crest (Figures 13a and 13b). The dome is broadly symmetric in this orientation, which crosses the two orthogonal contractional structures somewhat obliquely (Figure 12). The dome is interpreted to be cut by a small thrust fault on the

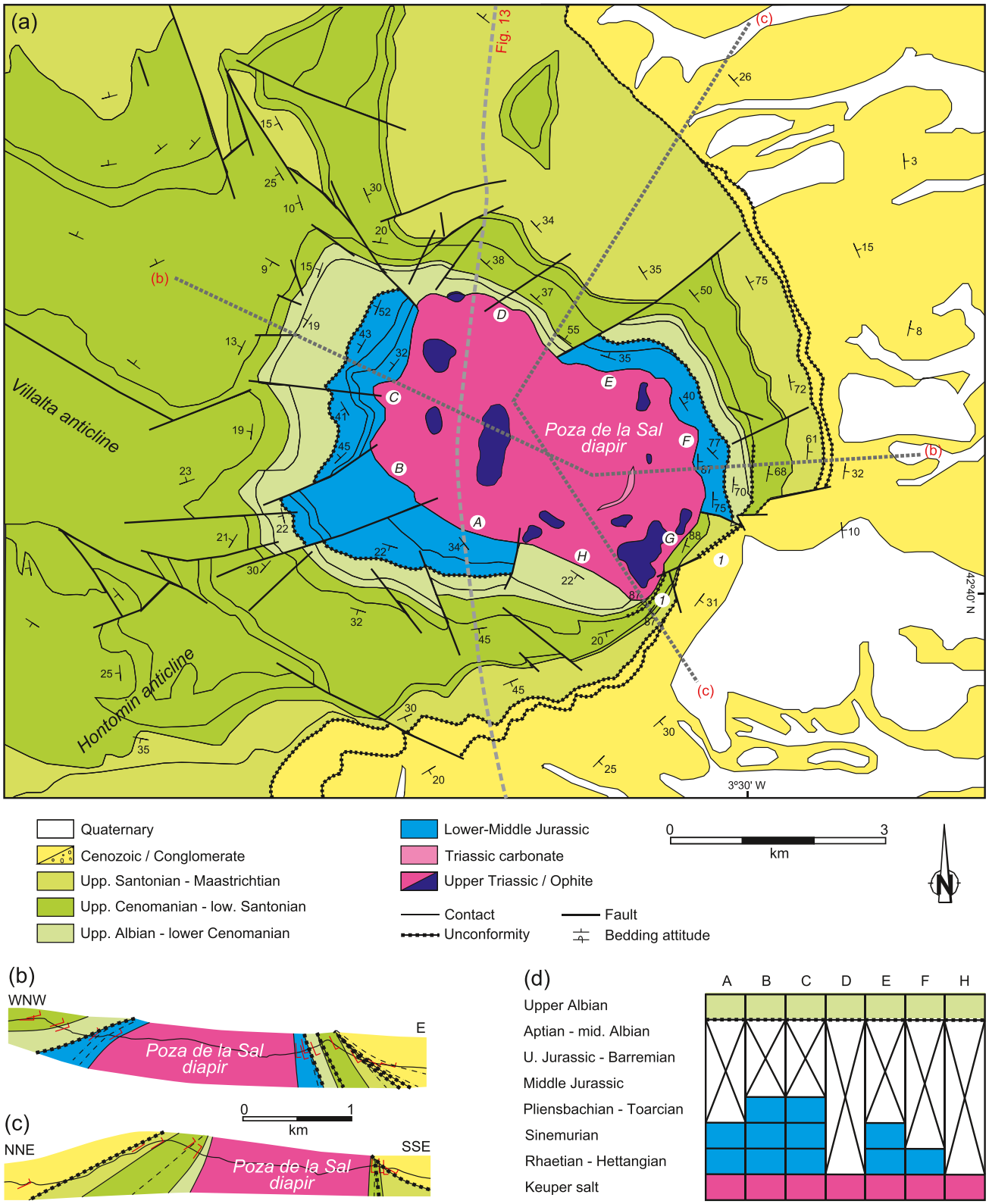

Figure 12. Surface observations at Poza de la Sal diapir: (a) geologic map (incorporating some data from Mas Tudó, 2011; Quintà et al., 2012; see Figure 2 for location); (b, c) local cross sections showing diapir-flanking stratal geometries (locations shown on map; data projected using Move™); (d) chart showing variable amount of missing section at base-upper Albian unconformity in different segments of the diapir margin (age not to scale). Numbers in circles in panel (a) indicate features discussed in the text; letters in circles denote the segments shown in panel (d).

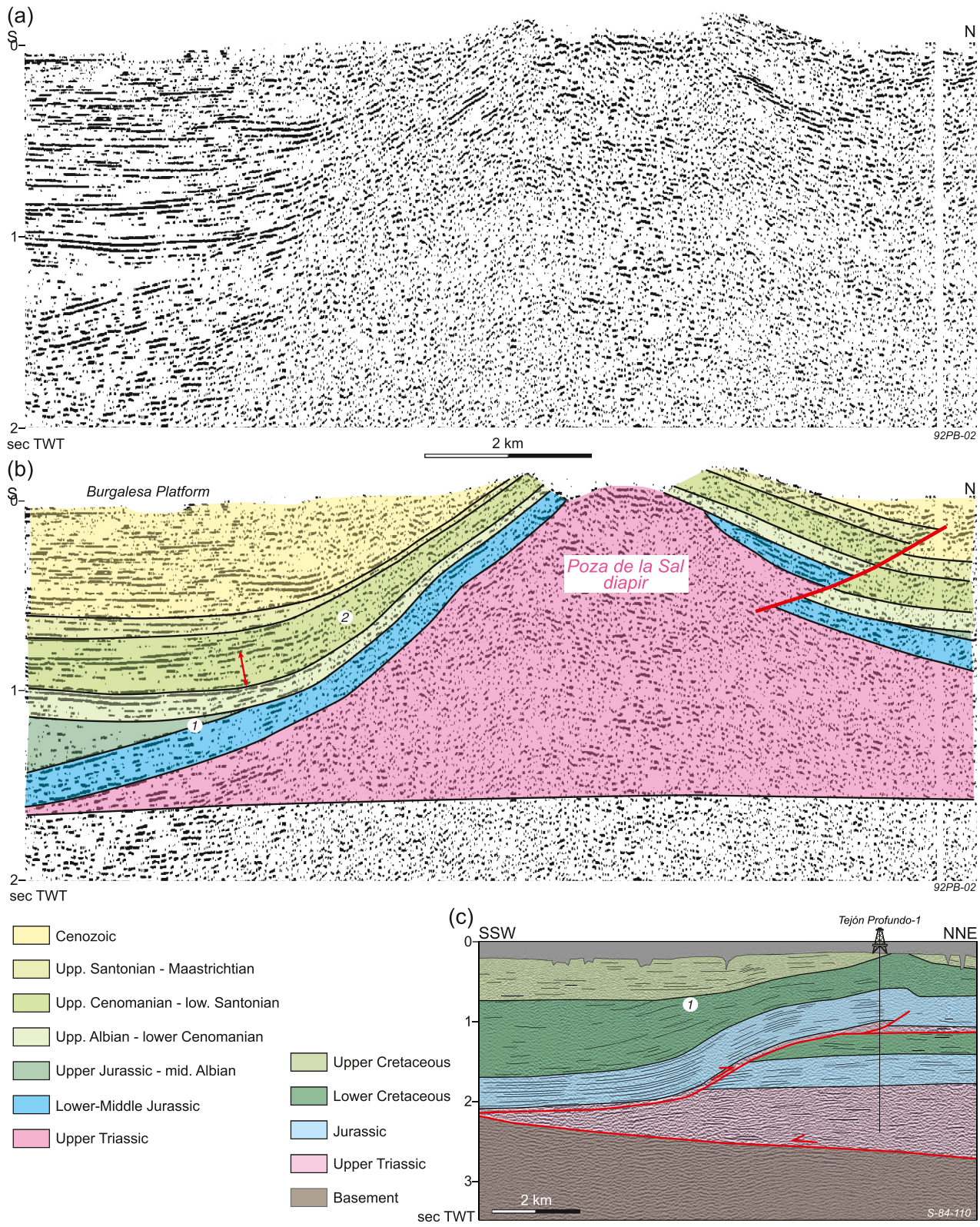

Figure 13.

northern limb (see also Cámara, 2017), presumably an equivalent of the thrust fault penetrated by the Tejón Profundo-1 well 17 km to the west-northwest (Figure 13c) and interpreted on seismic data between the well and the diapir on the Villalta anticline (Carola et al., 2015). Of particular note is the angular relationship at the base of the upper Albian, seen both at Poza de la Sal and along strike (Figure 13b, location ***1***, Figure 13c), interpreted as the middle-late Albian regional unconformity. There is also thinning of the postrift sequence visible at least on the southern limb of the dome (Figure 13b, location ***2***).

3.9. Burgalesa Platform

The Burgalesa Platform (Figures 2 and 3) is similar to the Alavesa Platform in that exposed postrift Upper Cretaceous rocks are broadly horizontal. It is bounded on the northeast and southwest by contractional structures, on the northwest by strata plunging off the Asturian Massif, and on the southeast by the contractional Hontomin anticline. Several minor NE-SW trending anticlines or monoclines cut across the platform, including the Hontomín anticline that has Poza de la Sal diapir at its NE end. The Burgalesa Platform is generally accepted to have experienced translation to the southeast during the Pyrenean orogeny, between the Bureba reentrant of the Ebro Basin to the northeast and the Duero basin to the southwest; accordingly, the structures bounding the platform to the southwest (Ubierna fault system) and northeast would have experienced sinistral and dextral displacement, respectively (Carola et al., 2013, 2015; Hernaiz, 1994; Tavani et al., 2011). Some of the wells along the southwestern margin of the platform penetrate either no or only thin parts of the Lower-Middle Jurassic prekinematic section above the salt (Figures 2 and 14).

Although the surface geometry is subhorizontal over most of the Burgalesa Platform, seismic data reveal tilted strata in the subsurface (Malagón et al., 1994). Between the subhorizontal Upper Cretaceous postrift strata and a mostly level Jurassic prerift interval (except for beneath the Villalta anticline) is a series of landward-dipping and -onlapping Lower Cretaceous synrift strata that define southwestward-shifting depocenters with pseudo-sigmoidal geometries (Figure 14). The domain of landward-dipping strata is up to 15 km wide in the dip direction and spans about 35 km along strike (Carola et al., 2015). Tavani et al. (2011) rejected interpretations as S-directed progradational clinoforms, a N-directed extensional rollover, or a S-directed expulsion rollover, and favored instead a slightly shifting drape fold over an underlying basement fault. In contrast, others have interpreted it as an expulsion rollover (Ramos et al., 2022a, 2022b) or as ramp-syncline basins formed by significant thin-skinned basinward translation over a step in the base salt (Carola et al., 2015).

3.10. Folded Band and Montorio Complex

The Folded Band is a domain roughly 10–12 km wide comprising short-wavelength anticlines and SW-vergent thrust faults along the boundary between the Basque-Cantabrian Pyrenees and the Duero Basin (Figures 2, 3, and 15). It is separated from the Burgalesa Platform by the Ubierna fault system, which had extensional displacement during rifting, as demonstrated by significant thickening of the Lower Cretaceous interval on its northern side (Figure 15b), but experienced dextral inversion during the Pyrenean Orogeny (Hernaiz, 1994; Tavani et al., 2011). In the vicinity of the transect, down-dropped and tilted Miocene rocks occur above an unconformity between strands of the fault system (Figures 15a and 15b, locations ***1***) and attest to a component of transtension, possibly in a releasing bend, during the latest stages of movement.

Salt bodies take several forms in what we term the Montorio complex (Figure 15b). First, Keuper salt occurs in the core of a NE-SW trending anticline flanked mostly by conformable and concordant uppermost Triassic and Jurassic strata (Figure 15a, location ***2***). On its NW edge, however, is a small extensional fault with prekinematic Rhaetian to Sinemurian strata, growth strata of Pliensbachian-Toarcian (Early Jurassic) age, and locally postkinematic Dogger strata (Figure 15a, location ***3***). Second, salt occurs in the hanging wall of a thrust fault, again with conformable and concordant uppermost Triassic and Lower Jurassic rocks (Figures 15a and 15b, locations ***4***). These are both simple contractional structures with the Upper Triassic salt in its normal, autochthonous

Figure 13. 2-D, time-migrated seismic profiles across the northeastern edge of the Burgalesa Platform: (a) uninterpreted and (b) interpreted versions of a line (92PB-02) over Poza de la Sal diapir (location shown in Figures 2 and 12a, interpretation constrained by both surface outcrops and well-tie seismic correlations, approximately 1:1 scale assuming an average velocity of 4,600 m/s); (c) geo-seismic line through the Tejón Profundo-1 well, located 17 km to the NW across the Huidobro anticline (location shown in Figure 2; modified from Carola et al., 2015). Numbers in circles in panels (b, c) indicate features discussed in the text. The red double-headed arrow in panel (b) highlights a local subtle depocenter in the oldest postrift strata.

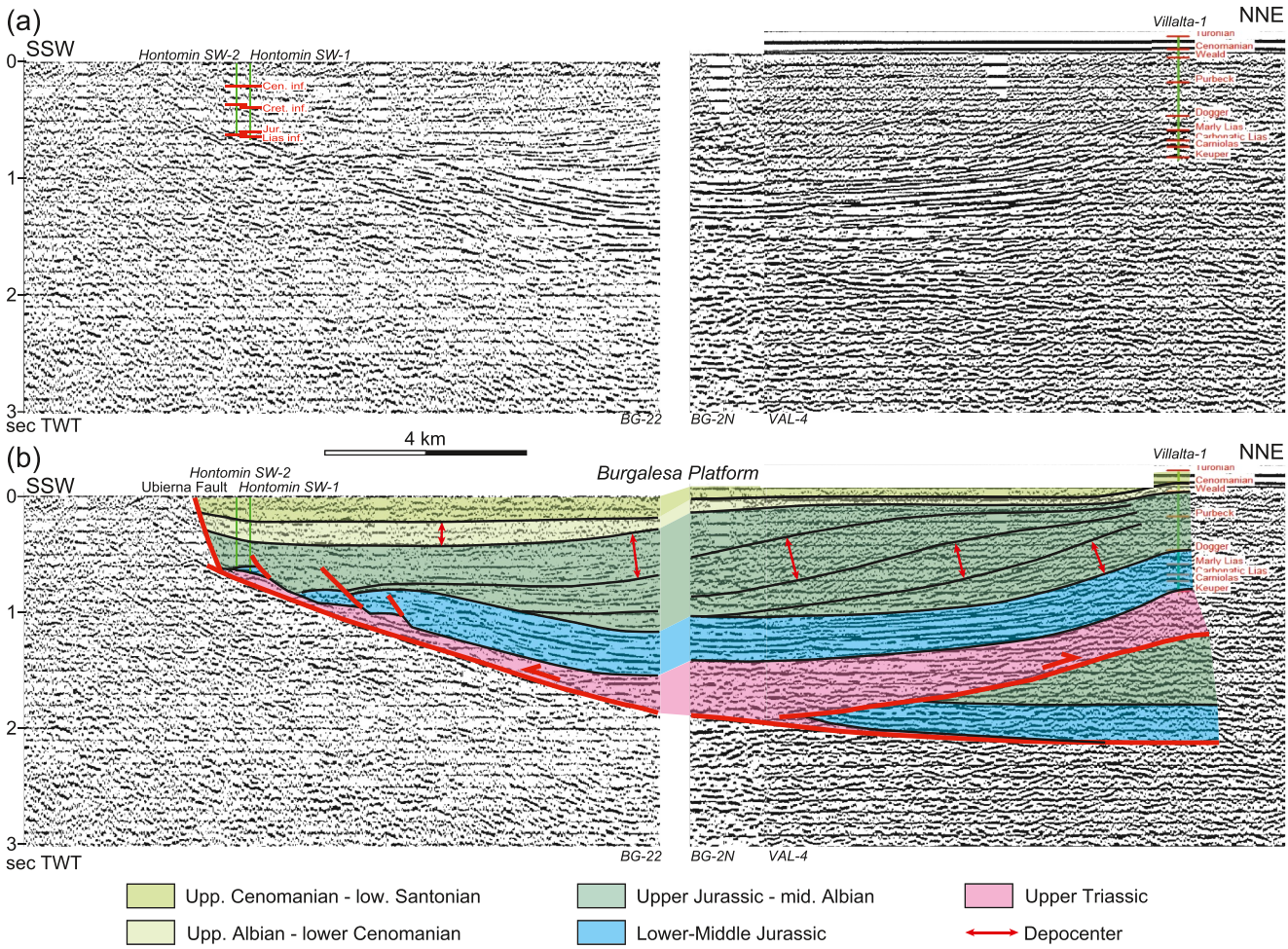

Figure 14. 2-D, time-migrated composite seismic profile (lines VAL-4, BG-2N, and BG-22) showing key features of the Burgalesa Platform (location indicated in Figure 2): (a) uninterpreted; (b) interpreted (constrained by both surface outcrops and well-tie seismic correlations). The profile is at approximately 1:1 scale assuming an average velocity of 4,600 m/s. The thrust fault beneath the Villalta anticline is adopted from Carola et al. (2015). Note that well tops for the Hontomin SW wells have been removed in panel (b) for clarity. The red double-headed arrows indicate landward/southward-shifting depocenters in synrift strata, and the profile has not been interpreted in the footwall of the Ubierna Fault.

position beneath mostly prekinematic Lower-Middle Jurassic strata. Third, an elongate band of Keuper rocks is found along the SW side of the Ubierna fault system over a distance of ~11 km (Figures 15a and 15b, locations ***5***). It is flanked on its SW side by upper Albian to lower Cenomanian rocks, although the contact and exact relationship is obscured by Quaternary fill. Finally, there is a local steep weld along the Ubierna fault system marked by a thin zone of Keuper facies (Figures 15a and 15b, locations ***6***). The weld separates low-dipping upper Albian rocks on the NE side from upper Cenomanian (postrift) strata on the SW side that form a small growth wedge with local upturn of bedding that decreases upward (Figure 15c).

3.11. Summary

The salt-related structures along the transect across the Basque-Cantabrian Pyrenees vary widely in several respects. First, the diapirs display a surprising range of relationships with surrounding strata that is not just a matter of exposure level. Second, they have varying plan-view geometries and structural positions within the orogenic belt. The Montorio and Sopelana welds are squeezed diapirs along complex zones of contractional deformation, but their full lateral extent is unclear. Poza de la Sal and Salinas de Rosío diapirs are associated with contractional anticlines, but whereas the main body of Salinas de Rosío is elongate along a faulted anticline, Poza de la Sal is more circular at the intersection of two nearly perpendicular contractional structures. Bakio diapir is also

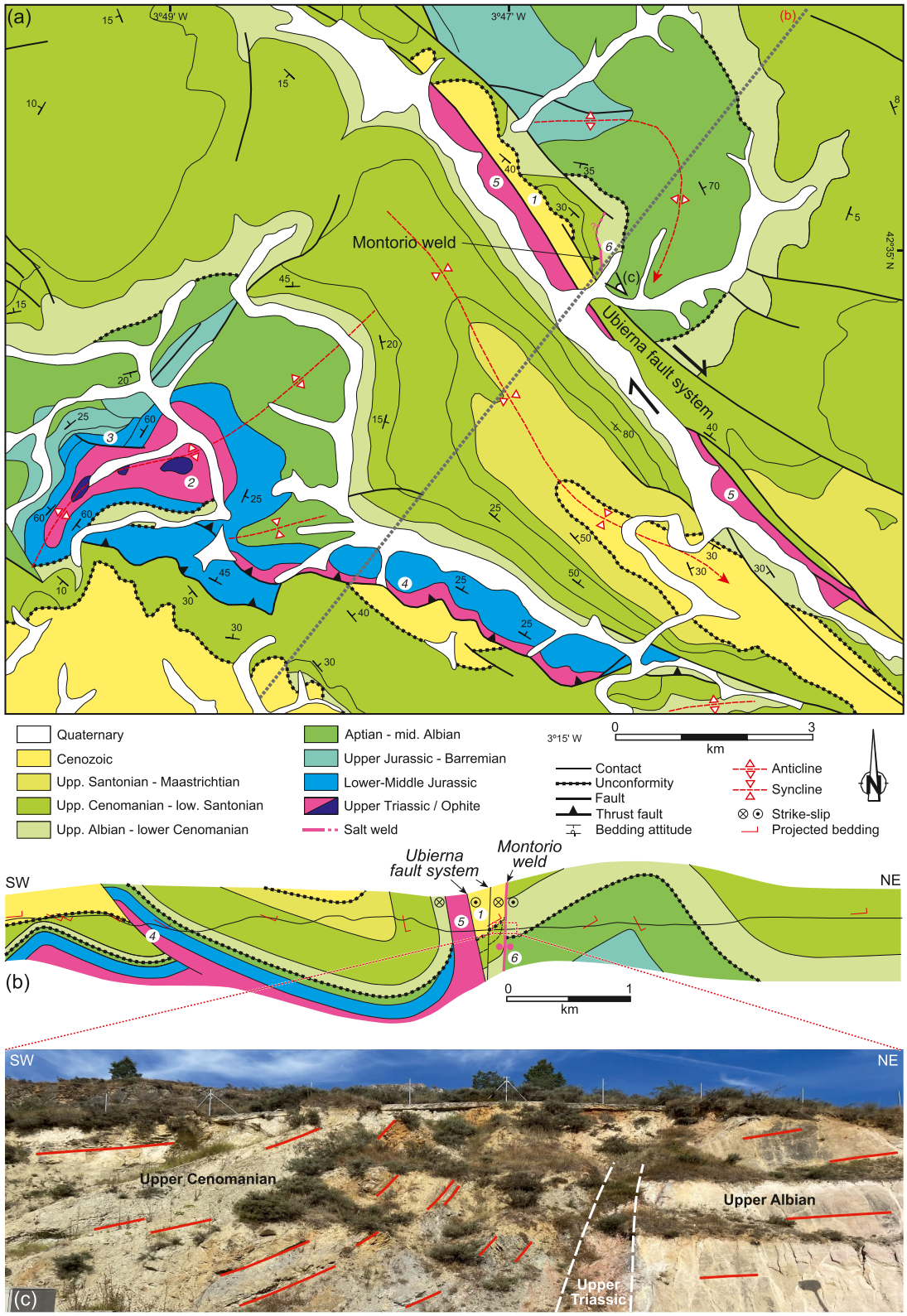

Figure 15.

elongate, but at an angle that is highly oblique to most of the folds and thrusts. The most anomalous diapir in this sense is Villasana de Mena, which is a nearly circular stock with no contractional structures in surrounding strata.

The relationships of the diapirs to stratal geometries in the intervening minibasins also vary. Two of the areas, the Burgalesa and Alavesa platforms, have clearly imaged landward-shifting depocenters that have regional extent (Miró et al., 2021, Figure 5), and a similar subsurface geometry has been suggested south of Bakio diapir (Roca et al., 2021). Yet the diapirs have different positions relative to these domains: (a) Bakio, Salinas de Rosío, and the Montorio weld are at the landward ends (Figures 5, 11, and 14); (b) Poza de la Sal is at the basinward end (Figure 14); and (c) Villasana de Mena is within the laterally-shifting depocenters (Figure 7).

4. Interpretation

In this section, we use a combination of the observed surface and subsurface features, cross-section restoration, conceptual models, and global analogs to interpret the salt-related geometries. We first address the internal composition of the diapirs before deciphering the origin and evolution of the different minibasins and diapirs and, in turn, proposing a general model for the salt-involved deformation during both rifting and inversion.

4.1. Salt Composition

Salt diapirs typically comprise a combination of halite, anhydrite, bittern salts, and non-evaporative lithologies such as siliciclastics, carbonates, and even igneous rocks (e.g., Rowan et al., 2019). Moreover, surface exposures are usually caprock assemblages that lack the more soluble evaporites such as halite due to dissolution by meteoric water (e.g., Warren, 2016). The Upper Triassic Keuper salt of the Basque-Cantabrian Pyrenees is no different. Surface exposures are dominated by gypsum and claystones, with subordinate amounts of carbonate and ophites. But wells show that halite is abundant and that gypsum is replaced by anhydrite in the subsurface (Lanaja, 1987). In addition, Hempel (1967) reported that rocksalt (halite) was found just 20–30 m beneath the surface at Poza de la Sal diapir even though none is exposed. Moreover, springs with saline water have been exploited for millennia at Poza de la Sal and Salinas de Rosío.

Clasts of non-evaporite rocks originally interbedded with or intruded into the salt basin are known as stringers and are easy to explain: more competent layers in the layered evaporite sequence get folded and disrupted by boudinage during salt flow into diapirs (e.g., Rowan et al., 2019). This is almost certainly the origin of the ophite stringers. More problematic are clasts of apparent Muschelkalk (middle Triassic) and/or uppermost Triassic (Rhaetian) carbonates in the Keuper evaporites. Some interpretations from this and other basins explain such occurrences of apparent subsalt or overburden strata in diapirs as basal plucking or roof foundering (e.g., Brinkmann & Lögters, 1968; Fernandez et al., 2017; Garrison & McMillan, 1999; Pflug, 1967). However, it is possible that these carbonates are actually Upper Triassic in age, as shown for supposed Muschelkalk carbonates at the western margin of the Basque-Cantabrian Pyrenees (Sopeña et al., 2009), and thus part of the Keuper salt *sensu stricto*. Alternatively, it has been suggested that the "Keuper" salt locally includes older and younger layers, spanning from the upper Buntsandstein to the Hettangian (Serrano & Martínez del Olmo, 1990; Serrano Oñate et al., 1989; see also, e.g., Wicker & Ford, 2021). Interestingly, carbonate stringers are most common in Villasana de Mena and Salinas de Rosío diapirs, in the center of the basin (Figures 8 and 10, respectively), with none identified at Bakio and only one at Poza de la Sal, closer to the basin margins (Figures 5 and 12, respectively). We therefore apply knowledge from the Zechstein salt in northern Europe, where anhydrites and carbonates are predominant in platform areas but halite is more common in more basinal areas (e.g., Clark et al., 1998; Grant et al., 2019; Pichat, 2022). Specifically, we suggest that the upper Buntsandstein to Muschelkalk and Rhaetian to Hettangian sequences had no halite near the margins of the Triassic depositional basin but had halite in the basin center. Thus, whereas the mobile salt comprised only the Keuper evaporites in the southern and northern proximal parts of the Basque-Cantabrian Pyrenees (left arrow in Figure 16), it would have included the underlying Muschelkalk and overlying latest Triassic to earliest Jurassic strata in the area of Villasana de Mena and Salinas

Figure 15. Surface observations at the Montorio complex: (a) geologic map (modified from Pineda Velasco, 1991; see Figure 2 for location); (b) cross section using data projected from out of the plane (location shown on map; data projected using Move™); (c) photo of the Upper Triassic Keuper weld, with upturned and thinned strata on SW side (see (a, b) for location of photo; height of outcrop is ~10 m). Numbers in circles in panel (a) indicate features discussed in the text; strike-slip symbols in panels (a, b) adopt interpretation of Tavani et al. (2011) in which the Ubierna fault system accommodated right-lateral movement during the Pyrenean Orogeny. Note also the large thickness increase of synrift strata across the Ubierna fault zone.

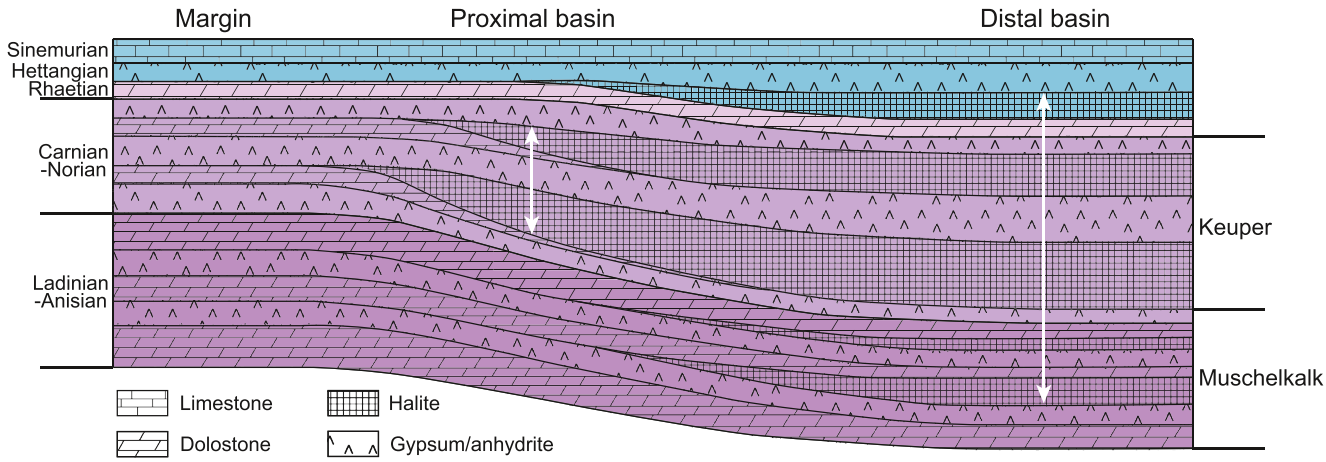

Figure 16. Highly schematic and simplified diagram showing proposed original distribution of different lithologies in the Middle Triassic to Early Jurassic. Note that siliciclastic layers and igneous intrusions or extrusions (ophites), although common in the Keuper, are not included; also, there would have been significantly more complex interbedding of even the lithologies shown. The white arrows denote the portion of the stratigraphy that would have deformed in a ductile manner as "salt" during extension, diapirism, and inversion.

de Rosío diapirs, closer to the basin center (right arrow in Figure 16). The carbonate stringers are simply interpreted as part of a more age-expansive layered evaporite sequence.

The rare Paleozoic, Cretaceous, and Cenozoic clasts are more enigmatic. It is notable that the Paleozoic stringers are observed in Villasana de Mena and Salinas de Rosío diapirs (Figures 8 and 10), where significant expansion of synrift sequences suggests probable involvement of subsalt extensional faults. Thus, rather than plucking by the salt, we favor an origin in which salt deposition accompanied rifting, with footwall basement blocks being eroded and redeposited into the evaporite basin and then subsequently getting disrupted and incorporated into the diapirs. The most likely origin of the younger (Cretaceous and Cenozoic) clasts, given the absence of Late Cretaceous or Cenozoic regional extension and thus associated diapir fall, is that they record halite dissolution and consequent collapse of roof strata into the tops of the diapirs.

4.2. Minibasins

Before addressing the diapirs themselves, it is important to decipher the intervening minibasin geometries for clues into the salt evolution. Synclinal minibasins, such as those to the west and east of Bakio diapir (Roca et al., 2021, Figure 5) or to the south of Salinas de Rosío diapir, likely formed by some combination of extension and salt evacuation, followed by Pyrenean shortening, and will not be examined further. However, those characterized by landward-shifting depocenters (see Miró et al., 2021) are more controversial, and we use the example of the Burgalesa Platform (Figure 14) to explain their development.

Several interpretations are possible. First, the shifting depocenters could represent sedimentary clinoforms related to progradation. However, they downlap in the wrong direction: sediment transport during the Aptian to Albian was generally from south to north (e.g., García-Mondéjar, 1990; Pujalte et al., 1996; Pujalte & Robles, 2008). Second, one might interpret them as extensional rollovers above a décollement, but this would require a detachment at an Upper Jurassic level. No such regional slip surface has ever been identified in the basin, and there is, of course, the very weak Keuper salt detachment just slightly deeper, so this possibility is also rejected. Third, the geometries could represent an expulsion-rollover structure caused by progressive evacuation of salt, whether driven by progradation (Ramos et al., 2022a, 2022b) or not. But such features drive salt generally from more proximal areas to more basinal areas, whether in rifted margins with deepwater deposition such as the northern Gulf of Mexico (Harding et al., 2016; Rowan, 2023; Wu et al., 1990), elongate rift basins with fluvio-deltaic to shallow-water deposition such as the Nordkapp Basin (Hassaan et al., 2021; Rojo et al., 2019; Rowan & Lindsø, 2017), or foreland basins with nonmarine deposition such as the Paradox Basin (Kluth & Duchene, 2009; Paz et al., 2009; Trudgill, 2011). Basinward movement of salt even occurs when sediment distribution is axial (Kluth & Duchene, 2009). Moreover, the salt evacuated from beneath expulsion-rollover structures typically ends up in large salt walls (see examples cited just above). Although salt is locally present along the Ubierna fault

system at the southwestern margin of the Burgalesa Platform, evidence of elongate, long-lived salt walls is absent. In any case, we know of no salt basin in the world where there has been large-scale movement of salt toward the sediment source terrane, as suggested for the Burgalesa Platform by Ramos et al. (2022a, 2022b).

Tavani et al. (2013) rightly pointed out the problems with the three possible interpretations discussed above. They suggested instead that the geometries represent forced (drape) folds due to underlying basement faulting (see also Tavani & Granado, 2015). While a link to underlying faults is valid to a degree, drape folds formed during decoupled thick-skinned extension result in at most only minor lateral shifting of depocenters (e.g., Ferrer, Carola, & McClay, 2023; Stewart et al., 1996; Withjack & Callaway, 2000), not the ~15 km observed in the Burgalesa Platform (Carola et al., 2015). Instead, the geometries are best interpreted as a ramp-syncline basin formed by thin-skinned translation of the salt and overburden above a step in the base salt (e.g., Dooley et al., 2017; Jackson & Hudec, 2005; Pichel et al., 2018), as suggested by Carola et al. (2015). This is shown in a quantitative restoration of the composite seismic profile of Figure 14, where the geometries record 18 km of basinward translation (Figure 17).

The ramp-syncline basin model is compatible with the interpretation of Early Cretaceous (synrift) contraction interpreted from the well and seismic data at the Tejón Profundo-1 location to the north of the landward-shifting depocenters (Figure 13c; Carola et al., 2015) and supported by the distribution and geometries of the prekinematic Lower-Middle Jurassic strata. Wells that penetrated Keuper salt without hitting this sequence have been recognized for decades (see distribution in Figure 2) and interpreted as having formed due to thin-skinned extension (Serrano et al., 1994; Serrano & Martínez del Olmo, 1990). We agree, and interpret a faulted hanging-wall rollover landward of shifting depocenters (Figures 14a and 14b), with the Hontomin SW wells missing the prekinematic section (#2) or just catching the tip of the rollover (#1). A matching footwall is postulated (Figure 17) but is assumed to have been removed by syn- or post-orogenic erosion at the thrust front in the Folded Band.

The landward-shifting depocenters of the Alavesa Platform and southern limb of the Bilbao Anticlinorium (see Miró et al., 2021) have similarly been interpreted as a south-directed expulsion-rollover structure (Pedrera et al., 2017; Ábalos et al., 2008). But for the same reasons cited above for the Burgalesa Platform, we interpret this as another, larger, ramp-syncline basin detached on salt (Figures 7 and 11), with proven gaps in the prekinematic Lower-Middle Jurassic section (Figure 2). Ironically, the southern limb of the Bilbao Anticlinorium has also been identified as being a ramp-syncline basin by Pedrera et al. (2021), but on a *south*-dipping *crustal* detachment with a ramp-flat geometry. They cite forward models in Pichel et al. (2018) in supporting their interpretation, but this is misleading: whereas ramp-syncline basins in the Pichel models of thick salt (see also, e.g., Dooley et al., 2017; Evans et al., 2021; Roma et al., 2018) always shift laterally over time in the direction opposite to overburden translation (i.e., landward), those in the Pedrera model with thick salt shift in the same direction as their proposed translation (Pedrera et al., 2021, Figure 13b). They use a restoration to support their model of thick salt being the differentiating factor, but a careful inspection shows that accommodation for the suprasalt basins is generated not by subsidence into thick salt, but by an artificial thinning of upper crustal blocks bounded by high-angle extensional faults (Pedrera et al., 2021, Figure 9, from steps D to B). In addition, the pattern of shifting depocenters in this area continues well into the postrift section (Figure 7b), implying a thin-skinned, gravity-driven component to the translation that is incompatible with solely basement-involved extensional deformation. Postrift, gravity-driven extension has also been documented in other parts of the southern Pyrenees (López-Mir et al., 2014; McClay et al., 2004; Saura et al., 2016).

The north-dipping band of brighter reflections near the base of the section in Figure 7 was interpreted by Pedrera et al. (2021) as part of a basement hanging-wall rollover on a south-dipping crustal extensional fault. Here, however, it is simply interpreted as the salt detachment. It dips about 20°, but these are time data, so although the scale approximates 1:1, the true present-day dip is unknown. In any case, what was the origin of the northerly dip? Although it could be that the salt is ramping down over one or more basement faults, at least some component of the dip is almost certainly due to a combination of postrift thermal and loading subsidence and later orogenic flexural loading. Thus, the dip at the time of extension is unknown.

4.3. Diapirs

We divide the six diapirs or welds along the transect into three groups. The first comprises the Sopelana and Montorio welds, where there is inadequate information to fully interpret their origins and evolution due to very

10.1029/2025TC008824

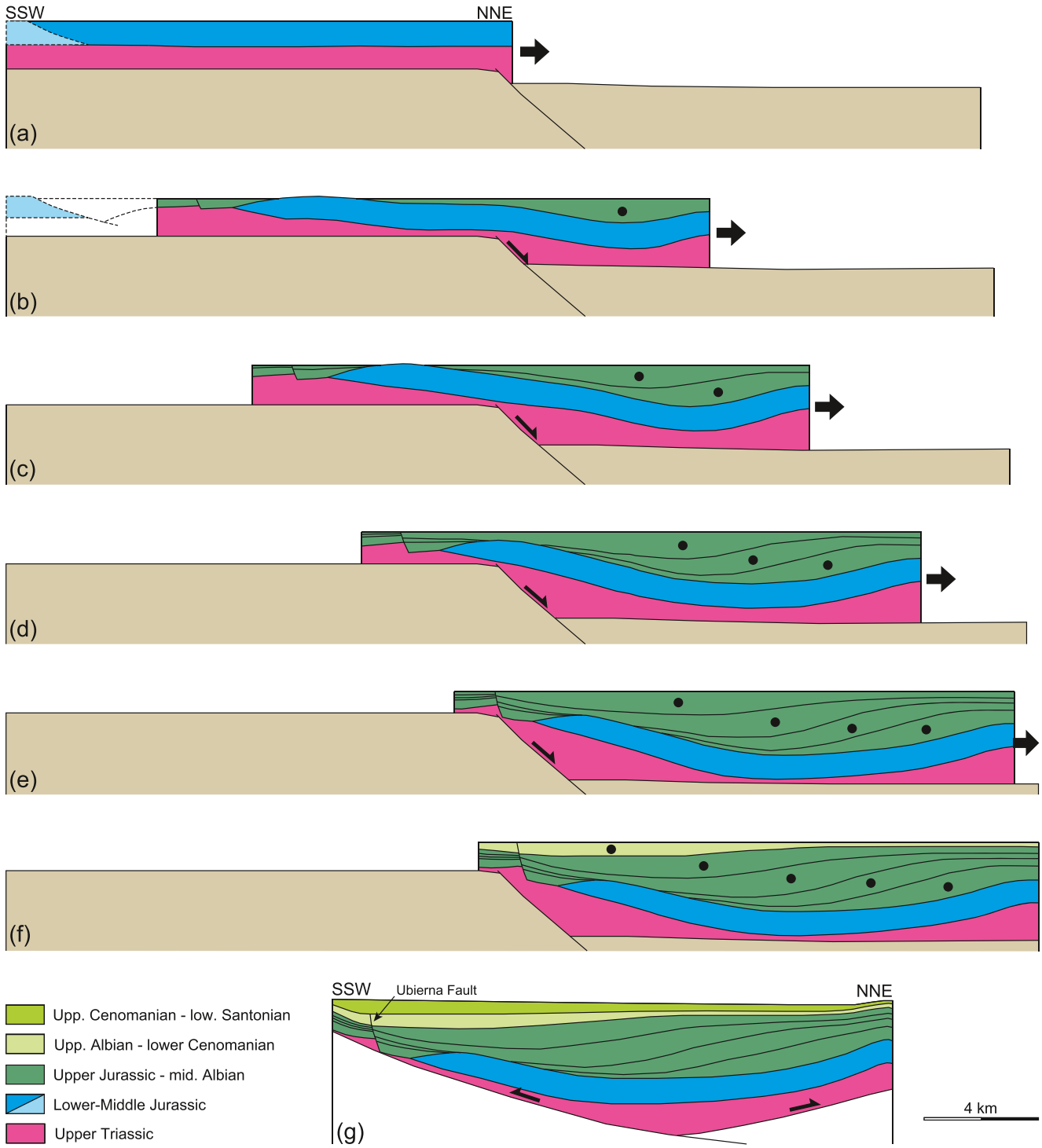

Figure 17. Evolution of the Burgalesa Platform shown by quantitative restoration of seismic profile of Figure 14, simplified in the Jurassic rollover and by ignoring late movement on the Ubierna Fault: (a) prekinematic Lower-Middle Jurassic with future listric fault (hanging wall in dark blue, postulated footwall in light blue); (b) initial stage of decoupled subsalt rifting and suprasalt extension and translation, resulting in first depocenter of ramp-syncline basin (black dot); (c–f) continued subsalt extension and decoupled extension (footwall not shown) and translation recorded by landward-shifting depocenters (black dots); (g) present-day geometry after Pyrenean inversion and thin-skinned thrusting to a position an unknown distance onto the footwall of the basement step of (a–f). Note that salt rollers such as that at the south end of the section could have locally evolved into passive diapirs, as postulated for the Montorio weld. Restoration carried out using StructureSolver™ and a flexural-slip algorithm, without decompaction or isostatic effects. Note that neither the footwall to the thrust fault in panel (g) or the Early Cretaceous shortening along the Villalta thrusted anticline to the NNE is shown. Vertical scale is in time, but set so that the section is at approximately 1:1 scale in depth.

limited exposures and lack of subsurface data. Each is in an area of more intense contractional deformation (the Biscay Synclinorium and Folded Band, respectively), and we infer that preexisting diapirs were squeezed shut during shortening. At Sopelana, the apparent vertical attitude of the weld and the observed moderately-dipping shear zone just south of the weld (Figure 6) suggests that there may be a component of diapir decapitation (see review of decapitation in nature and models in Rowan et al., 2022). At the Montorio weld (Figures 15a and 15b, location ***6***), the growth geometry in upper Cenomanian strata (Figure 15c) is interpreted as a halokinetic sequence (Giles & Rowan, 2012) documenting passive diapirism in the earliest postrift time. Given the location at the landward end of the Burgalesa Platform, it is possible that thin-skinned extension created a salt roller (see Figure 17) and that erosion by the regional mid-late Albian unconformity removed enough roof to initiate passive diapirism. The same might be true for the salt wall along the Ubierna fault, which has near-vertical upper Albian strata adjacent to the salt (Figures 15a and 15b, locations ***5***). It is highly unlikely, however, for two diapirs to initiate and grow within several hundred meters of each other, nor is it likely that one deep root splits upward to feed two shallow diapirs that close together. One possibility is that there was one diapir that collapsed during Neogene transtension, but the upper Cenomanian halokinetic sequence in between the Upper Triassic outcrops makes this problematic. Instead, we suggest that the diapir represented by the Montorio weld was originally located to the NW and moved into proximity of the salt wall during dextral movement on the Ubierna fault system; in other words, the two salt structures that are in close proximity to each other today formed far apart and were juxtaposed during later deformation. Using the current location and the estimated 15 km of strike-slip movement (Tavani et al., 2011), the now-welded Montorio diapir originally would have been positioned approximately 11 km along strike from the NW end of the salt wall that it is currently adjacent to (to the NW of the map in Figure 15a), a much more reasonable scenario.

The second grouping of two diapirs includes the Bakio and Villasana de Mena diapirs. Seismic data show that each is a tall, near-vertical diapir (Roca et al., 2021, Figures 5 and 9, respectively), and each has exposed flanking growth strata (Figures 5b and 8b–8c, respectively) interpreted as halokinetic sequences that record synrift to postrift passive diapirism. Given the ongoing synrift and pre-orogenic near-surface halokinetic growth, we infer that both were triggered by local extension, likely originating as reactive diapirs (whether symmetric or asymmetric) in the Late Jurassic to Early Cretaceous (see also Roca et al., 2021). With enough extension, the salt would have broken through in the active stage to subsequently grow as passive diapirs (see Rowan & Giles, 2021; Vendeville & Jackson, 1992). Interestingly, whereas Bakio diapir is a salt wall with evidence of contractional squeezing despite its oblique orientation, Villasana diapir is a near-circular stock with no evidence of any shortening. We return to this topic in the Discussion.

The final two diapirs, Poza de la Sal and Salinas de Rosío, have more unusual geometries and relationships because, unlike Bakio and Villasana de Mena, each is a local diapir above a larger salt anticline with mostly concordant overburden (Figures 11 and 13, respectively). Beyond that, however, they differ in details, and we address Poza de la Sal diapir first. Key aspects of Poza de la Sal (Figures 12 and 13) are that: (a) it is located near the lateral edge of the basinward end of a ramp-syncline basin; (b) the diapir is located near the termination of a structure with a well-imaged thrust fault that was partly active during the synrift Early Cretaceous; (c) strata that are synrift in age are folded upward and truncated beneath the regional base-upper Albian unconformity; (d) there is a local, low-angle unconformity in early postrift strata that we interpret as a halokinetic sequence boundary; and (e) the diapir is at the center of a domal contractional structure with Cenozoic growth strata. These observations are used to guide a restoration that shows the evolution of the diapir. Initially, the Keuper salt was covered by the prekinematic Lower-Middle Jurassic interval (Figure 18a). Salt inflation during synrift time is interpreted to have been caused by local minor shortening rather than differential loading (Figure 18b). Our reasoning is similar to that of Carola et al. (2015), who noted that the Villalta anticline along strike to the northwest has more thrust offset at the top Jurassic than at the top Lower Cretaceous, and is compatible with the observed Early Cretaceous basinward translation recorded by the ramp-syncline basin (Figure 17). Subsequently, erosion by the base-upper Albian unconformity removed the roof of the salt anticline and thereby initiated passive diapirism (Figure 18c), which continued during postrift time (Figure 18d) as evidenced by both a local halokinetic unconformity and the flanking depocenter in the oldest postrift strata (Figure 13a). Finally, Pyrenean contraction squeezed the salt to create a dome at the intersection of the Villalta anticline and the Hontomin anticline (Figure 18e), the latter formed due to southeastward movement (lateral escape) of the Burgalesa Platform on the Ubierna and other strike-slip faults (Carola et al., 2013; Tavani et al., 2011).

10.1029/2025TC008824

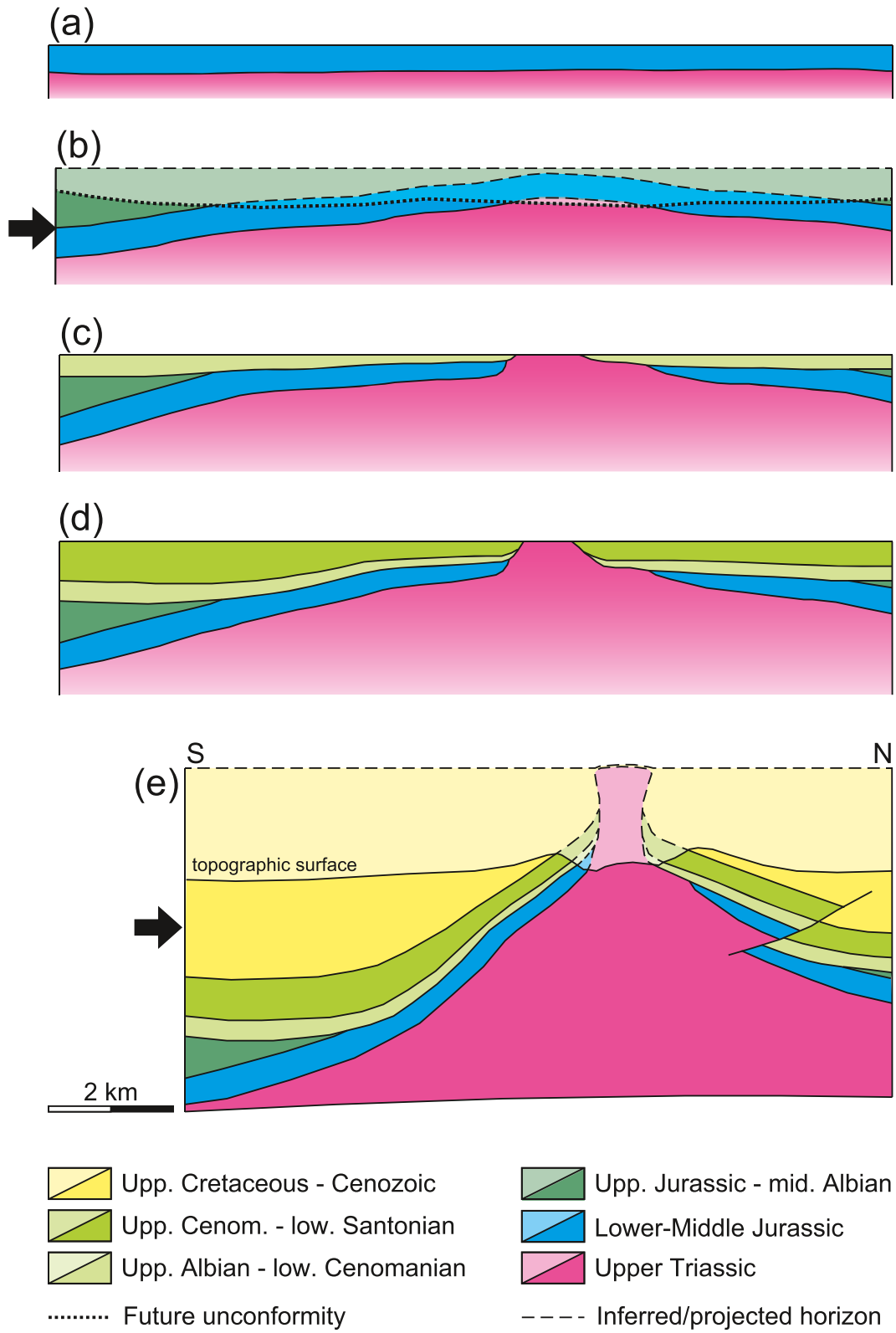

Figure 18.

Similarly, Salinas de Rosío diapir (Figures 10 and 11) has several key attributes: (a) in contrast to Poza de la Sal diapir, it is located at the *land*ward end of a large ramp-syncline basin; (b) the northern minibasin is elevated significantly relative to the much thinner southern minibasin, which comprises mostly Miocene synorogenic fill; (c) the diapir is along a contractional anticline, but the steep faults at both ends of the diapir have extensional origins; (d) there was periodic erosional removal of material over the salt high during both extension and contraction; (e) postrift to early synorogenic strata thin over a distance of several kilometers onto and over the diapir on its western and eastern ends; and (f) the same strata display short-wavelength folds just to the north of the diapir, such that the attitudes of flanking strata change dramatically along strike, in some places dipping away from the salt and in others dipping toward the salt. The thinned strata at both ends of the diapir have been interpreted as composite halokinetic sequences (Belenguer Oliver, 2017), but the thinning occurs over a distance of several kilometers rather than within less than 1 km as is the case with halokinetic sequences (see Rowan & Giles, 2023). Moreover, the geometries of upper Albian to Maastrichtian strata on the northern flank of the diapir are not those of halokinetic sequences. Thus, even though the base-upper Albian unconformity cut down to the salt on the western side of the diapir (Figure 10e), there is no evidence of salt breakthrough and then ongoing passive growth of a steep diapir during the Late Cretaceous.

The observations are used to constrain a restoration that illustrates a complex evolution (Figure 19). First, prekinematic Lower-Middle Jurassic strata were deposited above the footwall of a basement fault over which the Triassic salt is interpreted to have depositionally thickened (Figure 19a). The horizontal distance between these overburden strata and the deeper fault is unknown and can only be constrained by a more regional restoration. Latest Jurassic to middle Albian rifting was accommodated by decoupled thick-skinned extension, with increasing slip on the basement fault but thin-skinned extension and translation above the salt (Figure 19b). This resulted in drape folding of the overburden, deposition of thicker synrift strata over the basement-fault hanging wall, raft tectonics (complete separation) of the prekinematic sequence (see, e.g., Burollet, 1975; Duval et al., 1992), inflation of a salt anticline over the footwall (see analog models of decoupled thick-skinned extension by Ferrer Garcia, 2012; Warsitzka et al., 2015), and consequent erosion of one of the Jurassic rafts that was above the early salt high. Growth of the basement fault and thin-skinned translation of the overburden continued during the late Albian to early Cenomanian (Figure 19c), resulting in the formation of a ramp-syncline basin over the basement-fault hanging wall, continued vertical growth and extensional widening of the anticline, and erosion into the salt by the base-upper Albian unconformity. Lateral translation of the overburden continued even after the cessation of rifting, with consequent ongoing amplification of the anticline due to differential loading and further development of the ramp-syncline basin (Figure 19d). With the onset of Pyrenean contraction in the late Santonian, the salt anticline was squeezed slightly (Figure 19e), with occasional periods of crestal erosion such as within the Campanian and Maastrichtian. The main episode of shortening in the early Miocene led to an unknown amount of basement-fault inversion, further squeezing and amplification of the anticline (Figure 19f), significant crestal erosion, and salt breakout and lateral flow (farther to the east, not shown in restoration). Furthermore, the entire overburden, including the anticline and diapir, was thrust up and over the basement step some distance onto the footwall along the salt detachment, generating the asymmetric fold geometry and the differences in the regional structural elevation of both limbs of the anticline observed today (Figure 19f). Again, the amount of lateral translation can only be determined by a regional restoration.

Several aspects of this evolutionary model warrant further emphasis. First, some of the observed relationships are apparently contradictory. Salt was periodically exposed by erosion, and yet there was no consequent passive rise of a steep diapir and the development of halokinetic sequences, as seen at the other diapirs along the regional transect such as Poza de la Sal. Instead, the salt was repeatedly buried by ongoing deposition but nevertheless inflated so that strata thinned over multiple kilometers onto the salt high. Periodic unroofing and burial occurred during both extension and contraction (e.g., base upper Albian and intra-Maastrichtian, respectively). But why did salt not rise more vigorously, and thus steeply, after unroofing? The implication is that salt-rise rate was slow compared to sediment-accumulation rate. This is easily explained in the case of rifting, whether by extensional

Figure 18. Quantitative restoration of seismic profile across Poza de la Sal diapir (Figures 13a and 13b): (a) salt and prekinematic Lower-Middle Jurassic; (b) reconstruction of material eroded at base-upper Albian unconformity, showing minor contractional fold growth due to synrift translation of the overburden in the Burgalesa Platform; (c) end-rifting, with salt breakthrough due to erosion and consequent onset of passive diapirism; (d) ongoing diapirism during postrift; (e) present-day geometry, after Pyrenean contraction, with postulated eroded material at some arbitrary Cenozoic level. Restoration carried out using StructureSolver™ and a flexural-slip algorithm, without decompaction or isostatic effects. Vertical scale is in time, but set so that the section is at approximately 1:1 scale in depth.

10.1029/2025TC008824

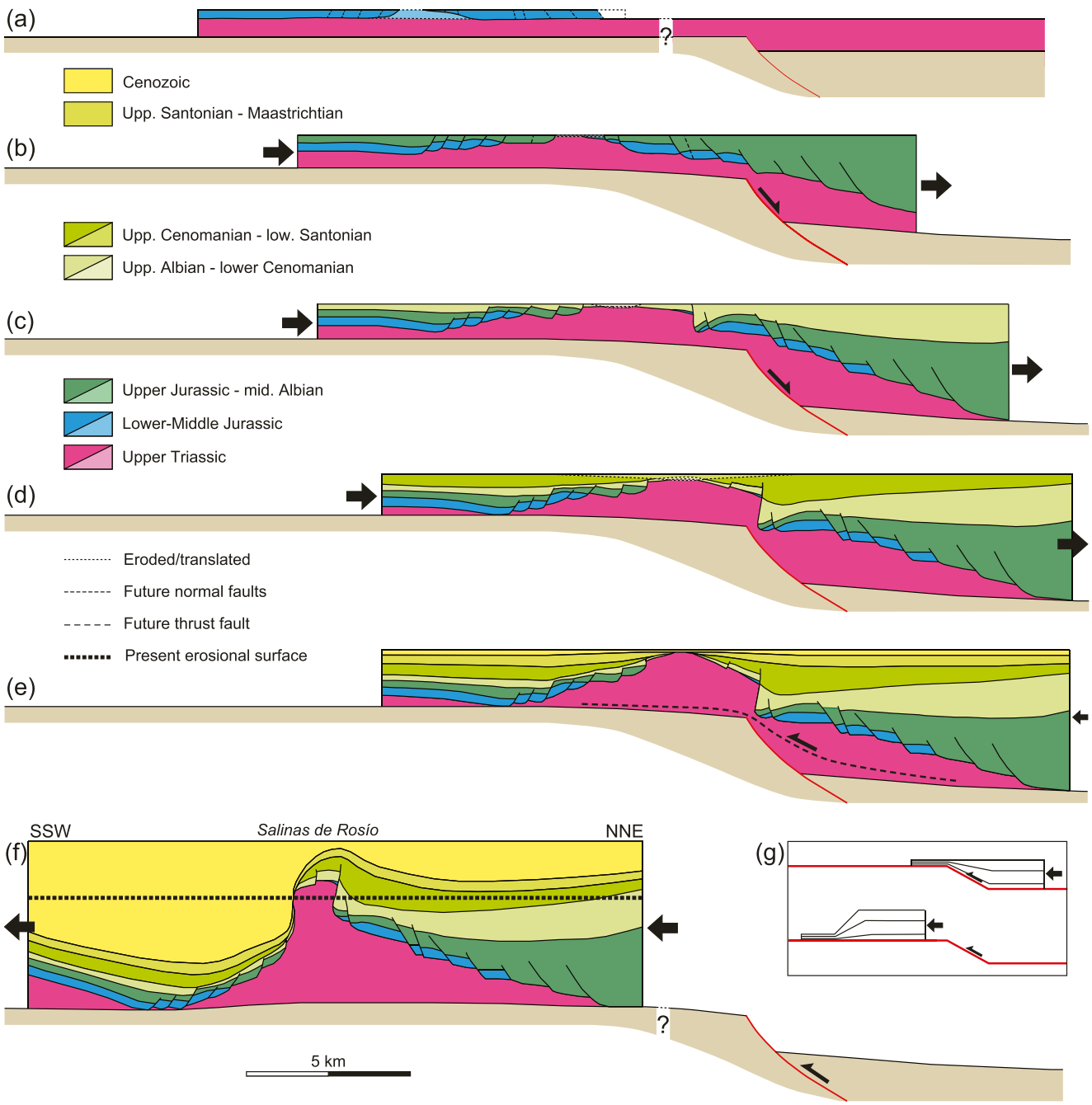

Figure 19. Quantitative restoration of a cross section combining the seismic profile through Salinas de Rosío diapir (Figure 11), the projected geometries west of the diapir (Figure 10b), and estimated geometries and thicknesses of eroded material: (a) prekinematic Lower-Middle Jurassic above the footwall of a basement fault but at an unknown distance from the fault; (b) decoupled thick-skinned extension and development of a broad salt anticline above the basement-fault footwall; (c) continued thick-skinned extension, widening of the salt anticline, and thin-skinned translation of the overburden; (d) cessation of rifting but ongoing gravity-driven translation and associated growth of the anticline during postrift time; (e) minor shortening (~100 m) during the latest Cretaceous to Paleocene, further amplifying the anticline; and (f) major Miocene shortening, with thin-skinned translation of the overburden strata an unknown distance onto the footwall of the inverted basement fault. (g) Generation of an asymmetric fold during thin-skinned translation of a depositional wedge over a ramp. Restoration carried out using StructureSolver™ and a flexural-slip algorithm, without decompaction or isostatic effects. Vertical scale is in time, but set so that the section is at approximately 1:1 scale in depth. The effects of flexural loading are shown schematically between (a and b), but not in subsequent time steps; eroded areas are depicted by dotted lines and lighter shades in panels (a–d); salt area is not maintained.

widening of the salt structure or dropping of the base of the salt in the hanging wall of the basement fault (depicted from Figures 19b–19c), both of which would have retarded upward salt rise. It is more problematic in the case of early contraction, but we infer that erosion was accompanied by or followed immediately by rapid deposition such that the salt remained buried enough to counter the effects of slow salt rise. Only during the main contractional event did squeezing increase salt-rise rate enough to overcome the rapid synorogenic deposition and cause salt breakout and sheet emplacement.

Second, the position of the diapir at the landward end of the ramp-syncline basin means that the broad salt anticline ended up over or near a basement fault at the end of lateral movement, having translated from a more proximal, footwall position. Note that Salinas de Rosío is part of a linear trend of diapirs along the landward edge of the Alavesa Platform (Figure 2), suggesting similar control by a large basement fault and similar overburden translation above that fault for at least 50 km along strike. Villasana de Mena is also along a linear trend of diapirs, but we address this in a later paper on the more regional aspects of our interpretation.

Third, thin-skinned contractional translation of a depositional wedge over a ramp in the base salt created what is effectively analogous to a large-scale fault-bend fold (compare Figures 19f and 19g). The consequent juxtaposition of thinning synrift strata in a steep monoclinal fold limb and an elevated, thicker panel of age-equivalent strata may easily be misinterpreted as forming due to local thick-skinned inversion of a basement fault, without any decoupling by the salt, rather than the large-scale thin-skinned translation proposed here.

5. Discussion

We have shown that different diapirs along the transect had very different histories. Some were long-lived passive diapirs that presumably were initially triggered by Late Jurassic to Early Cretaceous extension, but others started as salt anticlines, with roof erosion allowing salt to break through locally and begin passive diapirism. The timing and mode of deformation in these latter cases varied: Poza de la Sal diapir was marked by synrift shortening and late-Albian erosion and breakthrough; whereas Salinas de Rosío diapir was characterized by syn-to postrift loading and inflation that was subsequently enhanced during early stages of Pyrenean shortening, with erosion and breakthrough only during the main Cenozoic contractional stage.

This leads to an even more striking difference between the diapirs, namely how they responded to the Pyrenean orogenic event. At one end of the spectrum are the Sopelana and Montorio salt welds, which represent steep diapirs that were squeezed shut during the shortening. In contrast, although the Bakio, Salinas de Rosío, and Poza de la Sal diapirs all experienced shortening, as indicated by their location along contractional structures, they apparently remained open diapirs due to insufficient shortening to squeeze them shut. In the case of Bakio diapir, its orientation just slightly oblique to the regional shortening direction also played a role in keeping it open. The most enigmatic is Villasana de Mena diapir, which has no perceptible shortening, as indicated by the absence of adjacent contractional structures, despite its location in the center of an orogenic fold-and-thrust belt. The circular nature of diapirs such as Poza de la Sal was one of the arguments used by Ramos et al. (2022a, 2022b) to reject interpretations with large amounts of thin-skinned deformation because the diapirs would surely be squeezed. But this neglects the controlling role of the rocks surrounding the diapirs—if they are thick enough and strong enough to resist shortening, the diapirs will not be squeezed (see Rowan & Vendeville, 2006; Rowan et al., 2020; Vendeville & Nilsen, 1995; see also models by Callot et al., 2007; Santolaria et al., 2021). In fact, the pre-orogenic configuration of the Basque-Cantabrian Basin, with thin overburden near the basin margins and the thickest depocenters in the basin center, easily explains the variable amounts of observed diapir squeezing. This is most easily pictured as shortening of a wedge, with diapirs just local weak holes surrounded by stronger material. Contractional deformation, with folds and/or thrust faults extending away from squeezed/welded diapirs, will be concentrated near the tip of the wedge, that is, in marginal areas where the overburden is relatively thin and weak, as observed in analog models with shortening of a precontractional wedge (e.g., Muñoz et al., 2024; Smit et al., 2003). In the Basque-Cantabrian Pyrenees, this is in areas like the Folded Band (Figure 15b) and the opposite, northern margin. In contrast, diapirs like Villasana de Mena were surrounded by very thick postsalt strata and were simply translated above the salt detachment without being squeezed (see also Miró et al., 2021; Serrano & Martínez del Olmo, 1990). In an intermediate case like Poza de la Sal diapir, there was simply not enough shortening to squeeze the diapir shut to form a weld. And at Salinas de Rosío diapir, there was an elongate pre-orogenic salt anticline but no preexisting diapir; the diapir formed only late and there was insufficient subsequent shortening to squeeze it shut to form a weld.

If the geometry of diapirs (e.g., welded vs. undeformed) cannot be used to distinguish between thin-skinned translation and thick-skinned inversion, other criteria are needed. Needless to say, having clear evidence of inverted basement structures directly beneath diapirs and/or suprasalt folds or thrust faults would be ideal. But despite claims to the contrary (Pedrera et al., 2018), the legacy seismic data in the Basque-Cantabrian Pyrenees are largely inadequate for the task—there is more than enough uncertainty at base-salt and subsalt levels to allow for multiple interpretations. We suggest, therefore, that the critical observations are those of the relatively well-imaged minibasins. Specifically, key factors are the geometry of the prekinematic Lower-Middle Jurassic sequences, the patterns of synrift reflections, the nature of any suprasalt faults, and the observed thickness variations of synrift strata between different minibasins. The dramatic thickness changes, first from the Folded Band into the Burgalesa Platform (Figure 15b) and second from the Villarcayo Syncline into the Alavesa Platform (Figures 7 and 11), demonstrate significant changes in accommodation that almost certainly reflect basement fault control. But the overburden depocenters are not stacked vertically or with slight lateral offsets; instead, each change in accommodation marks the proximal end of synrift depocenters that shift landward ∼15 km in the Burgalesa Platform but at least 35 km in the Alavesa Platform and southern limb of the Bilbao Anticlinorium. These geometries record significant lateral translation over and across subsalt faults. This is corroborated by evidence of raft tectonics, with gaps in the prekinematic Lower-Middle Jurassic sequence, listric normal faults soling into the salt, and associated subtle rollover geometries (see also Cámara, 2017; Malagón et al., 1994; Serrano et al., 1994; Serrano & Martínez del Olmo, 1990).

No single factor is diagnostic, but we argue that the combination of observed geometries within minibasins is compatible only with an interpretation in which there was thin-skinned extension and consequent lateral translation. Thus, there was decoupled extension on a north-dipping salt detachment in the area from the Folded Band to the Bilbao Anticlinorium. This would have been the primary extensional detachment during rifting and argues against a south-dipping detachment as proposed by Pedrera et al. (2021). In our interpretation, there would have been a relatively minor south-dipping (antithetic) detachment only on the northern margin of the basin near Bakio diapir (Roca et al., 2021).

Given the postrift, pre-orogenic configuration of the Basque-Cantabrian Pyrenees, how was the subsequent orogenic shortening accommodated? One option is, again, thick-skinned, with inverted basement faults cutting through the salt and its overburden (Figure 3b; Pedrera et al., 2017, 2021; Quintana et al., 2015; Ramos et al., 2022a, 2022b; Tavani & Granado, 2015; Tavani et al., 2013). In this style of deformation, the major faults should be located at the boundaries between thin and thick overburden, that is, at the landward margins of the Burgalesa and Alavesa platforms. Since there is little, if any, present difference in structural level apparent at the base salt on either side of these boundaries (Figure 3), this would require near-total inversion, with the original extensional offset balanced almost exactly by later reverse slip. Coupled thick-skinned inversion should also create classic geometries of uplifted half-graben (modified by the presence of salt) with: steep, short forelimbs; long, planar, gently dipping backlimbs; and a return of the hanging wall to regional level away from the half-graben (e.g., Cooper & Warren, 2010; see Andrés et al., 2016, Figure 5). This style is not apparent along our transect.

A second option is one in which the deformation was spatially coupled but geometrically decoupled. In other words, both basement and overburden shortening occurred in the same locations, but with different geometries and little to no lateral translation (Cámara, 2017; Serrano et al., 1994). Confirmation of this interpretation would require either excellent seismic images of the basement structure or, failing that, overburden geometries incompatible with lateral translation as an important process. But the data and our analysis demonstrate that lateral translation was, in fact, an important aspect of the evolution.

The third option—and the one favored here—invokes significant decoupling of the overburden and basement deformation, consequent lateral translation of the overburden on the salt décollement, and a frontal (southern) thrust fault with significant displacement (Figure 3a; Carola et al., 2015; Hernaiz et al., 1994; Hernaiz Huerta & Solé Pont, 2000; Malagón et al., 1994; Miró et al., 2021; Muñoz, 2019). One underappreciated aspect of thin-skinned thrusting is that it can yield geometries superficially similar to those of thick-skinned inversion and thus be mistaken for coupled deformation. Thick strata that formed due to increased accommodation in the hanging wall of a subsalt extensional fault get transported over the ramp caused by the offset of the base salt and onto the footwall flat (Figure 19g). The result is an asymmetric structure—analogous to the frontal portion of a

fault-bend fold but with a thinning wedge—with a short, steep forelimb with thin strata and an elevated platform of thicker equivalent sequences. Thus, inverted basins are not diagnostic of coupled thick-skinned inversion.

One possible problem with an interpretation of decoupled thin-skinned deformation is that it requires a continuous salt layer for ongoing translation during extension and subsequent thin-skinned thrusting. Yet the amount of crustal extension in the Basque-Cantabrian Pyrenees, with shallow exhumation of mantle rocks, implies that the salt might have been completely offset by basement normal faults. However, as mentioned earlier, data from the Pyrenees s.s. demonstrate that salt can still be connected between the foot- and hanging walls of basement faults with 2–5 km of extensional throw (Ducoux et al., 2021; Ford & Vergés, 2021; Mencos et al., 2015). Moreover, analog and numerical models show that décollement continuity and consequent decoupling is favored by thicker salt (e.g., Ferrer, Carola, & McClay, 2023; Ferrer, Carola, McClay, & Bufaliza, 2023; Jourdon et al., 2020). We therefore suggest that the Keuper salt, at least in the area south of the Bilbao Anticlinorium, remained connected after the cessation of rifting and thus served as a regional detachment during subsequent decoupled inversion.

Many interpretations invoke strike-slip deformation in the Basque-Cantabrian Pyrenees during extension and/or contraction. While that bounding the Burgalesa Platform during orogenic escape tectonics on the Ubierna fault is well documented (Carola et al., 2013, 2015; Tavani et al., 2011, 2013), other more regional interpretations of wrench tectonics seem more speculative (e.g., Canérot et al., 2005; García-Mondéjar et al., 1996; Rat, 1988). Here we add only two comments. First, nothing in the diapir or minibasin geometries requires any strike-slip component to the deformation, but that of course does not rule it out. Second, the ramp-syncline basin of the Burgalesa Platform, combined with the geometry and gaps of Lower-Middle Jurassic strata at its landward edge, require that the Ubierna and associated strike-slip faults be decoupled from basement and confined to the suprasalt section (Cámara, 2017; Cámara et al., 2023; Carola et al., 2015; Miró et al., 2021; Muñoz, 2019), not thick-skinned structures that cut through the salt (Pedrera et al., 2021; Quintana et al., 2015; Ramos et al., 2022a, 2022b; Tavani et al., 2011, 2013; Tavani & Granado, 2015).

6. Concluding Remarks

The Basque-Cantabrian Pyrenees is a complex province even without salt, having experienced enough rifting to reach mantle exhumation and then subsequent inversion during the Pyrenean Orogeny. In addition, the Upper Triassic Keuper salt not only served as a décollement layer, but also sourced diapirs and provided extra accommodation for the development of both extensional and contractional depocenters. The resulting geometries observed today at the surface, combined with subsurface data of variable quality, have therefore been interpreted in fundamentally different ways. Key disagreements exist in the literature over the degree of decoupling between supra- and subsalt levels, the attendant continuity or discontinuity of the salt layer, the origin and evolution of both diapirs and minibasins, the amount of translation of the overburden relative to basement, the nature and dip direction of the primary detachment, the magnitudes of extension and later contraction, and the importance of any strike-slip deformation during each event. In this contribution, we use the observed salt and minibasin geometries to address many of these issues. We mostly ignore the subsalt deformation itself because of inadequate imaging at depth, and instead use surface and relatively well imaged, shallower subsurface data to unravel the salt-related deformation and thereby place constraints on the crustal interpretation.

We show that six diapirs along a transect across the Basque-Cantabrian Pyrenees had very different histories, some aspects of which are best explained by lateral translation detached on the salt. A key part of the analysis relies on the correct understanding of two sets of landward-shifting depocenters (the Burgalesa Platform and the Alavesa Platform to southern limb of the Bilbao Anticlinorium), as well as the distribution and geometry of the prekinematic Lower-Middle Jurassic sequence. No single feature is in itself diagnostic, but the combination strongly indicates decoupled extension and translation during rifting, with consequent rafts of the prekinematic strata and the formation of ramp-syncline basins in synrift strata due to translation over ramps in the base salt that marked the location of basement faults. Translation toward the center of the rift basin shows that the main detachment dipped to the north, not south, and was still connected rather than discontinuous when rifting ceased, at least from the southern limb of the Bilbao Anticlinorium southward. Moreover, continued translation during postrift time, recorded by the youngest ramp-syncline basins of the Alavesa Platform, attest to thin-skinned, gravity-driven deformation after extension ceased. Furthermore, inversion led to reverse movement on the detachment, with thick synrift strata in the hanging walls of the basement faults translating back up over the ramps

and onto the footwalls. Thus, although the locations of some of the diapirs were controlled by underlying basement faults, the diapirs are not above those faults today.

The results of this analysis and explanation of the salt tectonics along the single transect obviously can be applied to other areas of the Basque-Cantabrian Pyrenees. But it also has implications for unraveling others parts of the Pyrenees, whether farther to the east in the southern Pyrenees or in the northern Pyrenees of France. Furthermore, similar concepts may apply to other inverted rift basins with salt, from those with relatively low magnitudes of extension and contraction, such as the Atlas Mountains of Morocco or the Flinders Ranges of South Australia, to those with hyperextension and major orogenesis such as the French Alps or Northern Calcareous Alps of Austria. In all cases, the suitability of the results presented here will depend largely on when in the extensional history the salt was deposited, the consequent distribution and thickness of the salt, and the architecture and displacement magnitude of crustal faults.

Data Availability Statement

Seismic reflection profiles for this research are available and freely accessible in the SIGEOF repository, the Geophysical Information System of the IGME (Spanish Geological Survey), and the DIGITAL CSIC repository (IGME, 2025a). To access the data, use the web application (info.igme.es/SIGEOF/). Public-domain geological maps are available at: IGME (1:50.000 geological maps), https://info.igme.es/cartografiadigital/geologica/Magna50.aspx?language=es (IGME, 2025b); IGME (1:25.000 geological maps from Cantabria), (IGME, 2025c) https://info.igme.es/cartografiadigital/geologica/cantabria25.aspx; Basque country 1:25.000 geological maps (Ente Vasco de la Energia), EVE (2025), https://www.eve.eus/Conoce-la-Energia/La-energia-en-Euskadi/Publicaciones/Geologia/Mapa-Geologico-del-Pais-Vasco-a-escala-1-25-00-(1)?lang=es-es.

Acknowledgments
This collaboration grew out of putting together a field course on salt tectonics, based out of Bilbao and at the urging of Simon Baker, to whom we are therefore grateful. We also thank Stefano Tavani and Pablo Granado for discussions over the years, Mary Ford, Tim Dooley, and an anonymous reviewer for helpful comments and suggestions, B. López-Mir for the composite profile of Figure 7, and both StructureSolver and Petex for software. This work has been supported by the project PID2020-117598GB-I00, Structure and Deformation of Salt-Bearing Rifted Margins (SABREM), funded by MICIU/AEI/11.13039/501110011133 from the Spanish Ministry of Science and Innovation. The GEOMODELS Research Institute and the Grup de Geodinàmica i Anàlisi de Conques (2017SGR-596) are also acknowledged for their financial support. Partial funding for MR is through the Salt-Sediment Interaction Research Consortium at The University of Texas at El Paso, whose current sponsors are Chevron, Hess, PGS, and Woodside. The contributions of RU have been supported by postdoctoral research project POST1643103 2023-2 funded by Repsol S.A.

References

Ábalos, B., Alkorta, A., & Iríbar, V. (2008). Geological and isotopic constraints on the structure of the Bilbao anticlinorium (Basque-Cantabrian basin, North Spain). *Journal of Structural Geology*, *30*(11), 1354–1367. https://doi.org/10.1016/j.jsg.2008.07.008

Agirrezabala, L. M., Owen, H. G., & García-Mondéjar, J. (2002). Syntectonic deposits and punctuated limb-rotation in an Albian submarine transpressional fold (Mutriku village, Basque-Cantabrian basin, northern Spain). *Geological Society of America Bulletin*, *114*(3), 281–297. https://doi.org/10.1130/0016-7606(2002)114%3C0281:SDAPLR%3E2.0.CO;2

Andrés, J., Alcalde, J., Ayarza, P., Saura, E., Marzán, I., Martí, D., et al. (2016). Basement structure of the Hontomín CO_2 storage site (Spain) determined by integration of microgravity and 3-D seismic data. *Solid Earth*, *7*(3), 827–841. https://doi.org/10.5194/se-7-827-2016

Angrand, P., Mouthereau, F., Masini, E., & Asti, R. (2020). A reconstruction of Iberia accounting for western tethys–north Atlantic kinematics since the late-Permian–Triassic. *Solid Earth*, *11*(4), 1313–1332. https://doi.org/10.5194/se-11-1313-2020

Asti, R., Saspiturry, N., & Angrand, P. (2022). The Mesozoic Iberia-Eurasia diffuse plate boundary: A wide domain of distributed transtensional deformation progressively focusing along the North Pyrenean zone. *Earth-Science Reviews*, *230*, 104040. https://doi.org/10.1016/j.earscirev.2022.104040

Belenguer Oliver, J. (2017). *Mesozoic salt tectonics in the Jaeren High and Cod Terrace, northern Central Graben (offshore UK and Norway)* (Doctoral dissertation). Royal Holloway University of London.

Bodego, A., Iriarte, E., López-Horgue, M. A., & Álavarez, I. (2018). Rift-margin extensional forced folds and salt tectonics in the eastern Basque-Cantabrian rift basin (western Pyrenees). *Marine and Petroleum Geology*, *91*, 667–682. https://doi.org/10.1016/j.marpetgeo.2018.02.007

Boess, J. G. V. (1984). Der diapir von Gernika (Nordspanien). *Zeitschrift der Deutschen Geologischen Gesellschaft*, *135*(1), 7–21. https://doi.org/10.1127/zdgg/135/1984/7

Brinkmann, R., & Lögters, H. (1968). Diapirs in western Pyrenees and foreland, Spain. In J. Braunstein & G. D. O'Brien (Eds.), *Diapirs and Diapirism AAPG Memoir* (Vol. 8, pp. 244–260). American Association of Petroleum Geologists. https://doi.org/10.1306/M8361C18

Burollet, P. F. (1975). Tectonique en radeaux en Angola. *Bulletin de la Societe Geologique de France*, *XVII*(4), 503–504. https://doi.org/10.2113/gssgfbull.s7-xvii.4.503

Cadenas, P., Manatschal, G., & Fernández-Vijo, G. (2020). Unravelling the architecture and evolution of the inverted multi-stage North Iberian-Bay of Biscay rift. *Gondwana Research*, *88*, 67–87. https://doi.org/10.1016/j.gr.2020.06.026

Callot, J.-P., Jahani, S., & Letouzey, J. (2007). The role of pre-existing diapirs in fold and thrust best development. In: O. Lacombe, F. Roure, J. Lavé, & J. Vergés (Eds.), *Thrust belts and foreland basins* (pp. 309–325). Springer. https://doi.org/10.1007/978-3-540-69426-7_16

Cámara, P. (2017). Salt and strike-slip tectonics as main drivers in the structural evolution of the Basque-Cantabrian Basin, Spain. In J. I. Soto, J. F. Flinch, & G. Tari (Eds.), *Permo-triassic salt provinces of Europe, north Africa and the Atlantic margins: Tectonics and hydrocarbon potential* (pp. 371–393). Elsevier. https://doi.org/10.1016/B978-0-12-809417-4.00018-5

Cámara, P. (2020). Inverted turtle salt anticlines in the eastern Basque-Cantabrian basin, Spain. *Marine and Petroleum Geology*, *117*, 104358. https://doi.org/10.1016/j.marpetgeo.2020.104358

Cámara, P., Parés, J. M., & Suarez, J. (2023). Connecting the Iberian Range with the Basque-Cantabrian Basin: The structure of the Sierra de Atapuerco (Spain). *Marine and Petroleum Geology*, *155*. https://doi.org/10.1016/j.marpetgeo.2023.106417

Canérot, J., Hudec, M. R., & Rockenbauch, K. (2005). Mesozoic diapirism in the Pyrenean orogen: Salt tectonics on a transform plate boundary. *AAPG Bulletin*, *89*(2), 211–229. https://doi.org/10.1306/09170404007

Carola, E., Muñoz, J. A., & Roca, E. (2015). The transition from thick-skinned to thin-skinned tectonics in the Basque-Cantabrian Pyrenees: The Burgalesa platform and surroundings. *International Journal of Earth Sciences*, *104*, 2215–2239. https://doi.org/10.1007/s00531-015-1177-z

Carola, E., Tavani, S., Ferrer, O., Granado, P., Quintà, A., Butillé, M., & Muñoz, J. A. (2013). Along-strike extrusion at the transition between thin- and thick-skinned domains in the Pyrenean Orogen (northern Spain). In M. Nemčok, A. Mora, & J. W. Cosgrove (Eds.), *Thick-skinned-dominated orogens: From initial inversion to full accretion* (Vol. 377(1), pp. 119–140). Geological Society, London, Special Publication. https://doi.org/10.1144/SP377.3

Clark, J. A., Stewart, S. A., & Cartwright, J. A. (1998). Evolution of the NW margin of the North Permian basin, UK North Sea. *Journal of the Geological Society*, *155*(4), 663–676. https://doi.org/10.1144/gsjgs.155.4.0663

Clerc, C., & Lagabrielle, Y. (2014). Thermal control on the modes of crustal thinning leading to mantle exhumation: Insights from the Cretaceous Pyrenean hot paleomargins. *Tectonics*, *33*(7), 1340–1359. https://doi.org/10.1002/2013TC003471

Cooper, M., & Warren, M. J., (2010). The geometric characteristics, genesis and petroleum significance of inversion structures. In R. D. Law, R. W. H. Butler, R. E. Holdsworth, M. Krabbendam, & R. A. Strachan (Eds.), *Continental tectonics and mountain building: The legacy of Peach and Horne* (Vol. 335(1), 827–846). Geological Society, London, Special Publication. https://doi.org/10.1144/SP335.33

Cuevas, J., & Tubia, J. M. (1985). Estructuras diapiricas asociadas al sinclinorio de Vizcaya. *Munibe*, *37*, 1–4.

Cumberpatch, Z. A., Kane, I. A., Soutter, E. L., Hodgson, D. M., Jackson, C. A.-L., Kilhams, B. A., & Poprawski, Y. (2021). Interactions between deep-water gravity flows and active salt tectonics. *Journal of Sedimentary Research*, *91*(1), 34–65. https://doi.org/10.2110/jsr.2020.047

DeFelipe, I., Pedreira, D., Pulgar, J. A., van der Beek, P. A., Bernet, M., & Pik, R. (2019). Unraveling the Mesozoic and Cenozoic tectonothermal evolution of the eastern Basque-Cantabrian zone–western Pyrenees by low-temperature thermochronology. *Tectonics*, *38*(9), 3436–3461. https://doi.org/10.1029/2019TC005532

Dooley, T. P., & Hudec, M. R. (2020). Extension and inversion of salt-bearing rift systems. *Solid Earth*, *11*, 1–18. https://doi.org/10.5194/se-11-1-2020

Dooley, T. P., Hudec, M. R., Carruthers, D., Jackson, M. P. A., & Luo, G. (2017). The effects of base-salt relief on salt flow and suprasalt deformation patterns – Part 1: Flow across simple steps in the base of salt. *Interpretation*, *5*(1), SD1–SD23. https://doi.org/10.1190/INT-2016-0087.1

Dooley, T. P., Jackson, M. P. A., & Hudec, M. R. (2009). *Deformation styles and linkage of salt walls during oblique shortening*. AAPG Search and Discovery. Retrieved from https://www.searchanddiscovery.com/abstracts/html/2009/annual/abstracts/dooley.htm

Ducoux, M., Jolivet, L., Callot, J.-P., Aubourg, C., Masini, E., Lahfid, A., et al. (2020). The Nappes des Marbres unit of the Basque-Cantabrian Basin: The tectono-thermal evolution of a fossil hyperextended rift basin. *Tectonics*, *38*(11), 3881–3915. https://doi.org/10.1029/2018TC005348

Ducoux, M., Masini, E., Tugend, J., Gómez-Romeu, J., & Calassou, S. (2021). Basement-decoupled hyperextension rifting: The tectono-stratigraphic record of the salt-rich Pyrenean necking zone (Arzacq Basin, SW France). *Geological Society of America Bulletin*, *134*(3–4), 941–964. https://doi.org/10.1130/B35974.1

Duval, B., Cramez, C., & Jackson, M. P. A. (1992). Raft tectonics in the Kwanza basin, Angola. *Marine and Petroleum Geology*, *9*(4), 389–404. https://doi.org/10.1016/0264-8172(92)90050-O

Elorza, J. J., Orue-Etxebarria, X., & Lamolda, M. A. (1984). Existencia de una fracturacion intensa en el area de Sopelana-Meñakoz. *I Congreso Español de Geologia*, *3*, 177–178.

Evans, S. L., Jackson, C. A.-L., & Oppo, D. (2021). Taking the pulse of salt-detached gravity gliding in the Eastern Mediterranean. *Tectonics*, *40*(7). https://doi.org/10.1029/2020TC006476

EVE (Ente Vasco de la Energía). (2025). Mapa Geológico del País Vasco a escala 1:25.000 [Dataset]. https://www.eve.eus/Conoce-la-Energia/La-energia-en-Euskadi/Publicaciones/Geologia/Mapa-Geologico-del-Pais-Vasco-a-escala-1-25-00-(1)?lang=es-es

Fernandez, N., Duffy, O. B., Hudec, M. R., Jackson, M. P. A., Burg, G., Jackson, C. A.-L., & Dooley, T. P. (2017). The origin of salt-encased sediment packages: Observations from the SE Precaspian Basin (Kazakhstan). *Journal of Structural Geology*, *97*, 237–256. https://doi.org/10.1016/j.jsg.2017.01.008

Fernández-Mendiola, P. A., & García-Mondéjar, J. (1997). Isolated carbonate platform of Caniego, Spain: A test of the latest Albian worldwide sea-level changes. *Geological Society of America Bulletin*, *109*(2), 176–194. https://doi.org/10.1130/0016-7606(1997)109%3C0176:ICPOCS%3E2.3.CO;2

Ferrer, O., Carola, E., & McClay, K. (2023). Structural control of inherited salt structures during inversion of a domino basement-fault system from an analogue modelling approach. *Solid Earth*, *14*(5), 571–589. https://doi.org/10.5194/se-14-571-2023

Ferrer, O., Carola, E., McClay, K., & Bufaliza, N. (2023). Analogue modeling of domino-style extensional basement fault systems with pre-kinematic salt. *AAPG Bulletin*, *107*(1), 23–47. https://doi.org/10.1306/08072221188

Ferrer, O., Jackson, M. P. A., Roca, E., & Rubinat, M. (2012). Evolution of salt structures during extension and inversion in the offshore Parentis Basin (eastern Bay of Biscay). In G. I. Alsop, S. G. Archer, A. J. Hartley, N. T. Grant, & R. Hodgkinson (Eds.), *Salt tectonics, sediments and prospectivity* (Vol. 363, pp. 361–379). Geological Society, London, Special Publications. https://doi.org/10.1144/SP363.16

Ferrer, O., McClay, K., & Sellier, N. C. (2017). Influence of fault geometries and mechanical anisotropies on the growth and inversion of hanging-wall synclinal basins: Insights from sandbox models and natural examples. In: C. Childs, R. E. Holdsworth, C.A.-L. Jackson, T. Manzocchi, J. J. Walsh, & G. Yielding (Eds.), *The geometry and growth of normal faults* (Vol. 439, pp. 487–509). Geological Society, London, Special Publications. https://doi.org/10.1144/SP439.8

Ferrer Garcia, J. O. (2012). *Salt tectonics in the Parentis Basin (eastern Bay of Biscay)* (Doctoral dissertation). Universitat de Barcelona.

Ford, M., Masini, E., Vergés, J., Pik, R., Temois, S., Léger, J., et al. (2022). Evolution of a low convergence collisional orogen: A review of Pyrenean orogenesis. *BSGF – Earth Sciences Bulletin*, *193*, 19. https://doi.org/10.1051/bsgf/2022018

Ford, M., & Vergés, J. (2021). Evolution of a salt-rich transtensional rifted margin, eastern North Pyrenees, France. *Journal of the Geological Society*, *178*(1). https://doi.org/10.1144/jgs2019-157

Frankovic, A. (2010). *Análisis cinemático de la pared de sal Euskal Balea (Golfo de Viscaya) y do los diapiros salinos de Salinas de Añana y Maestu (Cuenca Vasco-Cantábrica, Álava)* (Doctoral dissertation). Universidad del País Vasco.

Frankovic, A., Eguiluz, L., & Martínez-Torres, L. M. (2016). Geodynamic evolution of the Salinas de Añana diapir in the Basque-Cantabrian Basin, western Pyrenees. *Journal of Structural Geology*, *83*, 13–27. https://doi.org/10.1016/j.jsg.2015.12.001

Frasca, G., Manatschal, G., Cadenas, P., Miró, J., & Lescoutre, R. (2021). A kinematic reconstruction of Iberia using intracontinental strike-slip corridors. *Terra Nova*, *33*(6), 573–581. https://doi.org/10.1111/ter.12549

García-Mondéjar, J. (1990). The Aptian-Albian carbonate episode of the Basque-Cantabrian Basin (northern Spain): General characteristics, controls and evolution. In M. E. Tucker, J. L. Wilson, P. D. Crevello, J. R. Sarg, & J. F. Fred (Eds.), *Carbonate platforms: Facies, sequences and evolution* (Vol. 9, pp. 257–290). International Association of Sedimentologists, Special Publication. https://doi.org/10.1002/9781444303834.ch10

García-Mondéjar, J., Agirrezabala, L. M., Aranburu, A., Fernández-Mendiola, P. A., Gómez-Pérez, I., López-Horgue, M., & Rosales, I. (1996). Aptian-Albian tectonic pattern of the Basque-Cantabrian Basin (northern Spain). *Geological Journal*, *31*(1), 13–45. https://doi.org/10.1002/(SICI)1099-1034(199603)31:1%3C13::AID-GJ689%3E3.0.CO;2-Y

García-Mondéjar, J., Fernández-Mendiola, P. A., Agirrezabala, L. M., Aranburu, A., López-Horgue, M. A., Iriarte, E., & Martínez de Rituerto, S. (2004). Aptiense-Albiense de la Cuenca Vasco-Cantábrica. In J. A. Vera (Ed.), *Geologia de España* (pp. 291–296). Sociedad Geológica de España-Instituto Geológico y Minero.

García-Mondéjar, J., Pujalte, V., & Robles, S. (1986). Caracteristicas sedimentologicas, secuenciales y tectoestrigraficas del Triasico de Cantabria y norte de Palencia. *Cuadernos de Geologia Iberica*, *10*, 151–172.

Garrison, J. M., & McMillan, N. J. (1999). Evidence for Jurassic continental rift magmatism in northeast Mexico: Allogenic meta-igneous blocks in El Papalote diapir, La Popa basin, Nuevo Leon, Mexico. In C. Bartolini, J. L. Wilson, & T. F. Lawton (Eds.), *Mesozoic sedimentary and tectonic history of north-central Mexico* (Vol. 340, pp. 319–332). Geological Society of America Special. https://doi.org/10.1130/0-8137-2340-X.319

Ghazian, R. K., & Buiter, S. J. H. (2014). Numerical modelling of the role of salt in continental collision: An application to the southeast Zagros fold-and-thrust belt. *Tectonophysics*, *632*, 96–110. https://doi.org/10.1016/j.tecto.2014.06.006

Giles, K. A., & Rowan, M. G. (2012). Concepts in halokinetic-sequence deformation and stratigraphy. In G. I. Alsop, S. G. Archer, A. J. Hartley, N. T. Grant, & R. Hodgkinson (Eds.), *Salt tectonics, sediments and prospectivity* (Vol. 363, pp. 7–31). Geological Society, London, Special Publications. https://doi.org/10.1144/SP363.2

Gomar, F., Ruh, J. B., Najafi, M., & Sobouti, F. (2024). Importance of basement faulting and salt decoupling for the structural evolution of the Fars Arc (Zagros fold-and-thrust belt): A numerical modeling approach. *Solid Earth*, *15*(12), 1479–1507. https://doi.org/10.5194/se-15-1479-2024

Gómez, M., Vergés, J., & Riaza, C. (2002). Inversion tectonics of the northern margin of the Basque-Cantabrian Basin. *Bulletin de la Societe Geologique de France*, *173*(5), 449–459. https://doi.org/10.2113/173.5.449

Grant, R. J., Underhill, J. R., Hernández-Casado, J., Jamieson, R. J., & Williams, R. M. (2019). The evolution of the Dowsing Graben System: Implications for petroleum prospectivity in the UK southern North Sea. *Petroleum Geoscience*, *27*(1). https://doi.org/10.1144/petgeo2018-064

Guerrero, J. (2017). Dissolution collapse of a growing diapir from radial, concentric, and salt-withdrawal faults overprinting in the Salinas de Oro salt diapir, northern Spain. *Quaternary Research*, *87*(2), 331–346. https://doi.org/10.1017/qua.2016.17

Guerrero, J., Bartolomé, M., & Gökkaya, E. (2023). The Quaternary activity of the Estella diapir from the uplift record of fluvial terraces, pediments and cave sediments in the Western Pyrenees, Spain. *Catena*, *233*, 107531. https://doi.org/10.1016/j.catena.2023.107531

Hansen, T. H., Clausen, O. R., & Andresen, K. J. (2021). Thick- and thin-skinned basin inversion in the Danish Central Graben, North Sea – The role of deep evaporites and basement kinematics. *Solid Earth*, *12*(8), 1719–1747. https://doi.org/10.5194/se-12-1719-2021

Harding, A., Walker, L., Ehlinger, S., & Chapman, T. (2016). The siliciclastic Upper Cretaceous play of eastern Mississippi Canyon. In C. M. Lowery, J. W. Snedden, & N. C. Rosen (Eds.), *Mesozoic of the Gulf Rim and beyond: New Progress in Science and Exploration of the Gulf of Mexico Basin. 35th annual GCSSEPM foundation Perkins-Rosen research conference* (pp. 215–225). https://doi.org/10.5724/gcs.15.35.0215

Hassaan, M., Faleide, J. I., Gabrielsen, R. H., Tsikalas, F., & Grimstad, S. (2021). Interplay between base-salt relief, progradational sediment loading and salt tectonics in the Nordkapp Basin, Barents Sea – Part II. *Basin Research*, *33*(6), 3256–3294. https://doi.org/10.1111/bre.12602

Hempel, P. M. (1967). Der diapir von Poza de la Salt (Nordspanien). *Beihefte zum Geologischen Jahrbuch*, *66*, 95–126.

Hernaiz, P. P. (1994). La falla de Ubierna (margen SO de la cuenca Cantábrica). *Geogaceta*, *16*, 39–42.

Hernaiz, P. P., Serrano, A., Malagón, J., & Rodríguez Cañas, C. (1994). Evolución estructural del margen SO de la cuenca Vasco Cantábrica. *Geogaceta*, *15*, 143–146.

Hernaiz Huerta, P. P., & Solé Pont, J. (2000). Las estructuras del diapiro de Salinas de Rosío y del alto de San Pedro-Iglesias y sus implicaciones en la evolución tectónica de la transversal Burgalesa de la Cordillera Vascocantábrica-Cuenca del Duero. *Revista de el Sociedad Geológica de España*, *13*(3–4), 471–486.

IGME (Instituto Geológico y Minero de España). (2025a). SIGEOF. Sistema de Información Geofísica [Dataset]. http://info.igme.es/SIGEOF/

IGME (Instituto Geológico y Minero de España). (2025b). Cartografía geológica [Dataset]. *Mapa Geologico de Espana - Escala 1:50 000*. https://info.igme.es/cartografiadigital/geologica/Magna50.aspx?language=es

IGME (Instituto Geológico y Minero de España). (2025c). Cartografía geológica [Dataset]. *Mapa Geológico Digital de Cantabria a escala 1: 25.000*. https://info.igme.es/cartografiadigital/geologica/cantabria25.aspx

Izquierdo-Llavall, E., Menant, A., Aubourg, C., Callot, J.-P., Hoareau, G., Camps, P., et al. (2020). Pre-orogenic folds and syn-orogenic tilts in an inverted hyperextended margin: The northern Pyrenees case study. *Tectonics*, *39*. https://doi.org/10.1029/2019TC005719

Jackson, M. P. A., & Hudec, M. R. (2005). Stratigraphic record of translation down ramps in a passive-margin salt detachment. *Journal of Structural Geology*, *27*(5), 889–911. https://doi.org/10.1016/j.jsg.2005.01.010

Jackson, M. P. A., & Hudec, M. R. (2017). *Salt tectonics: Principles and practice*. Cambridge University Press. https://doi.org/10.1017/9781139003988

Jackson, M. P. A., & Talbot, C. J. (1991). *A glossary of salt tectonics*. The University of Texas at Austin, Bureau of Economic Geology Geological Circular No. 91-4.

Jackson, M. P. A., & Vendeville, B. C. (1994). Regional extension as a geologic trigger for diapirism. *Geological Society of America Bulletin*, *106*(1), 57–73. https://doi.org/10.1130/0016-7606(1994)106%3C0057:REAAGT%3E2.3.CO;2

Jammes, S., Manatschal, G., & Lavier, L. (2010). Interaction between prerift salt and detachment faulting in hyperextended rift systems: The example of the Parentis and Mauléon basins (Bay of Biscay and western Pyrenees). *AAPG Bulletin*, *94*(7), 957–975. https://doi.org/10.1306/12090909116

Jourdon, A., Mouthereau, F., Le Pourhiet, L., & Callot, J.-P. (2020). Topographic and tectonic evolution of mountain belts controlled by salt thickness and rift architecture. *Tectonics*, *39*(1). https://doi.org/10.1029/2019TC005903

Klimowitz, J., Malagón, J., Quesada, S., & Serrano, A. (1999). Desarollo y evolución de estructuras salinas Mesozoicas en la parte suroccidental de la Cuenca Vasco-Cantábrica (Norte de España): Implicaciones exploratorias. In *Libro Homenaje a Jose Ramirez del Pozo* (pp. 159–166). AGGEP.

Kluth, C. F., & Duchene, H. R. (2009). Late Pennsylvanian and early Permian structural geology and tectonic history of the Paradox Basin and Uncompahgre uplift, Colorado and Utah. In W. S. Houston, L. L. Wray, & P. G. Moreland (Eds.), *The Paradox Basin revisited—New developments in petroleum systems and basin analysis* (pp. 178–197). Rocky Mountain Association of Geologists. Special Paper.

Labeaume, P., & Teixell, A. (2020). Evolution of salt structures of the Pyrenean rift (Chaînons Béarnais, France: From hyper-extension to tectonic inversion. *Tectonophysics*, *785*. https://doi.org/10.1016/j.tecto.2020.228451

Lagabrielle, Y., Asti, R., Duretz, T., Clerc, C., Fourcade, S., Teixell, A., et al. (2020). A review of Cretaceous smooth-slopes extensional basins along the Iberia-Eurasia plate boundary: How pre-rift salt controls the modes of continental rifting and mantle exhumation. *Earth-Science Reviews*, *201*, 103071. https://doi.org/10.1016/j.earscirev.2019.103071

Lagabrielle, Y., Asti, R., Fourcade, S., Corre, B., Poujol, M., Uzel, J., et al. (2019). Mantle exhumation at magma-poor passive continental margins. Part 1. 3D architecture and metasomatic evolution of a fossile exhumed mantle domain (Urdach lherzolite, north-western Pyrenees, France). *BSGF - Earth Sciences Bulletin*, *190*, 8. https://doi.org/10.1051/bsgf/2019007

Lanaja, J. M. (1987). *Contribución de la explotación petrolífera al conocimiento de la geologia de España*. Instituto Geológico y Minero de España.

Lescoutre, R., Manatschal, G., & Muñoz, J. A. (2021). Nature, origin, and evolution of the Pyrenean-Cantabrian junction. *Tectonics*, *40*(5). https://doi.org/10.1029/2020TC006134

Letouzey, J., Colletta, B., Vially, R., & Chermette, J. C. (1995). Evolution of salt-related structures in compressional settings. In M. P. A. Jackson, D. G. Roberts, & S. Snelson (Eds.), *Salt tectonics: A global perspective* (Vol. 65, pp. 41–60). AAPG Memoir. https://doi.org/10.1306/M65604C3

López-Gómez, J., Alonso-Azcárate, J., Arche, A., Arribas, J., Fernández Barrenechea, J., Borruel-Abadía, V., et al. (2019). Permian-Triassic rifting stage. In C. Quesada & J. T. Oliveira (Eds.), *The geology of Iberia: A geodynamic approach (169–249). Regional geological review*. Springer Nature. https://doi.org/10.1007/978-3-030-11295-0_3

López-Gómez, J., Martín-González, F., Heredia, N., de la Horra, R., Barrenechea, J. F., Cadenas, P., et al. (2019). New lithostratigraphy for the Cantabrian Mountains: A common tectono-stratigraphic evolution for the onset of the Alpine cycle in the W Pyrenean realm, N Spain. *Earth-Science Reviews*, *188*, 249–271. https://doi.org/10.1016/j.earscirev.2018.11.008

López-Mir, B., Muñoz, J. A., & García-Senz, J. (2014). Extensional salt tectonics in the partially inverted Cotiella post-rift basin (south-central Pyrenees): Structure and evolution. *International Journal of Earth Sciences*. https://doi.org/10.1007/s00531-014-1091-9

Lotze, F. (1953). Salzdiapirismus im nördlichen Spanien. *Zeitschrift der Deutschen Geologischen Gesellschaft*, *105*(4), 814–822. https://doi.org/10.1127/zdgg/105/1955/814

Malagón, J., Hernaiz, P. P., Rodríguez Cañas, C., & Serrano, A. (1994). Notas subre la inversión tectónica y aloctonia del la cuenca Vasco-Cantábrica. *Geogaceta*, *15*, 139–142.

Manatschal, G., Chenin, P., Lescoutre, R., Miró, J., Cadenas, P., Saspiturry, N., et al. (2021). The role of inheritance in forming rifts and rifted margins and building collisional orogens: A Biscay-Pyrenean perspective. *BSGF – Earth Sciences Bulletin*, *192*(55), 55. https://doi.org/10.1051/bsgf/2021042

Martín-Chivelet, J., Berástegui, X., Rosales, I., Vilas, L., Vera, J. A., Caus, E., et al. (2002). Cretaceous. In W. Gibbons, & M. T. Moreno (Eds.), *The geology of Spain* (pp. 255–292). The Geological Society.

Martín-Chivelet, J., López-Gómez, J., Aguado, R., Arias, C., Arribas, J., Arribas, M. E., et al. (2019). The late Jurassic-early Cretaceous rifting. In C. Quesada & J. T. Oliveira (Eds.), *The geology of Iberia: A geodynamic approach (regional geology reviews)* (pp. 169–250). Springer Nature. https://doi.org/10.1007/978-3-030-11295-0_9

Martinez-Braceras, N., Payros, A., Miniati, F., Arostegi, J., & Franceschetti, G. (2017). Contrasting environmental effects of astronomically driven climate change on three Eocene hemipelagic successions from the Basque-Cantabrian Basin. *Sedimentology*, *64*(4), 960–986. https://doi.org/10.1111/sed.12334

Mas Tudó, R. (2011). *Geometria i Cinemàtica del Diapir Salí de Poza de la Sal*. Universitat de Barcelona.

McClay, K., Muñoz, J. A., & García-Senz, J. (2004). Extensional salt tectonics in a contractional orogen: A newly identified tectonic event in the Spanish Pyrenees. *Geology*, *32*(9), 737–740. https://doi.org/10.1130/G20565.1

Mencos, J., Carrera, N., & Muñoz, J. A. (2015). Influence of rift basin geometry on the subsequent postrift sedimentation and basin inversion: The Organyà Basin and the Bóixols thrust sheet (south central Pyrenees). *Tectonics*, *34*, 1452–1474. https://doi.org/10.1002/2014TC003692

Miró, J., Ferrer, O., Muñoz, J. A., & Manatschal, G. (2023). Role of inheritance during tectonic inversion of a rift system in a thick-to thin-skin transition: Analogue modelling and application to the Pyrenean-Biscay system. *EGUsphere*. https://doi.org/10.5194/egusphere-2022-1175

Miró, J., Manatschal, G., Cadenas, P., & Muñoz, J. A. (2021). Reactivation of a hyperextended rift system: The Basque-Cantabrian Pyrenees case. *Basin Research*, *33*(6), 3077–3101. https://doi.org/10.1111/bre.12595

Mirumbrales Ayllón, S., Casas Sainz, A. M., & Román Berdiel, T. (2023). Los Montes Obarenes: Diapirismo e inversión tectónica en el margen sur de la Cuenca Vasco-Cantábrica. *Revista de la Sociedad Geologica de Espana*, *36*. https://doi.org/10.55407/rsge.99327

Muñoz, J. A. (2002). The Pyrenees. In W. Gibbons & M. T. Moreno (Eds.), *The geology of Spain* (pp. 370–385). The Geological Society.

Muñoz, J. A. (2019). Alpine orogeny: Deformation and structure in the northern Iberian margin (Pyrenees s.l.). In C. Quesada & J. T. Oliveira (Eds.), *The geology of Iberia: A geodynamic approach regional geology reviews* (pp. 433–451). Springer Nature. https://doi.org/10.1007/978-3-030-11295-0_9

Muñoz, J. A., Ferrer, O., Gratacós, O., & Roca, E. (2024). The influence of the geometry of salt detachments on thrust salient development: An analogue modelling approach based on the south-central Pyrenean thrust salient. *Journal of Structural Geology*, *180*, 105078. https://doi.org/10.1016/j.jsg.2024.105078

Payros, A., Orue-Etxebarria, X., & Pujalte, V. (2006). Covarying sedimentary and biotic fluctuations in lower-middle Eocene Pyrenean deep-sea deposits: Palaeoenvironmental implications. *Palaeogeography, Palaeoclimatology, Palaeoecology*, *234*(2–4), 258–276. https://doi.org/10.1016/j.palaeo.2005.10.013

Paz, M., Trudgill, B., & Kluth, C. (2009). *Salt system evolution of the northern Paradox Basin*. AAPG Search and Discovery. Retrieved from https://www.searchanddiscovery.com/documents/2009/30078paz/

Pedrera, A., García-Senz, J., Ayala, C., Ruiz-Constán, A., Rodríguez-Fernández, L. R., Robador, A., & González Menéndez, L. (2017). Reconstruction of the exhumed mantle across the north Iberian margin by crustal-scale 3-D gravity inversion and geological cross section. *Tectonics*, *36*(12), 3155–3177. https://doi.org/10.1002/2017TC004716

Pedrera, A., García-Senz, J., Ayala, C., Ruiz-Constán, A., Rodríguez-Fernández, L. R., Robador, A., & González Menéndez, L. (2018). Reply to comment by Pedreira et al. on "Reconstruction of the exhumed mantle across the north Iberian margin by crustal-scale 3-D gravity inversion and geological cross section". *Tectonics*, *37*(11), 4346–4356. https://doi.org/10.1029/2018TC005222

Pedrera, A., García-Senz, J., Peropadre, C., Robador, A., López-Mir, B., Díaz-Alvarado, J., & Rodríguez-Fernández, R. (2021). The Getxo crustal-scale cross-section: Testing tectonic models in the Bay of Biscay-Pyrenean rift system. *Earth-Science Reviews*, *212*, 103429. https://doi.org/10.1016/j.earscirev.2020.103429

Pedrera, A., García-Senz, J., Pueyo, E. L., López-Mir, B., Silva-Casal, R., & Díaz-Alvarado, J. (2023). Inhomogeneous rift inversion and the evolution of the Pyrenees. *Earth-Science Reviews*, *245*, 104555. https://doi.org/10.1016/j.earscirev.2023.104555

Pflug, R. (1967). El diapiro de Estella. *Beihefte zum Geologischen Jahrbuch*, *66*, 21–62.

Pichat, A. (2022). Stratigraphy, paleogeography and depositional setting of the K-Mg salts in the Zechstein Group of Netherlands – Implications for the development of salt caverns. *Minerals*, *12*(4), 486. https://doi.org/10.3390/min12040486

Pichel, L. M., Peel, F., Jackson, C. A.-L., & Huuse, M. (2018). Geometry and kinematics of salt-detached ramp syncline basins. *Journal of Structural Geology*, *115*, 208–230. https://doi.org/10.1016/j.jsg.2018.07.016

Pineda Velasco, A. (1991). *Mapa Geológico de España, 1:50,000, #167 (Montorio)*. Instituto Geológico y Minero de España.
Poprawski, Y., Basile, C., Agirrezabala, L. M., Jaillard, E., Gaudin, M., & Jacquin, T. (2014). Sedimentary and structural record of the Albian growth of the Bakio salt diapir (the Basque Country, northern Spain). *Basin Research*, *26*(6), 746–766. https://doi.org/10.1111/bre.12062
Poprawski, Y., Basile, C., Cumberpatch, Z., & Eude, A. (2021). Mass transport deposits in deep-water minibasins: Outcropping examples from the minibasins adjacent to the Bakio salt wall (Basque country, northern Spain). *Marine and Petroleum Geology*, *132*, 105194. https://doi.org/10.1016/j.marpetgeo.2021.105194
Poprawski, Y., Christophe, B., Etienne, J., Matthieu, G., & Michel, L. (2016). Halokinetic sequences in carbonate systems: An example from the middle Albian Bakio breccias formation (Basque Country, Spain). *Sedimentary Geology*, *334*, 34–52. https://doi.org/10.1016/j.sedgeo.2016.01.013
Pujalte, V., & Robles, S. (2008). Parasequencias transgresivo-regresivas en un cortejo transgresivo: Parte superior de la Fm Utrillas en Olleros de Pisuerga, Palencia. *Geogaceta*, *44*, 187–190.
Pujalte, V., Robles, S., & Hernández, J. M. (1996). La sedimentación continental del Grupo Campóo (Malm-Cretácio basal de Cantabria, Burgos y Palencia): Testimonio de un reajuste hidrográfico al inicio de una fase rift. *Cuadernos de Geologia Iberica*, *21*, 227–251.
Pujalte, V., Robles, S., Orue-Etxebarria, X., Baceta, J. I., Payros, A., & Larruzea, I. F. (2000). Uppermost Cretaceous-middle Eocene strata of the Basque-Cantabrian region and western Pyrenees: A sequence stratigraphic perspective. *Revista de la Sociedad Geologica de Espana*, *13*, 191–211.
Quintà, A., Tavani, S., & Roca, E. (2012). Fracture pattern analysis as a tool for constraining the interaction between regional and diapir-related stress fields: Poza de la Sal Diapir (Basque Pyrenees, Spain). In G. I. Alsop, S. G. Archer, A. J. Hartley, N. T. Grant, & R. Hodgkinson (Eds.), *Salt tectonics, sediments and prospectivity* (Vol. 363, pp. 521–532). Geological Society, London, Special Publications. https://doi.org/10.1144/sp363.25
Quintana, L., Pulgar, J. A., & Alonso, J. L. (2015). Displacement transfer from borders to interior of a plate: A crustal transect of Iberia. *Tectonophysics*, *663*, 378–398. https://doi.org/10.1016/j.tecto.2015.08.046
Ramos, A., García-Senz, J., Pedrera, A., Ayala, C., Rubio, F., Peropadre, C., & Mediato, J. (2022a). Salt control on the kinematic evolution of the southern Basque-Cantabrian Basin and its underground storage systems (northern Spain). *Tectonophysics*, *822*, 229178. https://doi.org/10.1016/j.tecto.2021.229178
Ramos, A., García-Senz, J., Pedrera, A., Ayala, C., Rubio, F., Peropadre, C., & Mediato, J. (2022b). Reply to Comment by Tavani et al. on "Salt control on the kinematic evolution of the southern Basque-Cantabrian Basin and its underground storage systems (northern Spain)". *Tectonophysics*, *837*, 229465. https://doi.org/10.1016/j.tecto.2022.229465
Rat, P. (1988). The Basque-Cantabrian Basin between the Iberian and European plates – Some facts but still many problems. *Revista de la Sociedad Geológico de España*, *1*(3–4), 327–348.
Roca, E., Ferrer, O., Rowan, M. G., Muñoz, J. A., Butillé, M., Giles, K. A., et al. (2021). Salt tectonics and controls on halokinetic-sequence development of an exposed deepwater diapir: The Bakio diapir, Basque-Cantabrian Basin, Pyrenees. *Marine and Petroleum Geology*, *123*, 104770. https://doi.org/10.1016/j.marpetgeo.2020.104770
Roca, E., Muñoz, J. A., Ferrer, O., & Ellouz, N. (2011). The role of the Bay of Biscay Mesozoic extensional structure in the configuration of the Pyrenean orogen: Constraints from the MARCONI deep seismic reflection survey. *Tectonics*, *30*(2), TC2001. https://doi.org/10.1029/2010TC002735
Rodríguez, L., Esteban, J. J., Vegas, N., & Cuevas, J. (2008). Inversion tectonics in the Sopelana beach (Basque Arc, Western Pyrenees). *Geogaceta*, *45*, 23–26.
Rodríguez Cañas, C., Hernaiz, P. P., Malagón, J., & Serrano, A. (1994). Notas sobre la estructura cabalgante de Rojas-Santa Casilda. *Geogaceta*, *15*, 135–138.
Rojo, L. A., Cardozo, N., Escalona, A., & Koyi, H. (2019). Structural style and evolution of the Nordkapp Basin, Norwegian Barents sea. *AAPG Bulletin*, *103*(9), 2177–2217. https://doi.org/10.1306/01301918028
Roma, M., Ferrer, O., Roca, O., Pla, O., Escosa, F. O., & Butillé, M. (2018). Formation and inversion of salt-detached ramp-syncline basins. Results from analog modeling and application to the Columbrets Basin (Western Mediterranean). *Tectonophysics*, *745*, 214–228. https://doi.org/10.1016/j.tecto.2018.08.012
Rowan, M. G. (2014). Passive-margin salt basins: Hyperextension, evaporite deposition, and salt tectonics. *Basin Research*, *26*(1), 154–182. https://doi.org/10.1111/bre.12043
Rowan, M. G. (2022). The ocean-Continent transition of late synrift salt basins: Extension and evaporite deposition in the southern Gulf of Mexico and global analogs. In C. Koeberl, P. Claeys, & S. Montanari (Eds.), *From the Guajira Desert to the Apennines, and from Mediterranean Microplates to the Mexico Killer Asteroid: Honoring the career of Walter Alvarez* (Vol. 557). https://doi.org/10.1130/2022.2557
Rowan, M. G. (2023). Structural architecture and evolution of eastern Mississippi Canyon, northern Gulf of Mexico. *Marine and Petroleum Geology*, *150*, 106127. https://doi.org/10.1016/j.marpetgeo.2023.106127
Rowan, M. G., & Giles, K. A. (2021). Passive versus active salt diapirism. *AAPG Bulletin*, *105*(1), 55–63. https://doi.org/10.1306/05212020001
Rowan, M. G., & Giles, K. A. (2023). Different scales of salt-sediment interaction flanking passive diapirs. *AAPG Bulletin*, *107*(1), 7–22. https://doi.org/10.1306/0104202221069
Rowan, M. G., & Jarvie, A. (2020). Crustal extension and salt tectonics of the Danmarkshavn Ridge and adjacent basins, NE Greenland. *Marine and Petroleum Geology*, *117*, 104339. https://doi.org/10.1016/j.marpetgeo.2020.104339
Rowan, M. G., & Krzywiec, P. (2014). The Szamotuły salt diapir and mid-Polish trough: Decoupling during both Triassic-Jurassic rifting and Alpine inversion. *Interpretation*, *2*(4), SM1–SM18. https://doi.org/10.1190/INT-2014-0028.1
Rowan, M. G., & Lindsø, S. (2017). Salt tectonics of the Norwegian Barents sea and northeast Greenland. In J. I. Soto, J. Flinch, & G. Tari (Eds.), *Permo-triassic salt provinces of Europe, north Africa and the Atlantic margins: Tectonics and hydrocarbon potential* (pp. 265–286). Elsevier. https://doi.org/10.1016/B978-0-12-809417-4.00013-6
Rowan, M. G., Muñoz, J. A., Giles, K. A., Roca, E., Hearon, T. E. I. V., Fiduk, J. C., et al. (2020). Folding and fracturing of rocks adjacent to salt diapirs. *Journal of Structural Geology*, *141*, 104187. https://doi.org/10.1016/j.jsg.2020.104187
Rowan, M. G., Muñoz, J. A., Roca, E., Ferrer, O., Santolaria, P., Granado, P., & Snidero, M. (2022). Linked detachment folds, thrust faults, and salt diapirs: Observations and analog models. *Journal of Structural Geology*, *155*, 104509. https://doi.org/10.1016/j.jsg.2022.104509
Rowan, M. G., Urai, J. L., Fiduk, J. C., & Kukla, P. A. (2019). Deformation of intrasalt competent layers in extension, contraction, differential loading, and passive diapirism. *Solid Earth*, *10*(3), 987–1013. https://doi.org/10.5194/se-10-987-2019
Rowan, M. G., & Vendeville, B. C. (2006). Foldbelts with early salt withdrawal and diapirism: Physical model and examples from the northern Gulf of Mexico and the Flinders ranges, Australia. *Marine and Petroleum Geology*, *23*(9–10), 871–891. https://doi.org/10.1016/j.marpetgeo.2006.08.003

Santolaria, P., Granado, P., Carrera, N., Schneider, C. L., Ferrer, O., Snidero, M., et al. (2021). From downbuilding to contractional reactivation of salt-sediment systems: Insights from analog modeling. *Tectonophysics*, *819*, 229078. https://doi.org/10.1016/j.tecto.2021.229078

Saura, E., Ardèvol I Orò, L., Teixell, A., & Vergés, J. (2016). Rising and falling diapirs, shifting depocenters, and flap overturning in the Cretaceous Sopeira and Sant Gervàs subbasins (Ribagorça Basin, southern Pyrenees). *Tectonics*, *35*(3), 638–662. https://doi.org/10.1002/2015TC004001

Schroeder, R., & Willems, H. (1983). Uber einem submarinen Durchbruch des diapirs von Villasana de Mena (Prov. Burgos, N-Spanien) an der Wende Unter-/Oberkreide. *Neues Jahrbuch für Geologie und Paläontologie - Abhandlungen*, *166*(1), 65–85. https://doi.org/10.1127/njgpa/166/1983/65

Serrano, A., Huerta, P. P. H., Malagón, J., & Cañas, C. R. (1994). Tectónica distensiva y halocinesis en el margen SO de la cuenca Vasco-Cantábrica. *Geogaceta*, *15*, 131–134.

Serrano, A., & Martínez del Olmo, W. (1990). Tectónica salina en el Dominio Cántabro-Navarro: Evolución, edad y origen de las estructuras salinas. In F. Ortí & J. M. Salvany (Eds.), *Formaciones evaporiticas de la Cuenca del Ebro y cadenas periféricas y de la zona de Levante* (pp. 39–53). Universitat de Barcelona.

Serrano, A., & Martínez del Olmo, W. (2004). Estructuras diapíricas de la zona meridional de la Cuenca Vasco-Cantábrica. In J. A. Vera (Ed.), *Geologia de España* (pp. 334–338). Sociedad Geológica de España-Instituto Geológico y Minero.

Serrano Oñate, A., Martinez del Olmo, W., & Cámara Rupelo, P. (1989). Diapirismo del Trías salino en el dominio Cántabro-Navarro. In *Libro Homenaje a Rafael soler* (pp. 115–121). A.G.G.E.E.P.

Smit, J. H. W., Brun, J. P., & Sokoutis, D. (2003). Deformation of brittle-ductile thrust wedges in experiments and nature. *Journal of Geophysical Research*, *108*(B10), 2480. https://doi.org/10.1029/2002JB002190

Sopeña, A., Sánchez-Moya, Y., & Barrón, E. (2009). New palynological and isotopic data for the Triassic of the western Cantabrian Mountains (Spain). *Journal of Iberian Geology*, *35*, 35–45.

Soto, R., Beamud, E., Roca, E., Carola, E., & Almar, Y. (2017). Distinguishing the effect of diapir growth on magnetic fabrics of syn-diapiric overburden rocks: Basque-Cantabrian Basin, northern Spain. *Terra Nova*, *29*(3), 191–201. https://doi.org/10.1111/ter.12262

Stampfli, G. M., & Hochard, C. (2009). Plate tectonics of the Alpine realm. In J. B. Murphy, J. D. Keppie, & A. J. Hynes (Eds.), *Ancient orogens and modern Analogues* (Vol. 327, pp. 89–111). Geological Society, London, Special Publications. https://doi.org/10.1144/sp327.6

Stewart, S. A. (2014). Detachment-controlled triangle zones in extension and inversion tectonics. *Interpretation*, *2*(4), SM29–SM38. https://doi.org/10.1190/INT-2014-0026.1

Stewart, S. A., & Clark, J. A. (1999). Impact of salt on the structure of the Central North Sea hydrocarbon fairways. In A. J. Fleet & S. A. R. Boldy (Eds.), *Petroleum geology of northwest Europe: Proceedings of the 5th Conference* (pp. 179–200). https://doi.org/10.1144/0050179

Stewart, S. A., Harvey, M. J., Otto, S. C., & Weston, P. J. (1996). Influence of salt on fault geometry: Examples from the UK salt basins. In G. I. Alsop, D. J. Blundell, & I. Davison (Eds.), *Salt tectonics* (Vol. 100, pp. 175–202). Geological Society, Special Publication. https://doi.org/10.1144/GSL.SP.1996.100.01.12

Tavani, S., Bertok, C., Granado, P., Piana, F., Salas, R., Vigna, B., & Muñoz, J. (2018). The Iberia-Eurasia plate boundary east of the Pyrenees. *Earth-Science Reviews*, *187*, 314–337. https://doi.org/10.1016/j.earscirev.2018.10.008

Tavani, S., Carola, E., Granado, P., Quintà, A., & Muñoz, J. A. (2013). Transpressive inversion of a Mesozoic extensional forced fold system with an intermediate décollement level in the Basque-Cantabrian Basin (Spain). *Tectonics*, *32*(2), 146–158. https://doi.org/10.1002/tect.20019

Tavani, S., & Granado, P. (2015). Along-strike evolution of folding, stretching and breaching of supra-salt strata in the Plataforma Burgalesa extensional forced fold system (northern Spain). *Basin Research*, *27*(4), 573–585. https://doi.org/10.1111/bre.12089

Tavani, S., Granado, P., Carola, E., Rowan, M. G., & Muñoz, J. A. (2022). Comment on Ramos et al. 2022: Salt control on the kinematic evolution of the Southern Basque-Cantabrian Basin and its underground storage systems (Northern Spain). *Tectonophysics*, *837*, 229460. https://doi.org/10.1016/j.tecto.2022.229460

Tavani, S., Quintà, A., & Granado, P. (2011). Cenozoic right-lateral wrench tectonics in the western Pyrenees (Spain): The Ubierna fault system. *Tectonophysics*, *509*(3–4), 238–253. https://doi.org/10.1016/j.tecto.2011.06.013

Teixell, A., Labaume, P., Ayarza, P., Espurt, N., de Saint Blanquat, M., & Lagabrielle, Y. (2018). Crustal structure and evolution of the Pyrenean-Cantabrian belt: A review and new interpretations from recent concepts and data. *Tectonophysics*, *724–725*, 146–170. https://doi.org/10.1016/j.tecto.2018.01.009

Trudgill, B. D. (2011). Evolution of salt structures in the northern Paradox Basin: Controls on evaporite deposition, salt wall growth and supra-salt stratigraphic architecture. *Basin Research*, *23*(2), 208–238. https://doi.org/10.1111/j.1365-2117.2010.00478.x

Tugend, J., Manatschal, G., Kusznir, N. J., Masini, E., Mohn, G., & Thinon, I. (2014). Formation and deformation of hyperextended rift systems: Insights from rift domain mapping in the Bay of Biscay-Pyrenees. *Tectonics*, *33*(7), 1239–1276. https://doi.org/10.1002/2014TC003529

Vendeville, B. C., & Jackson, M. P. A. (1992). The rise of diapirs during thin-skinned extension. *Marine and Petroleum Geology*, *9*(4), 331–353. https://doi.org/10.1016/0264-8172(92)90047-I

Vendeville, B. C., & Nilsen, K. T. (1995). Episodic growth of salt diapirs driven by horizontal shortening. In C. J. Travis, H. Harrison, M. R. Hudec, B. C. Vendeville, F. J. Peel, & B. F. Perkins (Eds.), *Salt, sediment, and hydrocarbons (285-295). SEPM Gulf coast section 16th annual research foundation conference*. https://doi.org/10.5724/gcs.95.16.0285

Warren, J. K. (2016). *Evaporites: A geological compendium* (2nd ed.). Springer.1813.

Warsitzka, M., Kley, J., & Kukowski, N. (2015). Analogue experiments of salt flow and pillow growth due to basement faulting and differential loading. *Solid Earth*, *6*(1), 9–31. https://doi.org/10.5194/se-6-9-2015

Wicker, V., & Ford, M. (2021). Assessment of the tectonic role of the Triassic evaporites in the North Toulon fold-thrust belt. *BSGF – Earth Sciences Bulletin*, *192*, 51. https://doi.org/10.1051/bsgf/2021033

Withjack, M. O., & Callaway, S. (2000). Active normal faulting beneath a salt layer: An experimental study of deformation patterns in the cover sequence. *AAPG Bulletin*, *84*, 627–651. https://doi.org/10.1306/C9EBCE73-1735-11D7-8645000102C1865D

Wu, S., Bally, A. W., & Cramez, C. (1990). Allochthonous salt, structure and stratigraphy of the north-eastern Gulf of Mexico. Part II. Structure. *Marine and Petroleum Geology*, *7*(4), 334–370. https://doi.org/10.1016/0264-8172(90)90014-8